From the
Chair for Molecular Animal Breeding and Biotechnology
(Prof. Dr. Eckhard Wolf)
and the
Chair for General Pathology and Pathological Anatomy
(Prof. Dr. Walter Hermanns)
Faculty of Veterinary Medicine of the
Ludwig-Maximilians University Munich

Under the supervision of Prof. Dr. Eckhard Wolf and Prof. Dr. Rüdiger Wanke

Transgenic pigs expressing a dominant-negative glucose-dependent insulinotropic polypeptide receptor – a novel animal model for studying the consequences of impaired incretin hormone function

Thesis for the attainment of the title Doctor in Veterinary Medicine
from the Faculty of Veterinary Medicine of the
Ludwig-Maximilians University Munich

by

Simone Renner
from Munich

Munich 2008

Aus dem
Lehrstuhl für Molekulare Tierzucht und Biotechnologie
(Prof. Dr. Eckhard Wolf)
und dem
Lehrstuhl für Allgemeine Pathologie und Pathologische Anatomie
(Prof. Dr. Walter Hermanns)
Tierärztliche Fakultät der
Ludwig-Maximilians Universität München

Unter der Betreuung von Prof. Dr. Eckhard Wolf und Prof. Dr. Rüdiger Wanke

Expression eines dominant-negativen Rezeptors für das Glukose-abhängige insulinotrope Polypeptid in transgenen Schweinen - ein neues Tiermodell zur Untersuchung der Auswirkungen einer verminderten Inkretinhormonfunktion

Inaugural Dissertation
zur Erlangung der tiermedizinischen Doktorwürde
der Tierärztlichen Fakultät der Ludwig-Maximilians Universität München

von

Simone Renner
aus München

München 2008

Gedruckt mit Genehmigung der Tierärztlichen Fakultät
der Ludwig-Maximilians Universität München

Dekan:	Univ.-Prof. Dr. J. Braun
Berichterstatter:	Univ.-Prof. Dr. E. Wolf
1. Korreferentin:	Univ.-Prof. Dr. H. Potschka
2. Korreferent:	Univ.-Prof. Dr. C. Knospe
3. Korreferent:	Univ.-Prof. Dr. H.-J. Gabius
4. Korreferent:	Univ.-Prof. Dr. K. Heinritzi

Tag der Promotion: 8. Februar 2008

To my family

Table of contents

1 Introduction

Diabetes mellitus type 2 is a chronic metabolic disorder of multiple etiology and characterized by insulin resistance and progressive dysfunction of pancreatic islet cells. The meal-stimulated insulin secretion from β-cells is reduced and fails to meet the demands of the insulin-resistant state (Kahn et al. 2006). The disease is considered to be a world health crisis. In conjunction with genetic susceptibility, particularly in certain ethnic groups, type 2 diabetes mellitus is brought on by environmental and behavioral factors such as a sedentary lifestyle, overly rich nutrition and obesity (Leahy 2005). At the turn of this century, 171 million individuals were estimated to have diabetes, 90 % of which were considered cases of type 2 diabetes mellitus. This number is expected to increase up to 366 million by 2030 (Wild et al. 2004). Due to its chronic character, gravity of secondary lesions and agents necessary to control these, type 2 diabetes mellitus is associated with very high expenses ($ 132 billion in 2002 in the U.S.A.) (Hogan et al. 2003). Importantly, a reduced relative β-cell mass coming along with increased β-cell apoptosis have been reported in type 2 diabetic patients (Butler et al. 2003; Sakuraba et al. 2002).

Glucose-dependent insulinotropic polypeptide (GIP) and glucagon-like peptide-1 (GLP-1) are defined as incretin hormones, mediating the incretin effect which describes the phenomenon that an oral glucose load leads to a higher insulin response than an intravenous glucose load (Elrick et al. 1964; McIntyre et al. 1964). Secreted from enteroendocrine cells within the intestine in response to nutrient ingestion, both incretin hormones bind to their specific receptor on the pancreatic β-cells and potentiate glucose-dependent insulin secretion, accounting for 20 to 60 % of total insulin secretion depending on the glucose load (Nauck et al. 1986a; Nauck et al. 1986b). One facet of type 2 diabetes mellitus is a reduced to almost absent incretin effect mainly originating from a significantly reduced insulinotropic action of GIP (Nauck et al. 1993). Based on the knowledge that the insulinotropic effect of the other incretin hormone, GLP-1, is vastly preserved, incretin hormone based therapeutics have already been established, but quite a few of them are still in the developmental phase.

Since the role of the GIP/GIP-receptor (GIPR) axis in the pathogenesis of type 2 diabetes mellitus needs to be clarified, the aim of this work was the generation and

genotypic as well as phenotypic characterization of transgenic pigs expressing a dominant-negative GIP-receptor under control of the rat insulin 2 *(Ins2)* gene promoter. A genetically modified large animal model is important to elucidate pathogenetic consequences associated with impairment of the GIP/GIPR axis as well as for translational studies, e.g. therapeutic trials.

Lentiviral gene transfer made it possible to efficiently generate a pig animal model which is more clinically relevant than rodent models owing to the high similarities of human and porcine anatomy and physiology.

2 Review of the literature

2.1 Viral transgenesis

Transgenic animals can be broadly defined as animals that contain recombinant DNA molecules in their genome that have been introduced by human intervention (Wall 1996). The principle of viral transgenensis is the introduction of foreign genes into preimplantation embryos with the aid of viruses. Retroviruses are characterized by their ability to reversely transcribe their viral genome into double-stranded (ds) DNA by using an enzyme called reverse-transcriptase and integrate it into the host genome as a so-called provirus. Thus, the virus serves as a shuttle for the transfer of external genes (transgenes) into the host genome. Integration of retroviruses carrying foreign DNA as well as germ line integration and transmission was first described by Jaenisch and coworkers using the murine leukemia virus (MLV) (Jaenisch et al. 1975; Jaenisch 1976).

2.1.1 Lentiviruses

The lentiviruses belong to the family of *Retroviridae* which possess the enzyme reverse transcriptase and maybe oncogenic. The family of retroviruses can be divided into two groups depending on the organization of their genome: simple and complex retroviruses. The genus *Lentivirinae* belongs to the latter group (Coffin 1992). They are enveloped viruses and their genome is a dimer of a single-stranded RNA of positive polarity. As all retroviruses, lentiviruses have *gag*, *pol* and *env* genes coding for structural virion proteins that form the matrix, capsid, and the nucleoprotein complex, viral enzymes (reverse transcriptase, integrase, protease) and envelope glycoproteins that are displayed on the surface of the virus (Goff 2001). In addition lentiviruses contain additional accessory and regulatory genes.

The most prominent and best studied representative of lentiviruses is the human immunodeficiency virus (HIV). But lentiviruses have also been isolated from other species, for example the visna/maedi virus in sheep, the equine infectious anemia virus (EIAV) in the horse and the feline immunodeficiency virus (FIV) in the cat.

2.1.2 Retroviral life cycle

Following infection of the host cell, reverse transcription of the virus RNA takes place in the cytoplasm. The viral genome is flanked by regulatory control sequences which are essential for reverse transcription and integration of viral genetic information (Starcich et al. 1985; Kao et al. 1987). The so-called R-region ("redundant") attaches directly to the *Cap*-structure at the 5'-end of the viral genome and also exists at the 3'-end with identical nucleotide sequence and orientation (Starcich et al. 1985). The U5-region ("unique") located at the 5'-end is important for the integration of the provirus into the host genome. A primer binding site (PB) is connected to the U5-region followed by a splice-donor-site. The splice-donor-site is probably responsible for the generation of all spliced mRNA molecules (Starcich et al. 1985). Additionally, a so-called ψ sequence is located at the 5'-end, which is essential for the packaging of viral RNA into the virus particle (Berglund et al. 1997; Clever et al. 2000); (Figure 2.1). The U3-region located at the 3'-end of the virus genome is reverse transcribed in duplicate and subsequently copied to the 5'-end while the U5-region at the 5'-end is copied to the 3'-end (LTR conversion) forming tandem repeats which are called long-terminal repeats (LTR's). LTR's are necessary for reverse transcription of the vector RNA and integration of the proviral DNA into the host genome. (Starcich et al. 1985).

Subsequently, the preintegration complex is translocated to the nucleus. Lentiviruses differ in their basic requirements for entering the nucleus from prototypic retroviruses. While simple retroviruses can only enter the nucleus during mitosis when the nuclear membrane is disassembled (Miller et al. 1990), lentiviruses are able to access the nucleus of non-dividing cells through the nuclear pores (Follenzi et al. 2000; Zennou et al. 2000). Thus, integration into the genome prior to the first cell division may minimize the risk of mosaic formation. As soon as virus DNA has reached the nucleus, DNA is integrated into the host genome forming a provirus. The provirus uses the host-cell machinery for gene expression. Therefore the U3-region contains promoters as well as cis-acting sequences which are binding sites for cellular proteins. Thus, the U3-region is also important for gene expression of the provirus. When translation of the virus genome is completed, new virus particles are assembled and released from the host cell by budding of the cell membrane (Pfeifer & Verma 2001).

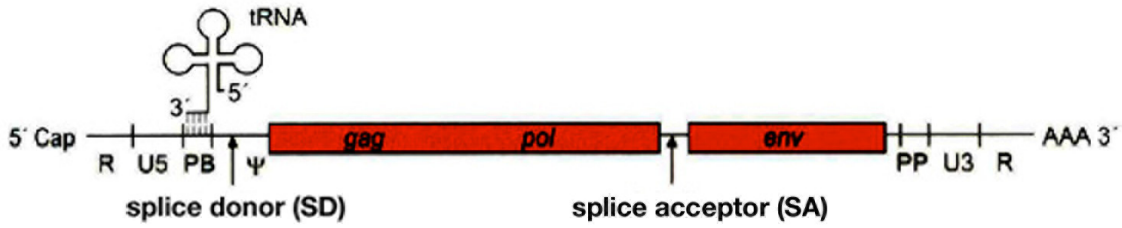

Figure 2.1: RNA genome of a retrovirus; figure from Modrow et al., 2003.

2.1.3 Basic outline of viral vectors

In general non-integrating and integrating viral vectors are known. While non-integrating vectors get lost after several cell divisions, integrating viral vectors integrate permanently into the host genome and outlast germline transmission. Lentiviruses, prototypic retroviruses or adeno-associated viruses (AAV) are most commonly used for construction of integrating vectors. To generate a viral vector, wild-type virus genes for infection, replication and pathogenesis are deleted. In such replication-defective viruses, the life cycle is cut down to one round of infection. Afterwards, the transgene is integrated into the viral vector together with the designated promoter and flanked by the LTR's. Last, the viral particles are produced by helper cells through the expression of essential viral proteins in *trans* (Pfeifer 2004). Being integrated into the host genome, the provirus is not able to form progeny virus, but the expression cassette on the vector can still be transcribed.

2.1.4 Lentiviral vectors

Lentiviral vectors are mostly based on the human immunodeficiency virus 1 (HIV-1). An advancement in biosafety has been the establishment of third generation HIV based vector systems (Dull et al. 1998). Apart from HIV-1, lentiviral vectors have been derived from HIV-2 (Poeschla et al. 1998a), feline immunodeficiency virus (FIV) (Poeschla et al. 1998b), equine infectious anemia virus (EIAV) (Olsen 1998), simian immunodeficiency virus (SIV) (Mangeot et al. 2000), and maedi/visna virus (Berkowitz et al. 2001).

Further advances have been achieved through the generation of so-called self-inactivating vectors (SIN-vectors) as viral enhancer and promoter sequences within the LTR's have been deleted in this vectors (Miyoshi et al. 1998; Zufferey et al. 1998). The risk for insertional activation of cellular oncogenes through the promoter and enhancer elements of the proviral LTR's was addressed with insertion of self-inactivating mutations in just these elements. In addition it was postulated that SIN vectors might avoid gene silencing as the active viral promoter sequence might attract the host silencing machinery to the integrated provirus (Pfeifer et al. 2002). This assumption proved false since epigenetic regulation was found in transgenic pigs generated by lentiviral gene transfer as well as in murine embryonic carcinoma P19 cells transduced with lentiviral SIN vectors (Hofmann et al. 2006; He et al. 2005). However, the extent of lentiviral silencing was much lower than in the initial studies using prototypic retroviruses (Jaenisch 1976). The lack of a viral promoter requires the incorporation of a heterologous promoter driving the transgene expression and so allowing ubiquitous as well as tissue-specific expression of the transgene (Pfeifer et al. 2002; Lois et al. 2002).

Another special feature is the incorporation of a polypurine tract (ppt) of the *pol* gene into the lentiviral vector which enhances the import of the viral genome into the nucleus (Follenzi et al. 2000; Zennou et al. 2000). In addition, the insertion of the posttranscriptional regulatory element of the woodchuck hepatitis virus enhances transgene expression in a promoter- and transgene-independent manner (Zufferey et al. 1999).

Besides genes located on the vector construct, several other viral elements are located on different packaging constructs. Usually, *gag* and *pol* proteins are needed. For ideal vector production the *rev* gene needs to be present which interacts with so-called RREs (*rev* responsive elements) and promotes the nuclear export of unspliced *gag-pol* mRNA and the genomic RNA of the lentiviral vector (Delenda 2004). Expression of the *rev* gene through a separate packaging construct could ameliorate biosafety (Gasmi et al. 1999). Finally, the gene coding for the *env* protein, determining the tropism of the virus, is located on a separate packaging vector. In order to expand the natural tropism of lentiviruses, *env* was replaced by envelope proteins of heterologous viruses. To provide a broad host range that can be infected, most of the lentiviral vectors are pseudotyped with the G-protein of the

vesiculostomatitis virus (VSV) (Akkina et al. 1996; Naldini et al. 1996). This method also stabilizes viral particles so they can easily be concentrated by ultracentrifugation and are more resistant to freezing and thawing processes (Lever et al. 2004). In addition, infection of host cells is no more carried out by fusion of the virus particle with the host cell but through the endocytosis signaling cascade (Aiken 1997). Packaging constructs are either transfected transiently into the packaging cells or a cell line is established that stably expresses the viral proteins. Mostly, HEK 293T cells, a human embryonic kidney cell line, transiently transfected with the vector and packaging plasmids are used. With this method high lentivirus titers (>10^9 infectious units (IU)/ml) can be achieved (Pfeifer & Verma 2001). Thus, the RNA is packaged into viral particles and the lentiviral virions are released into the culture medium of packaging/producer cells by budding.

2.1.5 Lentiviral transgenesis in the pig

Lentiviral transgenesis was first reported in mice and rats (Pfeifer et al. 2002; Lois et al. 2002). As the zona pellucida is a barrier for lentiviral infection, zygotes had to be denuded or the lentiviral particles had to be injected into the perivitelline space. The latter method turned out to be the only practical method for pigs due to high embryonic losses after denudation (Hofmann et al. 2003). Transgenic pigs generated by lentiviral gene transfer using a HIV-1 based vector system which carries the green fluorescent protein (GFP) under control of the ubiquitously expressing phosphoglycerate kinase promoter (PGK) were first described in 2003 (Hofmann et al. 2003). Seventy percent of animals born (13.1% of infected and transferred embryos) turned out to be transgenic. One to twenty lentiviral integrants were detected by Southern blot analyses. Thirty (94%) of the 32 transgenic pigs expressed the transgene. Also germline transmission was confirmed (Hofmann et al. 2003). Another group who generated transgenic pigs on the basis of an equine infectious anemia virus derived vector achieved 92% of transgenic pigs (31% of the transferred embryos). Ninety-five percent of the founder animals expressed the GFP transgene under the control of the human cytomegalovirus promoter (CMV). Pigs revealed one to five integrants. Germline transmission was not evaluated (Whitelaw et al. 2004). Thus, lentiviral transgenesis showed a 27- to 50-fold increase in efficiency compared

to DNA microinjection (Fassler 2004; Whitelaw et al. 2004). The efficiency of DNA microinjection, the most wide-spread technology to generate transgenic animals (Clark & Whitelaw 2003), is generally low. In the mouse, approximately 2.6% of transgenic offspring per injected and transferred embryos can be obtained while in the pig the efficiency is even lower, ranging around 0.9% (Wall 1996).

One reason for this is that the pronucleus of porcine zygotes can hardly be targeted with the injection capillary because the cytoplasm of porcine zygotes is opaque. Increased efficiency could considerably lower the costs incurred by generation of a transgenic pig which were estimated at $ 30,000 (Fassler 2004). However, the size of the transgene plus its internal promoter within the lentiviral construct is limited to 8 kb because the maximal packaging capacity of an HIV-1 based vector particle is ~10 kb while DNA transfer capacity of DNA-microinjection is basically unlimited. The phenomenon of DNA-hypermethylation was examined in pigs of the F1-generation after segregation of the integration sites had taken place. Actually, one third of the integration sites exhibited low expression levels and hypermethylation indicating that methylation plays a role in lentiviral expression (Hofmann et al. 2006). Also insertional mutagenesis or activation of proto-oncogenes following integration of the lentiviral construct close to a proto-oncogene promoter may be possible side-effects of lentiviral transgenesis (Pfeifer 2004). However, it has been shown that prototypic retroviruses tend to integrate in genomic sequences surrounding the transcriptional start site (Wu et al. 2003; Wu & Burgess 2004), while lentiviruses do not (Schroder et al. 2002).

2.2 The incretin hormone system

2.2.1 History of the incretin concept

As early as 1932, La Barre introduced the term “incretin” for the first time. He and his colleagues had performed cross-circulation experiments and demonstrated that the intravenous injection of crude secretin, a term which originally involved all ingredients of a mucosal extract from the small intestine, produced hypoglycemia in dogs via stimulation of the endocrine pancreas. They concluded that crude secretin contained two active principles: “incretin” stimulating the internal secretion of the pancreas and

“excretin” stimulating the exocrine pancreas (Creutzfeldt 2005). Over 20 years later, in 1964, as soon as it was possible to determine serum insulin concentrations by radioimmunoassay, the incretin effect was determined as the phenomenon of an oral glucose load eliciting a higher insulin response than an intravenous glucose load (Elrick et al. 1964; McIntyre et al. 1964). From this time, all known gastrointestinal hormones were proved for their properties of an incretin. Secretin, vasoactive intestinal polypeptide (VIP), glucagon, gastrin and cholecystokinin (CCK) for instance stimulated insulin secretion but only if given in supraphysiologic doses (Creutzfeldt 1979). At this point none of the known hormones met the criteria of an incretin which are as follows (Creutzfeldt 2005):

- Release from gut endocrine cells after ingestion of nutrients, especially glucose
- Glucose dependency of the glucose lowering effect, i. e. the glucose lowering effect occurs only in the presence of elevated blood glucose levels
- Stimulation of insulin secretion in a concentration that is easily achieved after nutrient ingestion (not only after administration of supraphysiological levels)

The first incretin hormone was discovered in 1970 by John C. Brown as a contaminant of impure cholecystokinin-pancreozymin extracts and was named gastric inhibitory polypeptide (GIP) due to its inhibitory effect on gastric acid secretion in dogs (Brown et al. 1970; Brown & Dryburgh 1971). A few years later the insulinotropic effect of GIP was discovered (Dupre et al. 1973) and the meaning of the acronym GIP changed into glucose-dependent insulinotropic polypeptide, since an inhibitory effect of GIP on gastric acid secretion was seen only at pharmacologic doses, whereas its incretin action occurred at physiologic levels. However, several different experimental approaches revealed that GIP cannot be the only incretin. In vivo immunoneutralization of GIP reduced but did not completely ablate the incretin effect in response to an oral glucose load. Significant insulin-releasing activities remained after removal of GIP from intestinal mucosa preparation as well as from venous perfusate of an isolated perfused rat intestine (Ebert & Creutzfeldt 1982; Ebert et al. 1983; Levin et al. 1979). Patients who underwent intestinal resection with near total loss of the ileum showed a smaller incretin effect than patients with larger

amounts of residual ileum, although GIP levels were identical in all groups (Lauritsen et al. 1980). In 1985, the insulinotropic effect of the second incretin, glucagon-like peptide 1 (GLP-1), was discovered (Schmidt et al. 1985).

2.2.2 Quantification of the incretin effect

The incretin effect describes the phenomenon that an oral glucose load leads to a much higher insulin secretory response than does an intravenous glucose load (Elrick et al. 1964; McIntyre et al. 1964). To precisely quantify the extent of the incretin effect related to the total insulin response following nutrient stimulation, a comparison of the insulin secretory response after oral and “isoglycemic” intravenous glucose administration is state of the art. Here “isoglycemic” describes an intravenous glucose infusion leading to a similar glycemic profile as after an oral glucose load (Nauck et al. 2004).

The quantitative impact of the incretin effect was shown to be dependent on the size of the glucose load and ranged between 20 and 60% (C-peptide response) in healthy human subjects following an oral glucose load of 25 to 100 g (Nauck et al. 1986a; Nauck et al. 1986b). It is also important to note that the two incretins, GIP and GLP-1, have additive but not potentiating effects on insulin secretion in humans (Nauck et al. 1993a). However, GIP was found to be able to release GLP-1 in rodents (Herrmann-Rinke et al. 1995). Quantitatively, the contribution of GIP to the incretin effect was reported to be more important (Nauck et al. 1993a). Despite similar glucose-concentration dependence of their insulinotropic activities, higher plasma concentrations of GIP, both in the basal and postprandial state, were detected compared to GLP-1 levels (Nauck 1999).

To define the contribution of both incretin hormones or either one of them on insulin secretion, numerous studies were carried out in rodents using GIP receptor (GIPR) and GLP-1 receptor (GLP-1R) antagonists. Studies performed in rats using the GIPR antagonist GIP (7-30)-NH_2 reduced postprandial insulin release by 72% (Tseng et al. 1996b). Application of the GLP-1 receptor antagonist Exendin (9-39) also led to a marked decrease of insulin secretion by 48% (Wang et al. 1995). Another study showed a reduction of insulin secretion by 32% and 54% after Exendin (9-39) and GIP (7-30)-NH_2 application following an intragastric glucose load (Tseng et al. 1999).

GIP (6-30)-amide was found to be a potent GIPR antagonist with an equivalent binding affinity to the GIPR compared to the bioactive GIP (1-42) and reduced cAMP rise by 58% in chinese hamster kidney (CHO-KI) cells stably expressing the rat pancreatic islet GIP receptor (Gelling et al. 1997a).

2.2.3 The enteroinsular axis

The term enteroinsular axis formed by Unger and Eisentraut comprises the collectivity of signaling pathways between the gut and the endocrine pancreas meaning nutrient, neural and hormonal signals (Unger & Eisentraut 1969).

2.2.4 Neural components

Vagal stimulation following nutrient ingestion is thought to augment insulin secretion. An example for this is the cephalic phase of insulin secretion which has been demonstrated in dogs, rats and humans (Ebert & Creutzfeldt 1987). It has been shown that several gastrointestinal neuropeptides with insulinotropic inhibitory or stimulatory activity are present in pancreatic nerves: stimulators such as gastrin-releasing peptide (GRP), cholecystokinin (CCK), gastrin and vasoactive intestinal polypeptide (VIP) as well as inhibitors such as somatostatin may function as neurotransmitters. The gastrointestinal neural system may participate in the entero-insular axis in two ways: regulation of the release of an incretin into the blood stream and by direct stimulation of the islets via nerve fibres (Creutzfeldt 1979). However, whether denervation of the pancreas impairs glucose tolerance is discussed controversial. In humans, the incretin effect of pancreas-kidney-transplanted type 1 diabetic patients, whose functioning pancreas is denervated, was shown to be preserved (Nauck et al. 1993b).

2.2.5 Glucagon-like peptide 1 (GLP-1)

GLP-1 is a tissue-specific posttranslational proteolytic product of the proglucagon gene that is released from intestinal L-cells in response to nutrient ingestion (Mojsov et al. 1987; Kreymann et al. 1987). L-cells are located mainly in the distal ileum and

the colon. Besides GLP-1, other gastrointestinal hormones like enteroglucagon, peptide YY and GLP-2 are secreted from L-cells following glucose and fat ingestion (Holst 1994). Secretion of GLP-1 occurs in a biphasic pattern starting with an early phase (within 10-15 minutes) that is followed by a longer (30-60 minutes) second phase (Herrmann et al. 1995). In humans, GLP-1 exists mainly as a COOH-terminally amidated form, GLP-1-(7-36)-amide, and a minor glycine extended form, GLP-1-(7-37) (Orskov et al. 1994). Both bioactive forms are equipotent concerning their insulinotropic activity. GLP-1 is a target for the dipeptidyl peptidase-4 (DPP-4) and the active forms are rapidly degraded ($t_{1/2}$ < 2 minutes) to GLP-1-(9-36)-amide and GLP-1-(9-37) (Deacon et al. 1995). GLP-1 exhibits biological functions in numerous tissues mediated through binding to its specific receptor, the GLP-1 receptor. In the pancreas it acts as an incretin hormone but also inhibits glucagon secretion (Nauck et al. 2002). Both actions are glucose-dependent. As a result of its impact on insulin and glucagon secretion, glucose production in the liver is lowered while glucose uptake and storage in peripheral tissues (fat, muscle) is increased. Additionally, GLP-1 triggers satiety, thus reduces calorie intake which was evaluated by intracerebroventricular as well as systemic application of GLP-1 (Turton et al. 1996; Flint et al. 1998). Further, glucagon-like peptide-1 reduces gastric emptying leading to a delayed nutrient transfer to the duodenum, resulting in a diminished rise of blood glucose levels. Surprisingly, the action of GLP-1 as an incretin hormone and its effect on gastric emptying act antidromic on total insulin secretion (Nauck et al. 1997). GLP-1 was found to exhibit mitogenic and anti-apoptotic functions on the β-cell in vitro and in vivo (Farilla et al. 2002; Farilla et al. 2003; Buteau et al. 2004). Moreover GLP-1 was reported to exhibit cardioprotection (Baggio & Drucker 2007).
Nearly sustained insulinotropic action of GLP-1 in type 2 diabetic patients revealed its therapeutic potential to correct the reduced incretin effect in type 2 diabetic patients mainly initiated by reduced insulinotropic action of GIP (Nauck et al. 1993).

2.2.6 Glucose-dependent insulinotropic polypeptide (GIP)

GIP is a single 42 amino acid peptide (Brown & Dryburgh 1971; Moody et al. 1984) which is highly conserved with more than 90% amino acid sequence homology comparing the human, bovine, porcine, mouse and rat GIP sequence (Yip & Wolfe

2000). Bioactive GIP itself is derived by proteolytic processing of its preprohormone precursor, 153-amino acids in length in humans (144-amino acids in length in rats) (Yip & Wolfe 2000). A signal peptide as well as a N-terminal peptide and a C-terminal peptide which functions are unknown so far flank the bioactive GIP (1-42). Studies performed in prohormone convertase (PC) 1/3 or PC2 knockout mice revealed PC1/3 to be responsible for processing of the proGIP protein. Moreover, different cell lines expressing either PC1/3 or PC2 and overexpressing preproGIP confirmed that PC2 can indeed mediate processing to GIP but PC1/3 seem to be mainly responsible for the release of bioactive GIP which is among other things related to the fact that PC2 was not found in intestinal GIP expressing cells (Ugleholdt et al. 2006). In rodents and humans, the GIP gene is expressed in stomach as well as in intestinal K-cells while in rats GIP was also found to be expressed in the submandibular salivary gland (Fehmann et al. 1995).

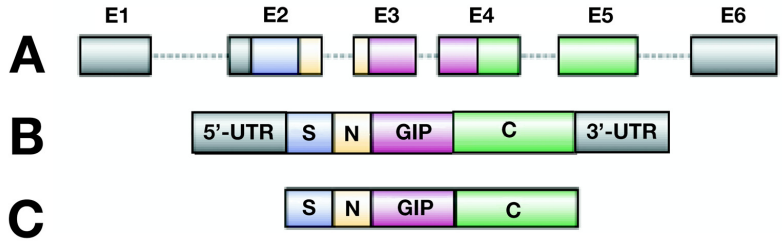

Figure 2.2: Generation of bioactive GIP

(A) proGIP gene, (B) proGIP mRNA, (C) proGIP protein, E1-E6: Exon 1 – Exon 6, S: signal peptide, N: N-terminal peptide, C: C-terminal peptide, figure modified from Baggio 2007.

2.2.7 GIP secretion, metabolism, degradation

GIP is synthesized in and released from enteroendocrine K-cells, the majority of which are located in the duodenum and the upper jejunum (Buffa et al. 1975; Thomas et al. 1977; Buchan et al. 1978). There are also some endocrine cells located in the mucosa of the upper small intestine where GIP and GLP-1 are colocalized and presumably secreted simultaneously (Mortensen et al. 2000; Mortensen et al. 2003; Theodorakis et al. 2006). However, endocrine cells that produce GLP-1 and GIP as well as cells that produce both peptides were found

throughout all regions of the rat, porcine and human small intestine (Mortensen et al. 2003; Theodorakis et al. 2006). Consistent with these findings, GIP mRNA was detected in the duodenum and small intestine by RT-PCR analyses and in situ hybridization (Usdin et al. 1993). The major secretion stimuli are glucose, few other mono- and disaccharides as well as triglycerides (Pederson et al. 1975; Ross & Dupre 1978; Cataland et al. 1974; Falko et al. 1975). More precisely, the rate of nutrient absorption is the decisive stimulus for GIP secretion. Depending on the assay used to measure total versus intact GIP, basal circulating GIP levels in humans range between 0.06 and 0.1 nmol/l and rise up to 0.2 - 0.5 nmol/l after a meal (Orskov et al. 1996; Vilsboll et al. 2001). Maximal circulating GIP concentrations are reached one to three hours after stimulation (Herrmann et al. 1995; Gallwitz et al. 2006) followed by a gradual decline. However, first rises of GIP are detected 15 minutes after ingestion of oral glucose or lipids, long before the ingested substrates are present in the gut. Therefore an involvement of the vagus nerve in the stimulation of GIP was discussed (Meier et al. 2002). This theory is put in doubt by the detection of glucokinase expression in the K-cells indicative for a glucose-sensing mechanism (Cheung et al. 2000). The half-life of intact biologically active GIP was reported to be less than two minutes in rodents (Kieffer et al. 1995) and 7-20 minutes in humans (Deacon et al. 2000; Gallwitz et al. 2006). Dipeptidyl peptidase-4 (DPP4) was clearly defined to be the primary enzyme responsible for degradation of both incretins by in vivo studies performed in humans and rats (Kieffer et al. 1995; Deacon et al. 2000). Bioactive peptides with N-terminal penultimate proline or alanine are good substrates for DPP-4 (Mentlein 1999). Thus, DPP-4 cleaves bioactive GIP (1-42) at the alanine 2 position, resulting in the N-terminally truncated biologically inactive GIP (3-42) fragment. DPP-4 is present in most vertebrate tissues, including endothelial cells of blood vessels and blood plasma (Mentlein 1999) suggesting, that the majority of incretin hormones is already inactivated once GIP and GLP-1 have reached portal circulation. The kidney was determined to play a major role in the final elimination of GIP and GLP-1 as patients suffering from chronic renal insufficiency revealed higher plasma GIP (3-42) and GLP-1 (9-36)-amide levels compared to control subjects (Meier et al. 2004). Further, GIP clearance was reduced in nephrectomized rats (Jorde et al. 1981). DPP-4 exists exceptionally concentrated in the kidney (Mentlein 1999). Studies in the anesthetized pig, measuring arteriovenous differences of GIP

levels across various organ beds, revealed an involvement of the liver and extremities besides the kidney in the elimination of exogenous intact GIP (Deacon et al. 2001).

2.2.8 The glucose-dependent insulinotropic polypeptide receptor (GIPR)

The GIP receptor (GIPR) was first cloned from a rat cerebral cortex cDNA library (Usdin et al. 1993). Cloning of the hamster (Yasuda et al. 1994), human (Gremlich et al. 1995; Yamada et al. 1995; Volz et al. 1995) and mouse (Miyawaki et al. 1999) GIPRs followed. The GIPR is a seven transmemebrane domain heterotrimeric G-protein coupled receptor consisting of three extracellular loops, three intracellular loops, an amino-terminal extracellular domain and an intracellular carboxyl terminus (Harmar 2001) and belongs to the subfamily B1 of G-protein coupled receptors. This group (Kolakowski 1994) also includes receptors like the GLP-1, GLP-2, glucagon, VIP, PACAP and GHRH receptor (Harmar 2001). The N-terminal extracellular domain extending to amino acid 132 (Gelling et al. 1997b) was found to be essential for ligand binding and selectivity, and the third intracellular loop turned out to be essential for G-protein coupling (Wheeler et al. 1993; Harmar 2001; Cypess et al. 1999; Hallbrink et al. 2001; Salapatek et al. 1999; Takhar et al. 1996). The majority of the C-terminal domain was found to be dispensable for signaling (Wheeler et al. 1999). The GIPR exhibits binding specificity for GIP, although some binding of Exendin-4, a GLP-1 receptor agonist, was noted at very high concentrations of 1-10 µM (Gremlich et al. 1995; Wheeler et al. 1993).

RT-PCR analyses detected mRNA of the GIPR in numerous tissues: pancreas, stomach, duodenum, proximal small intestine, fat, adrenal gland, several brain regions (telencephalon, diencephalon, brainstem, cerebellum, olfactory bulb and pituitary) (Usdin et al. 1993) and bone tissue (Bollag et al. 2000). No mRNA was found in spleen and liver tissue. In situ hybridization using tissue sections from adult rats as well as rat embryos (embryonic day 12, 17, 19) revealed the presence of GIPR mRNA in the pancreas, heart with particularly strong labelling of the cardiac endothelium, endothelium of major blood vessels, no clearly defined cells within bronchioles, inner layers of the adrenal cortex, adipose tissue and the epithelium of

the stomach, small and large intestine. Consistently, GIPR mRNA could not be detected in liver and spleen by in situ hybridization as was shown by RT-PCR analyses. In addition, in-situ hybridization of numerous brain regions was carried out to detect GIPR mRNA reaching the highest intensity in the olfactory bulb, cerebral cortex, ventral and dorsal hippocampus, mammilary bodies and the medial part of the inferior colliculus (Usdin et al. 1993).

2.2.9 GIPR signal transduction

GIP potentiates Ca^{2+}-dependent exocytosis of insulin. Binding of GIP to its receptor results in activation of a heterotrimeric stimulatory G-protein, followed by adenylate cyclase mediated cAMP accumulation and direct inhibition of ATP-dependent potassium channels (K_{ATP}) which leads to a depolarization of the β-cell membrane (Wheeler et al. 1995). Subsequently, mobilization of intracellular Ca^{2+} stores and activation of cell surface voltage-gated calcium channels to allow extracellular Ca^{2+} influx as well as activation of nonselective cation channels lead to an increase of intracellular Ca^{2+} levels (Wheeler et al. 1995). Closure of voltage-dependent (K_v) potassium channels and consequent reductions in K_v currents prevent repolarization of the β-cell. GIP also acts directly on insulin storage granule exocytosis by activation of the cAMP/PKA (protein kinase A) (Ding & Gromada 1997) and the PKA-independent cAMP/Epac2 modules (Kashima et al. 2001) in addition to phospholipase A_2 (PLA_2) (Ehses et al. 2001), protein kinase B (PKB) (Trumper et al. 2002; Trumper et al. 2001) and mitogen-activated protein kinase (MAPK) (Ehses et al. 2002). Recently, a role of GIP in the regulation of voltage-gated K-channel (K_v) expression on the β-cell surface could be identified in vitro and was supposed as a possible mechanism of GIP to modulate insulin secretion (Kim et al. 2005a).

2.2.10 Biological actions of GIP

2.2.10.1 Pancreatic actions of GIP

The major function of GIP is that of an incretin hormone. Following release from enteroendocrine cells (K-cells) in response to nutrient ingestion, GIP binds to its specific receptor on the β-cells and enhances glucose-dependent insulin secretion.

Initially, potentiation of insulin secretion by GIP was detected in the isolated perfused rat pancreas (Pederson & Brown 1978) as well as in dogs (Pederson et al. 1975) and humans (Dupre et al. 1973), but a distinct insulinotropic effect of GIP could only be observed in the presence of elevated glucose concentrations (Pederson et al. 1975; Pederson & Brown 1978; Nauck et al. 1986b). The glucose dependency of the insulinotropic GIP effects could be confirmed by stepwise hypo-, eu-, and hyperglycemic clamp experiments in combination with the infusion of GIP (Elahi et al. 1979; Kreymann et al. 1987; Nauck et al. 1993a). Hyperinsulinemia was shown to have no impact on GIP-stimulated insulin secretion (Andersen et al. 1978). Furthermore, GIP stimulates insulin gene transcription and protein synthesis in the β-cell (Fehmann et al. 1995; Wang et al. 1996) as well as the expression of components of β-cell glucose sensors (Wang et al. 1996). Also, GIP was discussed to exhibit proliferative and anti-apoptotic actions on the β-cell (see 2.2.10.2).

2.2.10.2 Proliferative and anti-apoptotic actions of GIP on the β-cell

As β-cell death is a major contributing factor to diabetes mellitus, an understanding of the underlying mechanisms that increase cell survival as well as protect β-cells against apoptosis is important. GIP was found to have antiapoptotic as well as proliferative functions on the β-cell. In INS-1 cells, GIP was determined to function as a mitogenic and anti-apoptotic factor by pleiotropic signaling being dependent on glucose metabolism and Ca^{2+} influx (Trumper et al. 2002; Trumper et al. 2001). In this context, pleiotropic stimulation of the mitogenic signaling modules PKA/CREB, MAPK and PI3K/PKB mediated by GIP and glucose was shown (Trumper et al. 2001). In another study, GIP was able to potentiate glucose (11 mM) mediated INS-1 cell proliferation to levels comparable to GH and GLP-1 (Ehses et al. 2003). It was also proposed that GIP is able to reverse caspase-3 activation in INS-1 cells mediated by inhibition of long-term p38 MAPK phosphorylation after cells were incubated in glucose- and serum-free media in the absence or presence of wortmannin (Ehses et al. 2003), an inhibitor of the PI3K/PKB pathway. Moreover, GIP was found to reduce apoptosis under glucolipotoxic conditions through down-regulation of *Bax* gene transcription via PI3K/PKB-mediated depletion of Foxo1 from the nucleus in INS-1 β-cells (Kim et al. 2005b). Similar protective effects of GIP could

be detected in wild-type C57BL/6 mouse islets but not in those from GIPR knockout ($GIPR^{-/-}$) mice (Kim et al. 2005b). Recently, GIP was shown to reduce biochemical markers associated with endoplasmatic reticulum (ER) stress in INS-1 cells treated with thapsigargin, a chemical inducer of ER stress (Yusta et al. 2006).

Only very limited information is available from in vivo studies. Infusion of GIP via a micro-osmotic pump into Vancouver diabetic fatty rats for two weeks, led to down-regulation of the pro-apoptotic *Bax* gene and up-regulation of the anti-apoptotic *Bcl2* gene (Kim et al. 2005b). $GIPR^{-/-}$ mice exhibited a paradoxical increase of relative β-cell area (referring to pancreas area) of ~45% (Pamir et al. 2003), whereas the total insulin content of pancreata and insulin mRNA levels in the fed state were significantly reduced compared to controls (Pamir et al. 2003). In another study, no histological abnormalities were found in the pancreas of $GIPR^{-/-}$ mice (Miyawaki et al. 1999). Additionally, $GIPR^{-/-}$ mice showed no aberrant glycemic excursions or insulin levels in an intraperitoneal glucose tolerance test, which would have pointed to changes in islet/β-cell mass (Miyawaki et al. 1999).

2.2.10.3 Extrapancreatic actions of GIP

2.2.10.3.1 Adipose tissue

Indicative for a biological function of GIP on adipose tissue is the fact that fat is a potent stimulus for GIP secretion in humans (Falko et al. 1975). Also, functional GIPRs were found to be expressed on rat adipocytes and 3T3-L1 cells (preadipocyte cell line) (Yip et al. 1998) and GIPR mRNA could be detected in adipose tissue (Usdin et al. 1993). In vitro studies, using cultured preadipocytes, revealed a dose-dependent enhancement of lipoprotein lipase activity by GIP (Eckel et al. 1979). Additionally, enhancement of insulin-stimulated fatty acid incorporation into triglycerides initiated by GIP could be shown in epididymal fat pads (Beck & Max 1983) and obese Zucker rats (Beck & Max 1987). Moreover, GIP stimulates fatty acid synthesis in explants of rat adipose tissue (Oben et al. 1991). Also, inhibitory effects of GIP on lipolytic glucagon action were identified in rat adipocytes (Dupre et al. 1976; Hauner et al. 1988). Interestingly, a high-fat diet did not lead to obesity in $GIPR^{-/-}$ mice being indicative for lipolytic effects of GIP (Miyawaki et al. 2002) (see 2.2.12.1).

2.2.10.3.2 Central nervous system

Findings on GIP expression in the central nervous system are controversial. GIP mRNA and protein were identified in the hippocampus (CA1–CA3 region and the dentate gyrus (DG), including the granule cell layer (GCL)) of rats by RT-PCR, quantitative real-time PCR, in situ hybridization and immunohistochemistry (Nyberg et al. 2005) while no GIP mRNA was detected anywhere in the rat brain using in situ hybridization (Usdin et al. 1993). GIPR mRNA and protein were observed in the hippocampus (Nyberg et al. 2005) as well as in several other brain regions, including cerebral cortex and olfactory bulb as was determined using RT-PCR and in situ hybridization (Usdin et al. 1993). Chronic intracerebroventricular infusion of GIP induced proliferation of hippocampal progenitor cells in rats in vivo as well as of adult-derived hippocampal progenitor cells cultured in vitro. This is in line with observations of a significantly lower number of newborn cells in the hippocampal dentate gyrus of $GIPR^{-/-}$ mice compared to non-transgenic control mice (Nyberg et al. 2005). Thus, according to the available data GIP might have a regulatory function in progenitor cell proliferation within the CNS.

2.2.10.3.3 Bone

Recently, an influence of GIP on bone tissue was discovered. GIPR mRNA and protein were detected by RT-PCR, Western blot analyses and indirect immunofluorescence in rat and human normal bone, osteoblast-like cell lines (Bollag et al. 2000) as well as in rodent osteoclast cells (Zhong et al. 2007). Application of GIP to osteoblast-like cells (SaOS2) resulted in elevated expression of collagen type-1 mRNA and an increase in alkaline phosphatase activity indicating anabolic actions of osteoblast-like cells (Bollag et al. 2000). GIP also increased bone mineral density in ovariectomized rats, which is a rodent model for postmenopausal osteoporosis (Bollag et al. 2001). Studies in $GIPR^{-/-}$ mice suggested an anabolic effect of GIP on bone mass and bone quality (Xie et al. 2005) which was supported by inhibitory effects of GIP on bone resorption determined in osteoclasts (Zhong et al. 2007). In correspondence to these findings, transgenic mice overexpressing GIP under the control of the metallothionein promoter were found to have increased bone mass (Xie et al. 2007). In humans, studies of the effects of long-term application of GIP on bone

turnover are pending. However, acute application has not shown to alter bone turnover in humans (Henriksen et al. 2003).

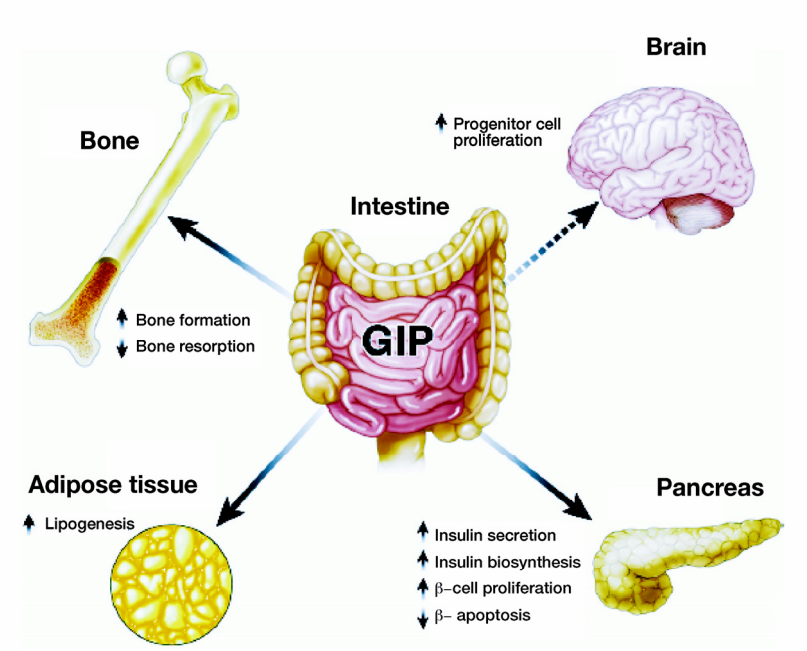

Figure 2.3: Biological actions of GIP, figure from Baggio 2007.

2.2.11 Incretin hormones in the context of type 2 diabetes mellitus

In type 2 diabetic patients, the incretin effect was found to be reduced to almost absent (Nauck et al. 1986a). Also, a substantial group (~50%) of first-degree relatives of type 2 diabetic patients showed a reduced incretin effect compared to control subjects but significantly higher GIP effects compared to type 2 diabetic patients in hyperglycemic clamp experiments combined with exogenous GIP infusion (Meier et al. 2001). In subjects with impaired glucose tolerance, the incretin effect is only partially affected (Muscelli et al. 2006). Further studies concentrated on searching for the cause leading to the impairment of the incretin effect by evaluation of GIP/GLP-1 secretion and action. Total and intact GLP-1 secretion were found to be decreased in type 2 diabetic patients especially two hours following meal ingestion (Vilsboll et al. 2001; Toft-Nielsen et al. 2001). According to the fact that the reduction in GLP-1 secretion of type 2 diabetic patients was relatively small and occurred late (two hours) in the response to nutrients, it was concluded that this cannot have a significant effect on insulin secretion. This assumption was supported among other

things by studies showing that antagonizing exogenous GLP-1 had minor effects on insulin secretion in healthy human subjects (Nauck et al. 2004). However, insulinotropic action of GLP-1 is vastly preserved in type 2 diabetic patients (Nauck et al. 1993) which is especially important for its therapeutic potential. In contrast, the insulinotropic action of GIP is greatly reduced to almost absent (Nauck et al. 1993; Vilsboll et al. 2002; Krarup et al. 1987; Elahi et al. 1994). Hyper- as well as hyposecretion of glucose-dependent insulinotropic polypeptide was found in type 2 diabetic patients, but most patients seemed to have normal GIP secretion (Vilsboll et al. 2001; Toft-Nielsen et al. 2001; Ross et al. 1977). Several mechanisms contributing to the reduced insulinotropic action of GIP in type 2 diabetic patients have been discussed. Decreased expression of the GIPR in the pancreatic islets was found by real-time RT-PCR in association with diminished β-cell response to GIP in Zucker diabetic fatty rats, a rodent model of type 2 diabetes (Lynn et al. 2003; Lynn et al. 2001). Recently, downregulation of the GIPR and surprisingly to a higher extent of the GLP-1 receptor initiated by hyperglycemia (exposition time four weeks) was shown in 90% pancreatectomized rats as well as in *db/db* mice, using semiquantitative radioactive multiplex PCR or real time RT-PCR and immunostaining. Downregulation of the incretin receptors came along with reduced insulin secretion in perifused islets of partially pancreatectomized rats following GIP/GLP-1 stimulation (Xu et al. 2007). Additionally, desensitization of the GIPR in type 2 diabetic patients was discussed. Such desensitization has been postulated due to the loss of insulinotropic activity of GIP after continuous intravenous infusion of GIP in rats (Tseng et al. 1996a) and in view of elevated GIP levels found in some studies in type 2 diabetic patients (Ross et al. 1977). Up to now this explanation seems not likely because no clear evidence of increased GIP levels in type 2 diabetic patients exists (Nauck et al. 2004). However, studies by Vilsboll et al., showing a relatively preserved incretin effect following a GIP bolus injection but impaired insulinotropic action of GIP after long-term GIP infusion (up to 240 minutes) during hyperglycemic clamp experiments would suggest underlying desensitization of the GIPR (Vilsboll et al. 2002). The presence of inactivating mutations within the exons of the GIPR gene was also considered as cause of the reduced insulinotropic effect of GIP. Actually, point mutations were found in the GIP receptor gene in human populations and some of them affected GIP signaling in cell models. However, it has

not been possible to consistently link these mutations to an increased frequency of type 2 diabetes (Almind et al. 1998; Kubota et al. 1996). Also, elimination rates of intact GIP and its primary metabolite, GIP (3-42), differed not significantly in type 2 diabetic patients compared to healthy subjects (Vilsboll et al. 2006). Interestingly, in human type 2 diabetic patients, a significant increase of L-cells as well as enteroendocrine cells containing GLP-1 and GIP but not of K-cells was detected in the duodenum compared to controls with normal glucose tolerance (Theodorakis et al. 2006). In conclusion, despite great efforts none of the suggested mechanisms resulting in a reduced to absent insulinotropic action of GIP has been surely proven so far.

2.2.12 Mouse models for studying the functions of the incretin hormone system

Several mouse models have been established to evaluate the impact of incretin hormones in general and in the context of type 2 diabetes mellitus.

2.2.12.1 GIPR knockout mice (GIPR$^{-/-}$)

The GIPR$^{-/-}$ mouse was established in 1999 by Miyawaki et al. (Miyawaki et al. 1999) on the C57BL/6 background. Knockout (KO) mice developed normally, showed normal blood glucose and insulin levels as well as insulin sensitivity in an insulin tolerance test but impaired glucose tolerance in an oral glucose tolerance test. No difference in glucose and insulin levels of GIPR$^{-/-}$ mice was seen following an intraperitoneal glucose tolerance test (IPGTT) compared to controls (Miyawaki et al. 1999; Hansotia et al. 2004; Pamir et al. 2003). GIPR$^{-/-}$ mice were shown to exhibit a paradoxical increase of relative β-cell area (referring to pancreas area) of ~45% whereas the total insulin content of pancreata and insulin mRNA levels in the fed state were significantly reduced compared to controls. Elsewhere, no histological abnormalities were found in the pancreas of GIPR$^{-/-}$ mice (Miyawaki et al. 1999). Additionally, GIPR$^{-/-}$ mice showed no changes in islet histology and endocrine cell distribution (Pamir et al. 2003). Interestingly, GIPR$^{-/-}$ mice did not develop insulin resistance and obesity in response to a high-fat diet fed from 7-50 weeks of age

compared to controls. Fat was found to be used as the preferred energy substrate in these mice and thus it was not efficiently accumulated in adipocytes (Miyawaki et al. 2002).

Recently, female GIPR$^{-/-}$ mice, evaluated between one and five months of age, showed that GIP modulates bone growth and bone turnover. GIPR$^{-/-}$ mice revealed significantly lower bone mineral density (BMD), bone mineral content (BMC), bone area (reflecting bone size), abnormal bone architecture (abnormal trabecular structure, decreased trabecular bone volume and bone connectivity) as well as impaired biomechanical properties and alterations in bone turnover (alkaline phosphatase and osteocalcin, biochemical markers for bone formation, were decreased in KO mice) compared to controls. However, reduction in BMD varied depending on the skeletal site and the age of the mice and differences became less apparent with age. On the basis of these results an anabolic effect of GIP on bone mass and bone quality was concluded and it was suggested that GIP might be a hormonal link between nutrient ingestion and bone formation (Xie et al. 2005).

Chronic intracerebroventricular infusion of GIP revealed reduced numbers of new proliferating cells in the hippocampal dentate gyrus of GIPR$^{-/-}$ mice leading to the assumption that GIP may be involved in neural progenitor cell proliferation (Nyberg et al. 2005). Islets from GIPR$^{-/-}$ mice were shown to exhibit increased sensitivity to exogenous GLP-1 which is indicative for a compensatory mechanism of the GLP-1/GLP-1 receptor axis (Pamir et al. 2003).

2.2.12.2 GLP-1 receptor knockout mice (GLP-1R$^{-/-}$)

GLP-1 receptor knockout mice revealed impaired glucose tolerance in an oral and intraperitoneal glucose tolerance test, being more pronounced in male than in female GLP-1R$^{-/-}$ mice. Fasting blood glucose levels were inconsistently elevated in male and female GLP-1R$^{-/-}$ mice determined at different age brackets on the CD1 background (Scrocchi et al. 1996), but turned out to be normal on the C57BL/6 background (Hansotia et al. 2004). Also, bypassing the incretin effect with an IPGTT led to elevated blood glucose levels, but not in all studies to reduced insulin levels of GLP-1R$^{-/-}$ mice (Hansotia et al. 2004; Scrocchi et al. 1996; Preitner et al. 2004). No changes in total β-cell volume and numbers were found and the insulin and glucagon

content of the pancreas were similar compared to controls. However, alterations in islet topography with α–cells being more centrally located than in controls and reduced formation of large β-cell clusters were determined in KO mice compared to controls (Ling et al. 2001). Despite evidence that GLP-1 is a potent inhibitor of short-term food intake, GLP-1 mice exhibit normal body weight and food intake (Scrocchi et al. 1996). The search for compensatory mechanisms of the GIP/GIPR axis in GLP-1R$^{-/-}$ knockout mice revealed increased GIP levels following oral glucose challenge as well as increased GIP stimulated insulin release from the perfused pancreas or isolated islets (Flamez et al. 1999; Pederson et al. 1998).

2.2.12.3 Double incretin receptor knockout mice (DIRKO)

Double incretin receptor knockout mice (DIRKO) lacking both a functional GIPR and a functional GLP-1R were found to exhibit more severe glucose intolerance than the individual mutants following oral glucose challenge. Similar to mice lacking a functional GLP-1 receptor, DIRKO mice exhibited abnormal glycemic excursions after an intraperitoneal glucose load. As in single incretin receptor knockout mice (SIRKO) mice, insulin sensitivity was unchanged compared to controls. Total pancreatic insulin content in the fasted state was normal and no apparent difference in the number and size of islets was seen compared to controls. Also, no differences were detected in growth, but DIRKO mice revealed increased food intake over a 24-h time period compared to control mice. Thus, disruption of both incretin receptors did not result in an overt diabetic phenotype indicated by normal fasting blood glucose levels (Hansotia et al. 2004; Preitner et al. 2004).

2.2.12.4 GIPR^{dn} transgenic mice

GIPR^{dn} transgenic mice expressing a dominant-negative GIPR under the control of the rat insulin 2 promoter show an overt diabetic phenotype due to a disturbed development of the endocrine pancreas. As early as three weeks of age, transgenic mice reveal severe glucosuria and hyperglycemia coming along with severe hypoinsulinemia from 30 days of age onwards. Immunohistochemical staining of the four principal islet cell hormones (insulin, glucagon, somatostatin, pancreatic polypeptide) revealed marked alterations of islet composition, namely a shift towards

cells expressing glucagon and somatostatin. Quantitative stereological analyses of the endocrine pancreas demonstrated severe reduction of total islet and total β-cell volumes within the pancreas first detected in 10-day-old animals and showing a progressive character with increasing age. In addition, the total volume of isolated β-cells (single β-cells and small β-cell clusters) turned out to be significantly reduced in $GIPR^{dn}$ transgenic mice compared to controls, indicative for disturbed islet neogenesis (Herbach et al. 2005). Additionally, alterations in the kidney including renal and glomerular hypertrophy, glomerulosclerosis and tubulo-interstitial changes could be detected (Herbach 2002).

2.2.12.5 Glucose-dependent insulinotropic polypeptide transgenic mice

Transgenic mice overexpressing GIP under the control of a heavy-metal inducible mouse metallothionein promoter (Palmiter et al. 1993) were created to examine the effect of GIP overexpression on the skeleton. RT-PCR analyses revealed high GIP expression in multiple tissues, including lung, liver, kidney, intestine and pancreas, with significant but lower expression in the brain and the heart. GIP transgenic mice showed a significant increase in markers of bone formation (elevated osteocalcin levels) and a decrease in markers of bone resorption (decreased levels of pyridinoline crosslinks). In addition, significantly increased bone mass (bone mineral content and bone mineral density) as measured by densitometry and histomorphometry could be determined which is consistent with the biochemical data. GIP transgenic mice were found to have normal serum glucose and insulin levels (Xie et al. 2007). Evaluations on behaviour of GIP transgenic mice revealed that the GIP receptor plays a role in the regulation of locomotor activity and exploration (Ding et al. 2006).

2.3 The pig as an animal model in diabetes research

Currently, pig animal models represent only a minor fraction in biomedical research. For this purpose *rodentiae* (mice/rats) as well as *lagomorphae* (rabbits) are used (Bundesministerium für Ernährung, 2006). Readily achievable animal welfare, high cost effectiveness and good standardization of experimentation argue for the usage of these small animal species. However, experimentation results obtained from these small animal models may not always mimic the human conditions faithfully enough. In contrast, a pig model has numerous advantages compared to rodent models. First, a great advantage is the size of the pig, allowing the imaging of internal vessels and organs using standard imaging techniques in human medicine as well as the collection of larger blood volumes in order to perform studies similar to those accomplished in humans. A pig animal model also warrants sufficient tissue for sample collection post-mortem. Moreover, pigs can be trained. This allows the performance of tests in conscious, unstressed animals as well as tests in relation to ingestion of meals like an oral glucose tolerance test.

2.3.1 Compatibilities between humans and pigs

Most importantly, many of the pig's organ systems, as well as physiological and pathophysiological responses resemble those of the human.

Pigs and humans have a high degree of similarity of the skin and subcutaneous tissue (Benech-Kieffer et al. 2000; Meyer 1996; Qvist et al. 2000) which is especially interesting for subcutaneous drug administration like insulin administration in diabetic patients. The morphology and physiology of the digestive system of the omnivores pig and human are much alike. Both of them are highly dependent on dietary quality because symbiotic microorganisms play a minor role in modifying ingested nutrients (Miller & Ullrey 1987). Ingesta transit times and digestive effectiveness are comparable (Miller & Ullrey 1987). The porcine pancreas resembles the human pancreas in size, shape and position. Islets from adult pigs are more similar to adult human islets because islet structure in young pigs is more diffuse and the reticular capsule separating endocrine from exocrine tissue is less evident than in humans (Wieczorek et al. 1998; van Deijnen et al. 1992; Ulrichs et al. 1995). Of all types of

experimental xenotransplantations, porcine islet transplantation was estimated to be the closest to clinical application on a large scale. Clinical trials have already been reported (Rood & Cooper 2006). Interestingly, islet amyloid polypeptide (IAPP) is expressed predominantly in β-cells but also in some α- and δ-cells in pigs and in humans (Lukinius et al. 1996). In contrast to humans, pigs are not prone to form pancreatic amyloid plaques (Larsen & Rolin 2004). Pig and human islets show similar sensitivity to damage induced by hydrogen peroxide, nitric oxide and superoxide, but are more resistant than rat islets (Wacker et al. 1995). Porcine and human insulin differ by only one amino acid at position 30 of the B-chain. Porcine insulin has even been used for almost 80 years to treat human diabetes (Bromberg & LeRoith 2006). Also blood glucose levels of pigs and humans range within similar limits (pig: 70 – 115 mg/dl; human: 65 – 100 mg/dl) (Kraft 1999; Swindle 2007). Human GIP amino acid sequence differs from porcine GIP only at residues 18 (human: His → porcine: Arg) and 34 (human: Asn → porcine: Ser) (Moody et al. 1984; Jornvall et al. 1981), while the GLP-1 amino acid sequence is fully conserved in both species (Orskov 1992). Porcine GIP has already been used in numerous human studies (Krarup et al. 1987; Jones et al. 1987; Amland et al. 1985).

2.3.2 Pig animal models of diabetes mellitus

Pig animal models of diabetes mellitus developed either spontaneously or have been generated by selective breeding or chemical induction.

In the 1970s two lines of Yucatan minipigs with altered glucose tolerance (one line with enhanced and one line with impaired glucose tolerance) were established by selective breeding. Females of the strain with impaired glucose tolerance rapidly became obese and some developed insulin resistance and diabetes. However, glucose intolerance was not detected in the F7 generation making these pigs currently not available for further investigations (Phillips et al. 1982). Male Göttingen minipigs fed a high-fat high-energy diet became obese (increased weight and body fat) and developed increased blood glucose and insulin levels (Larsen et al. 2001) while female pigs became obese and revealed increased insulin secretion, following an intravenous glucose tolerance test (Johansen et al. 2001). Chineze Guizhou minipigs fed a high-fed high-sucrose diet for six months revealed elevated blood

glucose levels, decreased insulin sensitivity, impaired glucose tolerance as well as increased levels of total cholesterol, triglycerides, free fatty acids and serum TNFα/β without chemical destruction of the islets. Also, atherosclerotic lesions were present in the aorta of these pigs (Xi et al. 2004). Osabaw pigs which lived in genetic isolation for a long time are generally considered obese. Obesity is considered a risk factor for the development of type 2 diabetes. Fed a high-fat high-cholesterol diet, pigs exhibit more severe obesity, but also insulin resistance, glucose intolerance, dyslipidemia and hypertension and are considered as a model for the human metabolic syndrome (Dyson et al. 2006). Familial hypercholesterolemic pigs, carrying a missense mutation within the low density lipoprotein (LDL) receptor, which is inherited in an autosomal fashion, were reported to show hypercholesterolemia and develop severe coronary and abdominal aortic atherosclerosis, while being fed a low fat pig diet (Prescott et al. 1991; Prescott et al. 1995).

Chemical induction of diabetes in pigs is still the primary means. For this purpose, substances like Streptozotocin (STZ) and Alloxan are available. STZ induces DNA strand breaks and subsequently activates repair mechanisms that result in a reduction of cellular Nicotinamide Adenine Dinucleotide (NAD) and ATP-levels below physiological levels, which leads to β-cell death. The mechanism of action of alloxan is similar (Yamamoto et al. 1981). These substances have been used in several pig breeds. For example Sinclair minipigs, treated with alloxan and fed an atherogenic diet developed dyslipidemia and atherosclerotic lesions in the carotid artery (Dixon et al. 1999). Göttingen minipigs treated either with STZ or Alloxan in combination with nicotinamide which partially protects the islets, are considered to be a good model for studying the pathophysiology and agents for treatment of diabetes (Larsen et al. 2003; Kjems et al. 2001).

Thus, there are already several pig models available, showing metabolic abnormalities as they are present in human type 2 or type 1 diabetic patients as well as cardiovascular complications. Considering cardiovascular complications, it is especially useful that pigs develop coronary, aortic, iliac and carotid atherosclerosis in anatomical locations relevant to the human condition also recapitulating the histopathology seen in humans namely proliferative lesions consisting of smooth muscle cells, macrophages, lymphocytes, foam cells, calcification, fibrous caps, necrotic and apoptotic cells, plaque hemorrhage and expanded extracellular matrices

(Prescott et al. 1991; Prescott et al. 1995; Brodala et al. 2005; Hasler-Rapacz et al. 1994; Gerrity et al. 2001; Nichols et al. 1992).

3 Animals, Materials and Methods

3.1 Pigs

Pigs were housed under conventional conditions on a planar-fixed basement with straw litter. Animals were fed a commercial diet once daily. Water was offered ad libitum. All animals investigated in this study were hemizygous male and female transgenic pigs and non-transgenic littermate control animals. During all study procedures, animals were housed in single pens under controlled conditions. Animals were trained carefully in all experimental procedures before the start of experiments. All animal experiments were carried out according to the German Animal Protection Law (209.1/211-2531-54/02).

Table 3.1: Composition of the different diets

Deuka primo care was fed to piglets up to 25 kg; deuka porfina U was fed to growing and adult sows and boars; ME: metabolizable energy

	Deuka primo care	Deuka porfina U
MJ ME/kg	14.0	12.6
Crude protein %	16.0	17.0
Crude fat %	4.3	3.0
Crude fiber %	4.5	6.5
Crude ash %	4.6	5.5
Lysin %	1.35	0.9
Calcium %	0.65	0.85
Phosphorus %	0.55	0.55
Sodium %	0.2	0.2

3.2 Material

3.2.1 Apparatuses

Accu-jet® pro pipette controller	Brand, Wertheim
Analytical balance	Sartorius, Göttingen
AU 400 autoanalyzer	Olympus, Hamburg
Multipette® plus	Eppendorf, Hamburg

Axiovert 135 microscope	Zeiss, Oberkochen
Benchtop 96 tube working rack	Stratagene, La Jolla, USA
Incubator	Heraeus, Munich
Staining box according to Schiefferdecker	Roth, Karlsruhe
Glass case for glass rack	Roth, Karlsruhe
Agarose gel electrophoresis chamber	MWG-Biotech, Ebersberg
HM 315 microtome	Microm, Walldorf
Heating plate with magnetic stirrer	IKA process equipment, Staufen
Hitachi 911 autoanalyzer	Roche, Mannheim
Hybridization oven	H. Saur, Reutlingen
Gel documentation system	Intas, Göttingen
Labotec thermo-cell-transporter	Labotec, Bovenden-Göttingen
Microwave	Siemens, Munich
MS1 Minishaker	IKA process equipment, Staufen
NanoDrop-1000 spectrophotometer	NanoDrop Technologies, Wilmington, USA
pH-meter	WTW, Weilheim
Power Pac 300	Bio Rad, Munich
Precision® Xceed™ Glucometer	Abbott, Wiesbaden
Phosphorimager Storm 860	GE Healthcare, Munich
Scintillation counter LS6500	Beckman, Palo Alto, USA
Thermomixer 5436	Eppendorf, Hamburg
UV-Crosslinker	Biometra, Göttingen
LB 2111 γ-counter	Berthold, Bad Wildbad
Videoplan® image analysis system	Zeiss-Kontron, Eching

Thermocycler:

Biometra Uno Thermoblock	Biometra, Göttingen
Biometra TProfessional	Biometra, Göttingen
Mastercycler® gradient	Eppendorf, Hamburg

Centrifuges:	
Heraeus Megafuge 1.0R	Heraeus, Munich
Rotanta 96	Hettich, Tuttlingen
Table centrifuge with cooling (5417R)	Eppendorf, Hamburg

3.2.2 Consumables

Cavafix® Certo® central venous catheter	B. Braun, Melsungen
Centrifuge tubes (15 ml, 50 ml)	Falcon®, Becton Dickinson, Heidelberg
Culture flasks with filter	Nunc, Wiesbaden
Culture dishes (diameter 10 cm)	Nunc, Wiesbaden
Disposable syringes (2, 5, 10, 20 ml)	Codan Medical ApS, Roedby, Denmark
Disposable tubes for γ-counter	Sarstedt, Nümbrecht
Disposable plastic pipettes	Falcon®, Becton Dickinson, Heidelberg
Uni-Link embedding cassettes	Engelbrecht, Edermünde
Hybond-N+ Nylon membrane	GE Healthcare, Munich
MicroSpin™ S-300 HR Columns	GE Healthcare, Munich
Millex™-GP syringe driven filter unit® (0.22 µm)	Millipore, Billerica, USA
Monovette® blood collection system (Serum, EDTA)	Sarstedt, Nümbrecht
Multi-well plates for cell culture	Greiner bio-one, Frickenhausen
OP-Cover (60 x 90 cm)	A. Albrecht, Aulendorf
Parafilm® M	American Can Company, Greenwich, USA
PCR reaction tubes (0.2 ml)	G. Kisker GbR, Steinfurt
Perfusor® cable (50 cm)	B. Braun, Melsungen
Precision Xtra™ Plus blood glucose stripes	Abbott, Wiesbaden
Safe-Lock reaction tubes (1.5 ml, 2 ml)	Eppendorf, Hamburg

Skin adhesive spray	A. Albrecht, Aulendorf
Sterican® cannulas (18 G, 20 G)	B. Braun, Melsungen
3-way-Stopcock	Fresenius Kabi, Bad Homburg
Storage phosphor screen	Bio Rad, Munich
Vasco® OP Protect gloves	B. Braun, Melsungen
Vascocan® indwelling venous catheter	B. Braun, Melsungen
Vicryl (2-0) suture material	Ethicon, Norderstedt

3.2.3 Chemicals

Comment: unless otherwise noted, all chemicals were used in p.a. quality

Acetic acid (glacial acetic acid)	Roth, Karlsruhe
Agar, granulated	Difco, Detroit, USA
Agarose	Invitrogen, Karlsruhe
Ampicillin	AppliChem, Darmstadt
Bacto™ Trypton	BD, Heidelberg
Bacto™ Yeast Extract	Difco, Detroit, USA
Bromophenolblue	Serva, Heidelberg
Chloroform	Merck, Darmstadt
DEPC (Diethylpyrocarbonate)	Sigma, Deisenhofen
3,3´ diaminobenzidine tetrahydrochloride	KemEnTec, Copenhagen, Denmark
DTT (100 mM)	Invitrogen, Karlsruhe
EDTA	Merck, Darmstadt
Ethanol	Roth, Karlsruhe
Ethidiumbromide (solution: 1 %)	Merck, Darmstadt
Formaldehyde solution, 37%	Sigma-Aldrich, Deisenhofen
D-(+)-glucose	Sigma-Aldrich, Deisenhofen
Disodiumhydrogenphosphate	Merck, Darmstadt
Glucose 50% solution	B. Braun, Melsungen
Glycerine	Roth, Karlsruhe
Hydrochloric acid (1 N)	Merck, Darmstadt

Hydrochloric acid (25%)	Merck, Darmstadt
Hydrogen peroxide 35%	Roth, Karlsruhe
Kalium chloride	Merck, Darmstadt
Kaliumdihydrogenphosphate	Merck, Darmstadt
Magnesium chloride (25 mM)	Qiagen, Hilden
Magnesium chloride	Merck, Darmstadt
Magnesium sulphate	Merck, Darmstadt
0.9% NaCl solution	B. Braun, Melsungen
2-Propanol	Merck, Darmstadt
Spermidine	Sigma, Deisenhofen
Sodiumacetate-trihydrate	Merck, Darmstadt
Sodium chloride	Merck, Darmstadt
Sodiumdodecylsulphate	Merck, Darmstadt
Sodium hydroxide	Roth, Karlsruhe
Tris-(hydroxymethyl)-aminomethane	Roth, Karlsruhe
X-gal (5-bromo-4-chloro-3-indolyl-β-D-galactoside)	Invitrogen, Karlsruhe
Xylol	SAV LP, Flintsbach a. Inn

3.2.4 Antibodies, drugs, enzymes and other reagents

3.2.4.1 Antibodies

Polyclonal guinea pig anti-porcine insulin	Dako Cytomation, Hamburg
HP conjugated polyclonal rabbit anti-guinea pig IgG	Dako Cytomation, Hamburg

3.2.4.2 Drugs

Altrenogest (Regumate®)	Serumwerk Bernburg, Bernburg
Cefquinom (Cobactan®)	Intervet, Unterschleißheim
Glucagon (GlucaGen®)	Novo Nordisk, Mainz
hCG (Ovogest®)	Intervet, Unterschleißheim
Heparin-Sodium (25.000 IE/5 ml)	B. Braun, Melsungen
Ketamine hydrochloride (Ursotamin®)	Serumwerk Bernburg, Bernburg
Metamizol-Sodium (Vetalgin®)	Intervet, Unterschleißheim

PMSG (Intergonan®)	Intervet, Unterschleißheim
Xylazine (Xylazin 2%)	WDT, Garbsen

3.2.4.3 Enzymes

DNase I (10 U/µl)	Roche, Mannheim
Proteinase K (20 mg/ml)	Roche, Mannheim
Herculase® enhanced DNA Polymerase	Stratagene, La Jolla, USA
HotStar Taq Polymerase (5 U/µl)	Qiagen, Hilden
Restriction enzymes and -buffers	Fermentas, St. Leon Roth
Restriction enzymes and -buffers	New England Biolabs, Boston, USA
RNase-Inhibitor (20 U/µl)	Applied Biosystems, Foster City, USA
Ribonuclease A (RNase-A) (0.2 U/µl)	Roche, Mannheim
Superscript™ II Reverse Transcriptase (200 U/µl)	Invitrogen, Karlsruhe
Taq Polymerase (5 U/ml)	Qiagen, Hilden
T4 DNA Ligase (2000 U/µl)	MBI Fermentas, St. Leon Rot

3.2.4.4 Other reagents

α-[^{32}P]-dCTP	GE Healthcare, Munich
Blood & Cell Culture DNA Midi Kit	Qiagen, Hilden
dNTPs (dATP, dCTP, dGTP, dTTP)	MBI Fermentas, St. Leon Roth
Eukitt®	Electron Microscopy Sciences, Hatfield, USA
5 x first strand buffer	Invitrogen, Karlsruhe
Gel blotting paper (GB002) (Whatman-paper)	Schleicher & Schüll, Dassel
Gentamycine sulphate	Sigma-Aldrich, Deisenhofen
Jetquick Gel extraction Spin Kit	Genomed, Löhne
Lamb serum	Invitrogen, Karlsruhe
10 x ligation buffer	MBI Fermentas, St. Leon Roth
Linear acrylamide (5 mg/ml)	Ambion, Austin, USA
10 x PCR buffer	Qiagen, Hilden

Porcine Insulin RIA Kit	Millipore, Billerica, USA
Porcine serum	Dako Cytomation, Hamburg
Q-solution	Qiagen, Hilden
QIAquick® Spin Miniprep Kit	Qiagen, Hilden
Rabbit serum	MP Biomedicals, Illkirch, France
Random Primers (3 mg/µl)	Invitrogen, Karlsruhe
Rapid-Hyb buffer	GE Healthcare, Munich
Synthetic porcine GIP	Bachem, Weil am Rhein
Synthetic Exendin-4	Bachem, Weil am Rhein
TOP 10 chemically competent E.coli	Invitrogen, Karlsruhe
TRIZOL Reagent	Invitrogen, Karlsruhe
Vet-Sept® solution (10%)	A. Albrecht, Aulendorf
Wizard® Genomic DNA Purification Kit	Promega, Mannheim

3.2.5 Buffers, media and solutions

Comment: unless otherwise noted, in a Millipore machine de-ionized water was used as solvent which is termed aqua bidest.

3.2.5.1 DEPC water (0,1 % (v/v))

Dissolve 1 ml DEPC in 1000 ml aqua bidest. overnight while stirring. For inactivation of DEPC autoclave at least three times. Storage at room temperature.

3.2.5.2 DNaseI buffer

10 mM	Tris
10 mM	$MgCl_2$
pH 7.4	

3.2.5.3 PBS buffer

137 mM	NaCl
10 mM	Na_2HPO_4

2.7 mM	KCl
2 mM	KH_2PO_4

3.2.5.4 Proteinase-K solution

20 mg	Proteinase K
1 ml	Aqua bidest.

Aliquotet; storage at -20°C

3.2.5.5 TBS buffer (10 x)

90 g	NaCl
60.5 g	Tris
ad 1000 ml	Aqua bidest.

pH 7.6

3.2.5.6 TE-buffer

10 mM	Tris/HCl (pH 8.0)
1 mM	EDTA (pH 8.0)

3.2.5.7 Buffers for agarose gels

3.2.5.7.1 TAE buffer (50 x)

242 g	Tris
57.1 ml	glacial acetic acid
100 ml	EDTA 0.5 M (pH 8.0)
ad 1000 ml	Aqua bidest.

3.2.5.7.2 TAE running buffer (1 x)

20 ml	50 x TAE buffer
ad 1000 ml	Aqua bidest.

3.2.5.7.3 Loading buffer for DNA (6 x)

3 ml	glycerine
7 ml	aqua bidest.

1 point of a
spatula bromophenolblue
Aliquotet, storage at -20°C

3.2.5.8 Solutions for Southern blotting

3.2.5.8.1 Denaturation solution

0.5 M NaOH
1.5 M NaCl

3.2.5.8.2 Neutralization solution

1 M NaCl
0.5 M Tris/HCl (pH 8.0)

3.2.5.8.3 SSC buffer (20 x)

3 M NaCl
0.3 M Sodiumacetate-trihydrate
pH 7.0

3.2.5.8.4 Washing solution I

2 x SSC
0.1% SDS

3.2.5.8.5 Washing solution II

1 x SSC
0.1% SDS

3.2.5.9 Solutions for bacterial culture

3.2.5.9.1 Luria-Bertani (LB)-medium

10 g bacto trypton
5 g bacto yeast extract
10 g NaCl

ad 1000 ml Aqua bidest.

pH 7.0 (adjust with 5 M NaOH)

Autoclave, storage at room temperature

3.2.5.9.2 SOC medium

2%	bacto trypton
0.5%	bacto yeast extract
0.05%	NaCl
10 mM	$MgCl_2$
10 mM	$MgSO_4$
0.4%	glucose

$MgCl_2$, $MgSO_4$ and glucose were added after autoclaving

3.2.5.9.3 Agar-LB-plates

1000 ml	LB-medium
15 g	agar, granulated

After autoclaving solution was cooled down to 50°C under constant stirring on a magnetic stirrer before ampicillin (100 µg/ml) was added. Then the solution was effused in 90 mm petri dishes. Petri dishes were stored at 4°C overarm after hardening of the agar.

3.2.6 Oligonucleotides

RIP2 (sense):	5'-TAGTCGACCCCCAACCACTCCAAGTGGAG-3'
RIP2 (antisense):	5'-CAGCCCTAACTCTAGACTCGAGGGATCCTA-3'
$GIPR^{dn}$ (sense):	5'-TTTTTATCCGCATTCTTACACGG-3'
$GIPR^{dn}$ (antisense):	5'-ATCTTCCTCAGCTCCTTCCAGG-3'
Actin (sense):	5'-TGGACTTCGAGCAGAGATGG-3'
Actin (antisense):	5'-CCTCTACGCCAACACGGTG-3'

3.2.7 DNA molecular weight markers

Gene Ruler™ (1 kb DNA Ladder)	MBI Fermentas, St. Leon Roth
Lambda DNA/*Eco*RI + *Hin*dIII-Marker	MBI Fermentas, St. Leon Roth
pUC Mix Marker 8	MBI Fermentas, St. Leon Roth

3.3 Methods

3.3.1 Generation of the RIP2-GIPR^{dn} expression vector

3.3.1.1 Restriction digest

The utilized amount of DNA was incubated together with the restriction endonuclease, its recommended buffer at the recommended temperature for 90 minutes in a total volume of 20 µl. Usually, 10 units of the enzyme per µg DNA were used.

3.3.1.2 Ligation of DNA fragments

Ligation means the connection of the 3' hydroxy-end and the 5' phosphorus-end of a nucleic acid using an enzyme called ligase. Here, 100 ng vector DNA were incubated with a two to three times molar overage of insert DNA in a total volume of 20 µl together with 2 µl of T4 DNA Ligase and 2 µl 10 x ligation buffer for two hours at RT. The required amount of insert DNA was calculated as follows:

$$\text{Insert (ng)} = \frac{\text{ng vector} * \text{kb-size insert} * \text{molar (vector : insert) DNA ratio}}{\text{kb-size of the vector}}$$

3.3.1.3 Transformation of E. coli

A 100-µl aliquot of transformation-competent E. coli TOP10-cells stored at -80°C was slowly thawed. 1 µg of plasmid DNA or up to 10 µl of a ligation batch was added to the bacteria solution, gently mixed and incubated on ice for 30 minutes. After that, a

heat shock was applied for exactly 45 seconds followed by an incubation step of 2-3 minutes on ice. Subsequently, 800 µl of SOC medium (without antibiotics) were added to the transformation batch and the mix was incubated at 37°C for one hour on a thermoblock. The transformed bacteria were then plated with a bended sterile pasteur glass-pipette on agar-LB-plates (+ 50 µg/ml ampicillin) and incubated at 37°C overnight. After twelve to sixteen hours of incubation single colonies were visible.

3.3.1.4 Isolation of plasmid DNA from E. coli

Single colonies were picked with a sterile pipette tip and transferred in 3 ml of ampicillin containing LB-medium. Following incubation at 37°C for 8-10 hours on a shaking incubator, bacteria containing medium was centrifuged at 20,800 x g and 4°C for 10 minutes. Isolation of plasmid DNA was carried out using the QIAquick® Spin Miniprep Kit according to the manufacturer's instructions.

3.3.2 Lentiviral construct

The expression cassette consisting of the rat insulin 2 gene promoter (RIP2) and the cDNA of a human dominant-negative glucose-dependent insulinotropic polypeptide receptor ($hGIPR^{dn}$) was described previously (Herbach et al. 2005). The construct was cloned into the lentiviral vector LV-pGFP (Pfeifer et al. 2002) via the *Cla*I and *Sal*I restriction sites by Prof. A. Pfeifer and coworkers (Institute of Pharmacology and Toxicology, University of Bonn, Germany; Figure 3.1). Recombinant lentivirus was produced by Prof. A. Pfeifer and coworkers as previously described (Pfeifer et al. 2002).

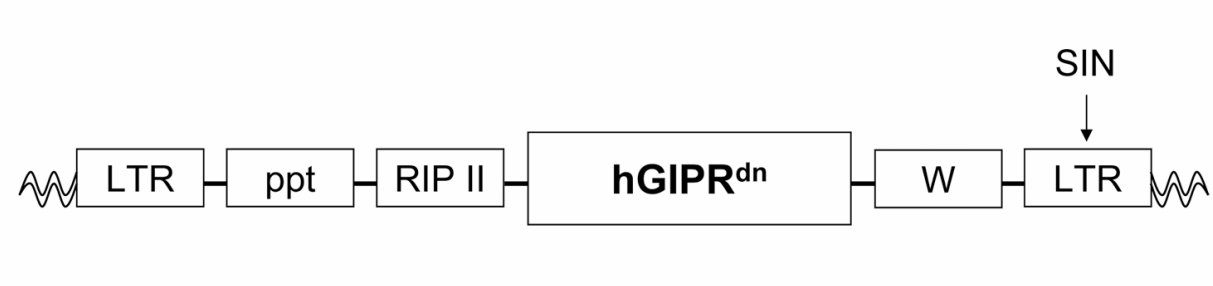

Figure 3.1: Lentiviral construct

The lentiviral vector (LV-GIPR^{dn}) carrying the cDNA of the human dominant-negative GIP-receptor (hGIPR^{dn}) under the control of the rat insulin 2 gene promoter (RIP2); LTR: long terminal repeat; ppt: polypurine tract; W: woodchuck hepatitis posttranscriptional regulatory element; wavy lines: pig genome; SIN: self-inactivating mutation.

3.3.3 Generation of transgenic animals

3.3.3.1 Zygote collection and injection of the lentiviral construct

Gilts, 6-7 months of age, were used as zygote donors. Superovulation was performed by an intramuscular injection of 1200 IU of pregnant mare serum gonadotropin (PMSG) (Intergonan®, Intervet) and 72 hours later ovulation was stimulated by an intramuscular injection of 750 IU of human chorionic gonadotropin (hCG) (Ovogest®, Intervet). Twenty-four and 36 hours after hCG injection, donors were artificially inseminated with $3x10^9$ sperms of a German Landrace boar suspended in 100 ml of a commercial BTS extender (Beltsville). Thirty-two to 34 hours after the first insemination, donor gilts were slaughtered and genital tracts were collected. After transport to the laboratory in a 37°C temperated box (Labotec thermo-cell-transporter, Labotec), corpora lutea were counted and oviducts were flushed into a polystyrene culture dish (diameter 10 cm, Nunc). The flushing medium consisted of PBS supplemented with 20% heat-inactivated lamb serum (Invitrogen) and 50 mg/l gentamicin sulphate (Sigma-Aldrich). Zygotes were collected followed by subzonal virus injection into the perivitelline space under an inverted microscope (Axiovert 135, Zeiss) using glass capillaries. Embryo transfer was performed the same day.

3.3.3.2 Embryo transfer

Six-month-old German Landrace gilts were used as recipients. Synchronization by oral administration of altrenogest (Regumate®, Serumwerk Bernburg) over a 15-day period was followed by administration of 750 IU PMSG. Ovulation was induced 72 hours later with 750 IU hCG. Embryo transfers were performed laparoscopically according to the procedure of Besenfelder et al. (Besenfelder et al. 1997) under general anesthesia using a combination of 2 ml per 10 kg body weight (BW) ketamine hydrochloride (Ursotamin®, Serumwerk Bernburg) and 0.5 ml per 10 kg xylazine (Xylazin 2%, WDT) injected intravenously. Thirty to 50 injected embryos were transferred into one oviduct of each recipient. Twenty-one to 25 days after the transfer, recipients were checked ultrasonographically for pregnancy.

3.3.4 Identification of transgenic animals

GIPR^{dn} transgenic pigs were identified by PCR as well as by Southern blot analysis. Thereby Southern blot analysis served not only for discrimination of transgenic pigs from wild-type animals, but also for determination of the number of integration sites of the transgene as well as determination of different integration sites.

3.3.4.1 Polymerase chain reaction (PCR)

3.3.4.1.1 Isolation of genomic DNA from ear punches

Ear punches were obtained from 2-day-old piglets and stored at –20°C until further processing. For isolation of genomic DNA the Wizard DNA Extraction Kit® (Promega) was used according to the manufacturer's instructions. In brief, ear punches, 3-5 mm in diameter, were transferred into 1.5 ml reaction tubes and incubated overnight at 55°C on a shaker after addition of the following mastermix:

Mastermix:	120 µl	0.5 M EDTA pH 8.0
	500 µl	Nuclei Lysis Solution
	17.5 µl	Proteinase K

The following day samples were centrifuged at 14,000 x g, 20°C to remove undigested constituents and the supernatant was transferred in new 1.5-ml reaction tubes. RNA removal was accomplished by addition of RNase-A. For protein precipitation, 200 µl protein precipitation solution were added followed by a centrifugation step. Afterwards DNA precipitation was carried out with 600 µl isopropanol and the DNA pellet was washed twice with 70% ethanol. Then the pellet was air-dried, resuspended in 50-100 µl DNA rehydration solution and incubated at 65°C on a shaker for one hour. To ensure that DNA has totally dissolved, DNA was stored at 4°C overnight.

The next day, DNA concentration was measured using a NanoDrop-1000 spectrophotometer (NanoDrop Technologies) and the concentration was adjusted to 100 ng/µl for PCR use.

3.3.4.1.2 PCR conditions

For identification of GIPR^{dn} transgenic pigs the following transgene-specific primers were used:

RIP2 (sense): 5'-TAGTCGACCCCCAACCACTCCAAGTGGAG-3'

RIP2 (antisense): 5'-CAGCCCTAACTCTAGACTCGAGGGATCCTA-3'

The amplification of so-called house-keeping genes which are being expressed independently of cell type, cell cycle or external influences serves as proof for the integrity of the isolated genomic DNA. Here, the β-actin gene was chosen and the following gene-specific primers were used:

β-actin (sense): 5'-TGGACTTCGAGCAGAGATGG-3'

β-actin (antisense): 5'-CCTCTACGCCAACACGGTG-3'

The PCR reactions with a total volume of 20 µl were prepared on ice in 0.2-µl reaction tubes as follows:

Table 3.2: Reaction batch RIP2-hGIPR^{dn} PCR

	RIP2-hGIPR^{dn}
10 x buffer (Qiagen)	2 µl
$MgCl_2$ (25 mM) (Qiagen)	1.25 µl
dNTPs (1 mM)	2 µl
Sense Primer (2 µM)	2 µl
Antisense Primer (2 µM)	2 µl
HotStar Taq DNA Polymerase (5 U/µl) (Qiagen)	0.1 µl
Aqua bidest.	9.65 µl
Template (100 ng/µl)	1 µl
Total volume	20 µl

Table 3.3: Reaction batch β-actin PCR

	β-actin
10 x buffer (Qiagen)	2 µl
$MgCl_2$ (25 mM) (Qiagen)	1.25 µl
Q-solution (Qiagen)	4 µl
dNTPs (1 mM)	1 µl
Sense Primer (2 µM)	1 µl
Antisense Primer (2 µM)	1 µl
Taq DNA Polymerase (5 U/µl) (Qiagen)	0.1 µl
Aqua bidest.	8.65 µl
Template	1 µl
Total volume	20 µl

The PCR conditions used are listed below:

Table 3.4: Reaction conditions RIP2-hGIPR^{dn} PCR

	RIP2-hGIPR^{dn}		
Denaturation	95°C	15 min	
Denaturation	94°C	1 min	35 x
Annealing	62°C	1 min	
Elongation	72°C	1 min	
Final elongation	72°C	10 min	

Table 3.5: Reaction conditions β-actin PCR

	β-actin		
Denaturation	94°C	4 min	
Denaturation	94°C	1 min	35 x
Annealing	58°C	1 min	
Elongation	72°C	1 min	
Final elongation	72°C	10 min	

Finally, the thermocycler cooled down to 4°C. For short-term storage samples were kept in the refrigerator and for long-term storage at –20°C. As positive control, plasmid DNA including the RIP2-GIPR^{dn} construct or genomic DNA of a previously genotyped transgenic pig was used. Aqua bidest. served as negative control (non-template control).

3.3.4.1.3 Agarose gel electrophoresis

The agarose gel electrophoresis allows separation of DNA strands according to their size. For separation of the DNA TAE-agarose gels were used. The gel solution was boiled in the microwave and thereafter ethidiumbromide, a dye which intercalates between the bases of nucleic acids whereby DNA can be visualized under UV-light,

was added at a final concentration of 0.5 µg/ml. Samples as well as a DNA molecular weight standard were mixed with 6x loading dye so that the progression of the gel electrophoresis could be estimated and pipetted into the gel slots before gel electrophoresis was started. All agarose gels were documented under UV-light (254 nm) using a gel documentation system (Intas).

3.3.4.2 Southern Blot

3.3.4.2.1 Isolation of genomic DNA from EDTA blood

Genomic DNA was isolated from 5 ml EDTA blood using the Blood & Cell Culture DNA Midi Kit® (Qiagen) according to the manufacturer's instructions.

3.3.4.2.2 Restriction digest

Genomic DNA (8 µg) was incubated overnight along with 30 U of the restriction enzyme *Apa*I, its appropriate buffer as well as 0.1 M spermidine in a total volume of 30 µl at 37°C. The next day another 10 U of the restriction enzyme were added per sample followed by an incubation step of one hour. Subsequently, 6x loading dye was added to all samples before they were used for agarose gel electrophoresis.

3.3.4.2.3 Gelelectorphoresis and transfer of genomic DNA

DNA fragments were separated using a 0.9% TAE agarose gel and the 1 kb ladder as DNA molecular weight standard. Gelelectrophoresis was discontinued as soon as the samples, visualized by the bromophenol blue containing 6 x loading dye, had been reached the end of the gel and documented under UV-light using a gel documentation system. After that the gel was pivoted in 0.25 M hydrochloric acid for about 20 minutes depending on the color shift of the bromophenol blue bands to yellow. Then the gel was washed with aqua bidest. and incubated in denaturation solution until the color of the bands turned back to blue (around 45 minutes). Subsequently, the previously digested and separated genomic DNA was transferred to a positive loaded Nylon membrane (Nylon-N+, GE Healthcare) by capillary transfer. The assembly of a Southern blot is shown in Figure 3.2. After a transfer time

of 18-24 hours, the membrane was soaked in neutralization solution for five minutes and then air-dried. Cross linking of the transferred DNA with the membrane was accomplished under UV light (120 J/cm^2) before the membrane could be stored at room temperature until further processing.

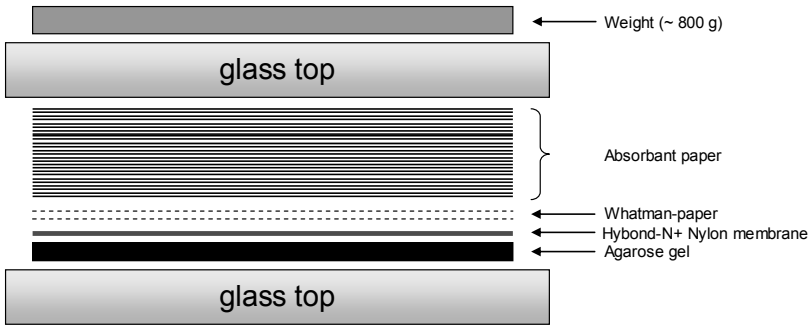

Figure 3.2: Schematic description of the assembly of a Southern blot.

3.3.4.2.4 Probe establishment

A 720-bp probe was created using the primers RIP2-sense and RIP2-antisense (see also chapter 3.3.4.1.2). Plasmid DNA containing the RIP2-hGIPR^{dn} construct in a concentration of 7 ng/µl served as template.

Table 3.6: Reaction batch probe Southern blot PCR

	Probe Southern blot
10 x Herculase buffer	10 µl
dNTPs (10 mM)	2 µl
Sense primer (100 µM)	0.5 µl
Antisense primer (100 µM)	0.5 µl
Aqua bidest.	83.5 µl
Herculase Taq Polymerase	0.5 µl
Template	3 µl
Total volume	100 µl

Table 3.7: PCR conditions probe Southern blot PCR

Probe Southern blot			
Denaturation	94°C	4 min	
Denaturation	94°C	1 min	34 x
Annealing	62°C	1 min	
Elongation	72°C	3.03 min	
Final elongation	72°C	10 min	

The PCR product was applied to a 1% TAE-agarose gel after addition of 20 µl 6x loading dye. Then, the designated band was excised using a scalpel blade and DNA was extracted from the gel using the Jetquick Gel Extraction Spin Kit according to the manufacturer's instructions. Then 2 µl of each extracted DNA sample as well as of the molecular weight standard Lambda/ *Hind*III + *Eco*RI were loaded on a 1% TAE agarose gel. DNA concentration was estimated by comparison of the band intensity of the DNA samples with the different band intensities of the known DNA concentration of the molecular weight standard Lambda/ *Hind*III + *Eco*RI.

3.3.4.2.5 Radioactive labeling of the probe

50-70 ng of the probe were radioactively labeled with 50 *µ*Ci α-[^{32}P]-dCTP (GE Healthcare) using the Rediprime II Random Prime Labeling System® according to the manufacturer's instructions. Random priming is a method to label DNA. Here previously denatured single strand DNA is hybridized with oligonucleotides of accidental sequence. The labeling is carried out by the integration of radioactive nucleotides. The Klenow fragment of Polymerase I is used as Polymerase. All not incorporated nucleotides are removed with a MicroSpin™ S-300 HR column. Nuclear radiation per minute (cpm: counts per minute) is measured using a scintillation counter. For this 5 µl of a 1:100 dilution of the labeled probe were utilized. The cpm value per µl of the labeled probe was calculated according to the following formula where Cerenkov is a correction factor for the calculation without scintillation liquid:

cpm/µl = cpm * 20 (dilution) * 1.55 (Cerenkov)

3.3.4.2.6 Hybridization, washing and signal detection

Prior to hybridization the Nylon membrane was prehybridized in Rapid-Hyb buffer® for two hours at 65°C in a hybridization oven. The hybridization was carried out overnight also at 65°C. For this, the labeled probe was utilized in a concentration of 2 x 10^6 cpm per µl Rapid-Hyb buffer®. The adequate amount of probe was denatured for five minutes at 95°C, chilled on ice and added to the prehybridization solution. The following day three washing steps were performed to remove nonspecific bound radioactivity: 1 x washing solution I for 20 minutes (RT); 2 x washing solution II for 20 minutes (65°C). Blots were exposed in a Phosphor-Imager cassette and visualized with a Phosphor-Imager (Storm 860).

3.3.4.2.7 Stripping of the membrane

Before application of another probe the previously used probe was removed by stripping of the membrane. For this, the moist Nylon membrane was transferred to a hybridization glass tube filled with boiling hot 0.1% SDS solution. After ten minutes the solution was renewed and the glass tube rolled until it had reached room temperature. Then the membrane was either immediately reused or air-dried.

3.3.5 Expression analysis by Reverse Transcriptase-PCR (RT-PCR)

Expression of the $GIPR^{dn}$ transgene on RNA level was investigated in porcine islets of Langerhans.

3.3.5.1 Isolation of total RNA from porcine islets of Langerhans

Total RNA was extracted using TRIzol® Reagent, a monophasic solution of phenol and guanidinium isothiocyanate, according to the manufacturer's instructions. Therefore, porcine islets of Langerhans (transgenic animals: 4,000-5,000 IEQ; wild-type animals: 10,000 IEQ) in culture media were centrifuged at 350 rpm (Rotanta 96; Hettich) for three minutes, the supernatant was discarded and the pellet resuspended in 1 ml TRIzol® Reagent. A former washing step with PBS was neglected because this could have led to an elevated mRNA degradation. Linear acrylamide was used as coprecipitate (5 µg per sample) because of the small number of islet equivalents

available per sample, especially in the transgenic animals. Quantification of total RNA was conducted using a NanoDrop-1000 spectrophotometer.

3.3.5.2 DNaseI digest and reverse transcription

In order to eliminate a possible DNA contamination of the RNA sample, about 1.4 µg of total RNA were incubated with 20 U of DNaseI in a total volume of 20 µl at 37°C for 30 minutes. The enzyme was inactivated at 75°C for ten minutes.

Total RNA	x µl (= 1.4 µg)
DNaseI reaction buffer	2 µl
DNaseI, RNase-free	2 µl
Deionized water	ad 20 µl

The RNA was quantified again using a NanoDrop-1000 spectrophotometer and 400 ng of total RNA were used for reverse transcription with the SuperScript™ II Reverse Transcriptase (Invitrogen) in a total volume of 20 µl.

Random Primers (3 µg/µl)	1 µl
dNTPs (10 mM)	1 µl
RNA, DNaseI digested (400 ng)	x µl
Deionized water	ad 12 µl
→ Incubation 5 min, 65°C	
→ chill on ice	

5 x first strand buffer	3 µl
DTT (100 mM)	2 µl
RNase OUT	1 µl
→ Incubation 2 min, 25°C	

5 x first strand buffer	1 µl
SuperScript™II RT (200 U/µl)	1 µl
→ Incubation 10 min, 25°C	

→ Incubation 50 min, 42°C

→ Incubation 15 min, 70°C

Following the inactivation of the enzyme at 70°C, the cDNA was chilled on ice, centrifuged and stored at -20°C until further processing. The integrity of the DNaseI digest was tested by a minus RT reaction of all samples. Both, RNA of all three wild-type animals and RNA of the transgenic pigs were pooled in two separate reaction tubes and reverse transcription was performed according to the previously described protocol. Instead of Superscript^{TM}II Reverse Transcriptase, 1 µl of deionized water was added.

3.3.5.3 RT-PCR

For determination of the transgene expression, the following transgene-specific primers were applied:

GIPR^{dn} (sense): 5'-TTTTTATCCGCATTCTTACACGG-3'

GIPR^{dn} (antisense): 5'-ATCTTCCTCAGCTCCTTCCAGG-3'

As template 2 µl of the cDNA were set in the following PCR-reaction:

Table 3.8: Reaction batch GIPR^{dn} RT-PCR

10 x buffer (Qiagen)	2 µl
$MgCl_2$ (25 mM) (Qiagen)	1.25 µl
dNTPs (1 mM)	2 µl
Sense Primer (2 µM)	2 µl
Antisense Primer (2 µM)	2 µl
HotStar Taq DNA Polymerase (5 U/µl) (Qiagen)	0.1 µl
Aqua bidest.	8.65 µl
Template (cDNA)	2 µl
Total volume	20 µl

Table 3.9: PCR conditions GIPR^{dn} RT-PCR

Denaturation	95°C	15 min	
Denaturation	94°C	1 min	35 x
Annealing	62°C	1 min	
Elongation	72°C	1 min	
Final elongation	72°C	10 min	

The β-actin PCR reaction batch and conditions were used as described in Table 3.3 and Table 3.5. Gel electrophoresis for visualization of the PCR result was carried out as described in 3.3.4.1.3.

3.3.6 Analysis of glucose metabolism

The glucose metabolism was analyzed through baseline parameters like blood/serum glucose and serum fructosamine determination as well as through different provocation assays, i.e., oral glucose tolerance test (OGTT), intravenous glucose tolerance test (IVGTT), GIP or Exendin-4 stimulation test and glucagon stimulation test (GST).

3.3.6.1 Blood glucose and serum fructosamine levels

For determination of blood glucose levels in pigs, a small drop of blood was collected from the ear vein with a lancet. This method causes minimal stress for the animals. Blood glucose was immediately determined using a plasma calibrated Precision® Xceed™ Glucometer (Abbott) with Xtra™ *Plus* control stripes (Abbott).

Blood samples for determination of serum fructosamine levels were taken from the jugular vein in restrained animals as this parameter is not influenced by stress and a larger volume of blood is needed. After an incubation period of 20 minutes at room temperature, serum was separated by centrifugation (20 minutes, 10,000xg) and stored at -80°C until assayed. Fructosamine levels were determined in the Medical Small Animal Clinic (LMU, Munich), using a Hitachi 911 autoanalyzer (Roche) and adapted reagents (Roche). Both parameters were analyzed once in unfasted pigs

before weaning and several times in fasted pigs (18-hour fasting period) after weaning. The number of animals investigated included five transgenic animals as well as five non-transgenic littermate controls.

3.3.6.2 Preliminary work for the provocation tests

During all study procedures, animals were housed in single pens under controlled conditions. At the beginning of all provocation tests, animals were well trained and accustomed to the person conducting the analyses in order to generate an environment with as minimal stress as possible. Additionally, pigs were trained to eat food supplemented with glucose so they would eat glucose within the preset time-frame during an OGTT.

3.3.6.3 Non-surgical implantation of a central venous catheter

One central venous catheter was inserted non-surgically in 5-month-old pigs used for an oral glucose tolerance test (OGTT). The procedure was performed by a modified method of Matte (Matte 1999) under general anesthesia, using a combination of 2 ml per 10 kg BW ketamine hydrochloride (Ursotamin®, Serumwerk Bernburg) and 0.5 ml per 10 kg BW xylazine (Xylazin 2%, WDT) injected intravenously. Pigs were restrained in dorsal recumbency with the head downwards at an angle of approximately 30° with the table. One jugular grove was shaved, washed carefully with Vet-Sept® solution (10%) and disinfected with alcohol (70%). A central venous catheter (Cavafix®Certo®, B. Braun Melsungen) was aseptically placed into the external jugular vein according to the manufacturer's instructions. External fixation was carried out by a single suture of adhesive tape, placed around the catheter, to the skin. Further, the catheter was covered with sterile gauze and adhesive tape up to the withers level where it was coiled in a pouch to provide easy access. An antibiotic (Cobactan® 2.5%, Intervet) was administered once (0.5 ml/10 kg BW) after catheter placement. The catheter was flushed with 250 IU heparin/ml 0.9% isotonic NaCl solution (Heparin-Natrium, B. Braun, 0.9% NaCl, B. Braun) once daily.

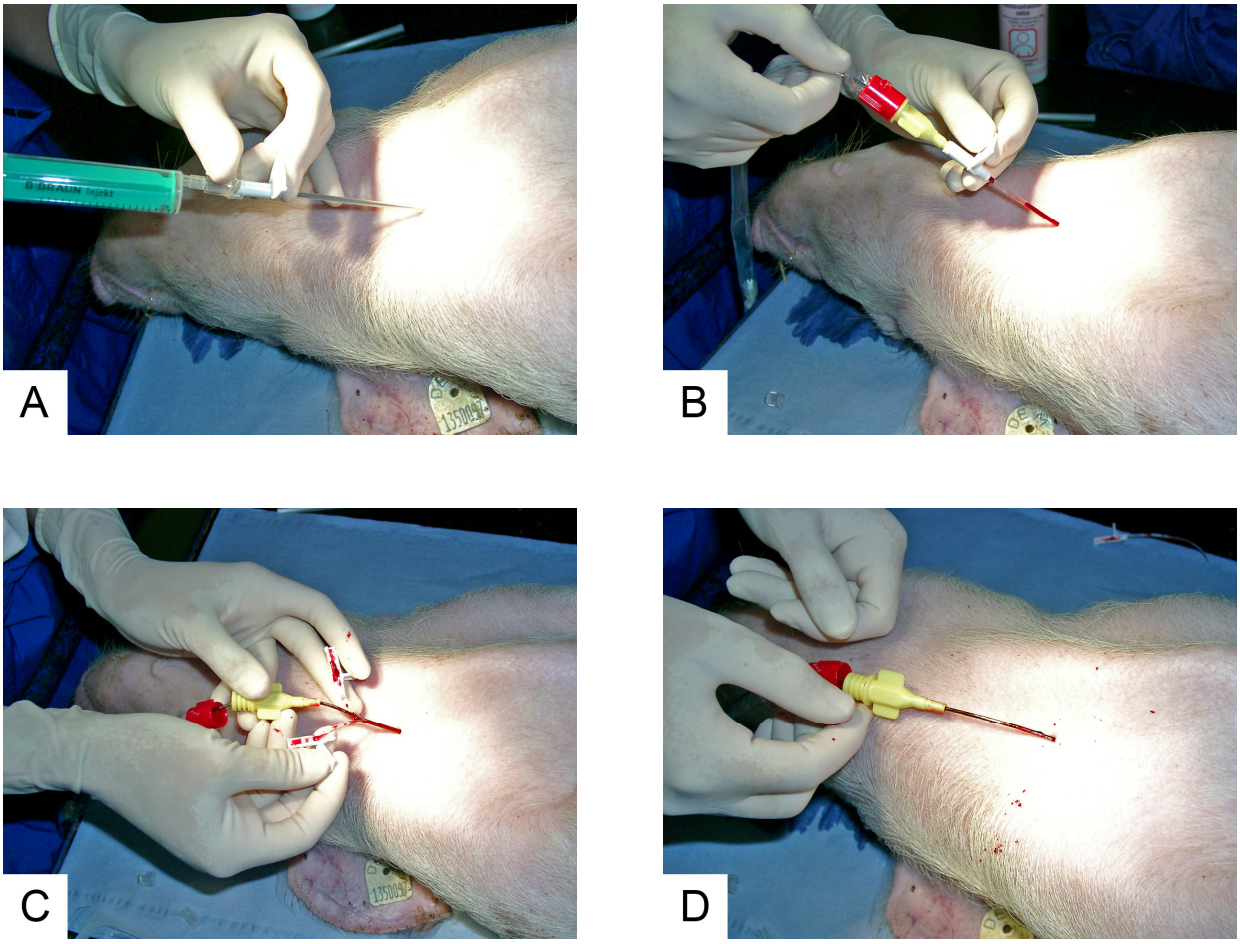

Figure 3.3: Non-surgical placement of a central venous catheter

(A) puncture of the external jugular vein with a puncture cannula under aspiration; after successful puncture removal of the steel cannula; **(B)** insertion of the catheter through the guiding plastic cannula; **(C)** removal of the guiding plastic cannula by splitting the cannula in two parts; **(D)** Cavafix® Certo® central venous catheter placed in the external jugular vein; part of the catheter outside of the vein surrounded by a plastic protection cover.

3.3.6.4 Surgical placement of a central venous catheter

For accomplishment of the intravenous glucose tolerance test as well as the glucagon stimulation test and GIP/Exendin-4 stimulation test, two central venous catheters (Cavafix® Certo®, B. Braun) were surgically inserted into the external jugular vein under general anesthesia, using a combination of 2 ml per 10 kg BW ketamine hydrochloride (Ursotamin®, Serumwerk Bernburg) and 0.5 ml per 10 kg BW xylazine (Xylazin 2%, WDT) injected intravenously. After aseptic preparation of the surgical field a skin incision, five centimeters in length, was made followed by the exposure of the external jugular vein. One holding suture was placed proximally and distally to the intended site of cannulation, a venotomy was made and the catheters were inserted 15 cm into the vein. A ligature was placed proximally and distally of the venotomy site and the incision was closed in two layers. External fixation of the catheters was performed as described in 3.3.6.3. Peri- and postsurgical analgesia were maintained by intramuscular injection of 1 ml/10 kg BW Metamizol (Vetalgin®, Intervet). Postsurgical infection of the surgical site was prevented by intramuscular injection of 0.5 ml/kg BW Cefquinom (Cobactan® 2.5%, Intervet) once daily for three days. The catheters were flushed with 250 IU heparin/ml 0.9% isotonic NaCl solution (Heparin-Natrium, B. Braun, 0.9% NaCl, B. Braun) once daily.

At the beginning of the study period, all animals had fully recovered from the surgical procedure as was indicated by the presence of normal behavior and food intake.

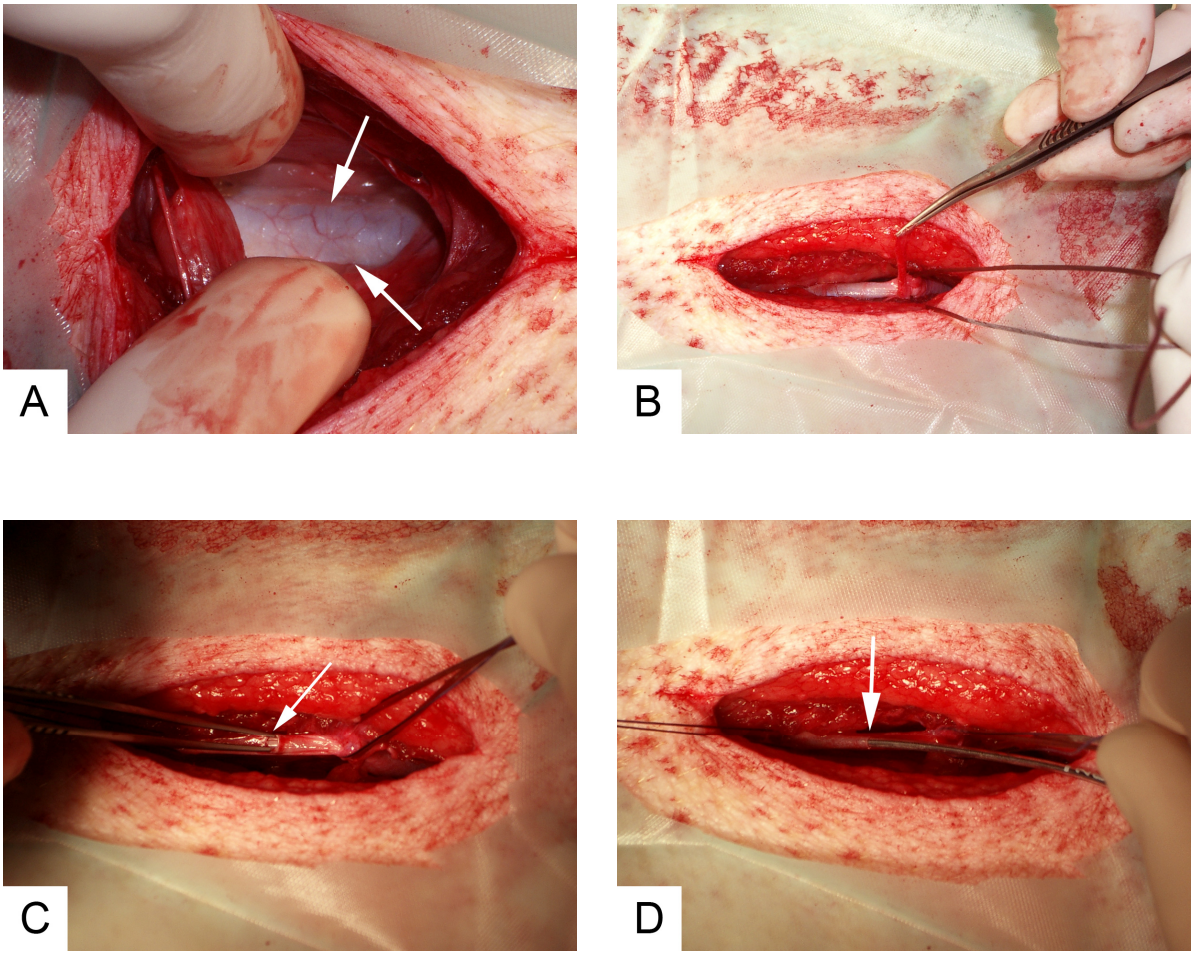

Figure 3.4: Surgical placement of a central venous catheter

(A) Exposed external jugular vein; white arrows indicate the outline of the vein; **(B)** external jugular vein advanced by a retention stitch; removal of the adjacent connective tissue; **(C)** vein after venotomy; **(D)** two Cavafix® Certo® catheters located in the external jugular vein.

3.3.6.5 Oral glucose tolerance test

The OGTT was performed in 5-month-old non restrained freely moving animals. After an 18-h overnight fast, animals were fed 2 g/kg BW glucose (Larsen et al. 2003) mixed with 100 g of commercial pig fodder. The meal was eaten from a bowl under supervision. Blood samples were obtained from the jugular vein catheter at -15, -5, 0, 15, 30, 45, 60, 90, 120, 150 and 180 minutes relative to the glucose load. Blood glucose was immediately determined using a Precision® Xceed™ Glucometer (Abbott). For insulin measurement, blood was collected in serum monovettes and

immediately put on ice. Separation of serum by centrifugation (20 minutes, 10,000 xg) was followed by storage at -80°C until samples were assayed. Serum insulin levels were determined using a porcine insulin radioimmunoassay kit (Millipore) as described in 3.3.6.10.

3.3.6.6 Intravenous glucose tolerance test

The IVGTT was performed in pigs 8 weeks, 7 month (28-36 weeks) and 10 month (45 weeks ± 2 weeks) of age. After an 18-h overnight fast, a bolus injection of concentrated 50% glucose solution (0.5 g glucose/kg BW) was administered (Kobayashi et al. 2004) through the central venous catheter number one. Subsequently, catheter one was flushed with 40 ml of 0.9% isotonic NaCl solution. Blood was collected through catheter number two at -15, -5, 0, 1, 3, 5, 10, 20, 30, 40, 50, 60, 120 and 180 minutes relative to the glucose load in 7- and 10-month-old pigs and at -15, 0, 1, 5, 10, 20, 30, 40, 60 minutes relative to the glucose load in 8-week-old animals. For serum glucose and insulin measurements, blood was collected in serum monovettes and immediately put on ice. Separation of serum by centrifugation (20 minutes, 10,000 xg) was followed by storage at -80°C until samples were assayed. Serum glucose levels were measured using an AU 400 autoanalyzer (Olympus). Serum insulin levels were determined by RIA as described in 3.3.6.10.

3.3.6.7 GIP stimulation test

The GIP stimulation test was performed in 8-week- and 7-month-old (28-36 weeks) non-restrained freely moving animals. Following an 18-hour fasting period, 0.5 g/kg BW of 50% glucose solution (Kobayashi et al. 2004) were administered as a bolus through a central venous catheter. Three minutes later, 20 pmol/kg BW of synthetic porcine GIP (Bachem) were mixed with 5% porcine serum in 5 ml of 0.9% NaCl and immediately administered intravenously. Blood samples were collected at -10, 0, 1, 6, 9, 11, 13, 18, 23, 28, 33, 48 and 60 minutes relative to the glucose load in 7-month-old pigs and at -10, 0, 1, 5, 10, 13, 18, 20, 23, 30, 40 and 60 minutes relative to the glucose load in 8-week-old pigs. Sample handling as well as serum glucose and serum insulin determination was performed as described in 3.3.6.6. The day before the GIP stimulation test, an IVGTT using 0.5 g/kg BW of 50% glucose solution was

performed and serum glucose and insulin levels were determined at time points as indicated in 3.3.6.6.

3.3.6.8 Exendin-4 stimulation test

The Exendin-4 stimulation test was performed in 8-week- and 7-month-old (28-36 weeks) non-restrained freely moving animals. Following an 18-hour fasting period, 0.5 g/kg BW of 50% glucose solution (Kobayashi et al. 2004) were administered as a bolus through the central venous catheter. Three minutes later 10 pmol/kg BW of synthetic Exendin-4 (Bachem) were mixed with 5% porcine serum in 5 ml of 0.9% NaCl and administered immediately intravenously. Blood samples were collected at -10, 0, 1, 6, 9, 11, 13, 18, 23, 28, 33, 48 and 60 minutes relative to the glucose load in 7-month-old pigs and at -10, 0, 1, 5, 10, 13, 18, 20, 23, 30, 40 and 60 minutes relative to the glucose load in 8-week-old pigs. Serum glucose and serum insulin levels were determined as described in 3.3.6.6. Two days before the Exendin-4 stimulation test, an IVGTT using 0.5 g/kg BW of 50% glucose solution was performed and serum glucose and insulin levels were determined at time points as indicated in 3.3.6.6.

3.3.6.9 Glucagon stimulation test (GST)

The glucagon stimulation test evaluates insulin secretion in response to maximal stimulation by glucagon. In human medicine this test is routinely used to estimate the remaining β-cell reserve and therefore the need of exogenous insulin in diabetic patients. In the present study, GST was used to estimate the insulin secretory capacity of $GIPR^{dn}$ transgenic pigs compared to non-transgenic control animals. The test was performed in 45-week-old pigs on average. Animals were fasted overnight (18 hours) before administration of 1 mg of Glucagon (GlucaGen®, Novo Nordisk) through the central venous catheter number one. Immediately afterwards, the catheter was flushed with 20 ml of 0.9% isotonic NaCl solution. Blood samples were obtained at -10, -5, 0, 2, 4, 6, 8, 10, 15, 20, 25, 30, 35 and 40 minutes relative to the glucose load. Sample handling as well as serum glucose and serum insulin determination was performed as described in 3.3.6.6.

3.3.6.10 Determination of serum insulin concentrations by radioimmunoassay (RIA)

To analyze serum insulin levels over the course of an OGTT, GIP/Exendin-4 stimulation test, IVGTT and GST, a porcine insulin RIA kit (Millipore, Billerica), which is a competitive radioimmunoassay, was used according to the manufacturer's instructions. In this RIA, a fixed concentration of labeled tracer antigen (^{125}I labeled insulin) was incubated with a constant dilution of anti-porcine insulin antiserum such that the concentration of antigen binding sites on the antibody was limited. If unlabeled insulin in the form of a serum sample was added to this system, there was competition between labeled tracer and unlabeled insulin for the limited and constant number of binding sites on the antibody. Thus, the amount of tracer bound to antibody decreased as the concentration of unlabeled antigen increased. This was measured after separating antibody-bound from free tracer and counting the antibody-bound fraction in a γ-counter. A calibration or standard curve was set up with increasing concentrations of standard unlabeled insulin and from this curve the amount of insulin in unknown samples was calculated. All samples were measured in duplicate. Only duplicates with a coefficient of variance (CV) less than 10% were accepted.

3.3.7 Isolation of porcine islets of Langerhans

3.3.7.1 Islet isolation procedure

Pancreatic islets were isolated from GIPR^{dn} transgenic pigs (n=3; two females, one male; 220 kg) and littermate control pigs (n=3; three females; 220 kg). Pancreata were harvested from slaughtered pigs under semi-sterile conditions on four consecutive days. The organs were crudely dissected from fat, blood vessels and connective tissue and explanted *in toto*. Total warm ischemia time was five minutes. After canulating the major pancreatic duct with a Cavafix® Certo 18G catheter (B. Braun, Melsungen, Germany) the organs were transferred to ice-cold HBSS solution (pH 7.2; Cell Concepts, Umkirch, Germany), and shipped on ice to the laboratory where a final dissection of fat, blood vessels and connective tissue was performed. For separation of the left pancreatic lobe which was used for islet isolation, the small

incision at the basis of the lobe right before it fades to the rest of the organ was marked on one side of the lobe. To recover the same point on the opposite side of the lobe base, the distance between the previously described incision and the tip of the lobe was measured using a compass and the same distance was marked out on the other side of the lobe. The left pancreatic lobe was then separated using a sharp blade following an imaginary line connecting the two previously marked points. Subsequently, both parts were weighed and the rest of the pancreas lacking the left lobe was prefixed in 10% neutral buffered formalin for approximately six hours for subsequent stereological analyses (see also 3.3.8). The left lobe of the pancreas was then distended, via the catheter, with 200 ml of 20°C warm University of Wisconsin (UW) solution, containing 4 PZ units NB8 collagenase (Nordmark, Uetersen, Germany) per gram of organ and 0.7 DMC units neutral protease (Nordmark). The pancreata were digested using a modification of the half-automated digestion-filtration method previously described by Ricordi et al. and Heiser et al. (Ricordi et al. 1990; Heiser et al. 1994). In brief, the organ was cut into five pieces that were placed into the digestion chamber containing a stainless steel mesh with 500 µm pore size and four stainless steel marbles. The system was filled with UW solution that passed a heating circuit to maintain a stable temperature of 32-37°C during the digestion process. Samples were taken every minute from minute 15 onwards and stained with dithizone (Sigma, Taufkirchen, Germany) to monitor the degree of tissue digestion (see also 3.3.7.4.1) (Latif et al. 1988). The isolation process was stopped after 20-25 minutes by flushing the system with ice-cold HBSS that contained 25 mM KH_2PO_4 buffer and 13% heat-inactivated FCS (FCS; Cell Concepts) when the first islet, free of surrounding exocrine tissue, was detected in the biopsy. The digest was collected in plastic tubes, washed twice at 250 xg and stored for 1 hour on ice in 10% FCS and 50 mM nicotinamide-containing UW solution. The non-digested tissue from the digestion chamber was weighed and not considered for calculation of the isolation result.

Purification of the isolated islets from the digest was performed with the discontinuous OptiPrep™ density gradient (Progen, Heidelberg, Germany) in the COBE 2991 cell processor (short: COBE; COBE Inc., Colorado, USA) (Krickhahn et al. 2001; van der Burg & Graham 2003). The digest was washed at 200 xg, resuspended in 200 ml UW solution, mixed with 120 ml working solution (two times

concentrated UW solution, and the same amount of OptiPrep™ at a density of 1.206 g/ml) and loaded into the COBE. During centrifugation at 1,000 rpm, 96 ml of low-density solution (a mixture of working solution and UW solution with a density of 1.206 g/ml) and 120 ml UW solution were loaded into the COBE. After further centrifugation for five minutes at 1,000 rpm the COBE was unloaded. The first 50 ml were discarded; the remaining suspension was collected in fractions of 30 ml on ice. Purified islets were washed with UW solution, were resuspended and transferred to two 30-ml culture flasks (Greiner, Nürtingen, Germany) and were cultured overnight in 30 ml HAM'S F12 culture medium (Cell Concepts; supplemented with 10% FCS, 1% amphotericine B, 1% L-glutamine, 1% ampicilline/gentamycine and 50 mM nicotinamide) at 24°C and 5% CO_2 in air.

3.3.7.2 Determination of islet numbers

After enzymatic digestion and purification, islet numbers were determined. 100-µl islet samples (triplicates) were stained with dithizone (DTZ) for differentiation of islets of Langerhans and exocrine tissue and counted under an Axiovert 25 microscope (Zeiss, Oberkochen, Germany) with a calibrated grid in the eyepiece. Counted islets were grouped into size categories and converted into islet equivalents (IEQ), i.e., islets with an average diameter of 150 µm. The isolation result was then indicated as total IEQ and IEQ per gram of digested organ (Krickhahn et al. 2001).

3.3.7.3 Determination of islet purity and islet vitality

To determine the purity of the islets, 50-µl samples (triplicates) were taken from the culture flasks, transferred to glass slides and mixed with 50 µl DTZ solution each. The percentage of contaminating exocrine debris (unstained) was estimated and compared to the red-stained islets.

Vitality of the islets was examined at a wavelength of 488 nm underneath a BX50 fluorescence microscope (Olympus, Hamburg, Germany) and fluorescence was visualized using a 530 ± 20 nm bandpass filter. 1.5 µl of freshly prepared fluorescein diacetate solution (FDA, Sigma-Aldrich; 1 mg in 1 ml acetone) and 10 µl propidium iodide (PI, Sigma-Aldrich; 5 mg in 10 ml PBS) were added to 20-30 islets in 1 ml

HAM'S F12 culture medium. The islet suspension was then screened under the microscope and vitality was estimated by two independent individuals.

FDA is a non-polar ester which passes through plasma membranes and is hydrolyzed by intracellular esterases to produce free fluorescein. The polar fluorescein is unable to pass through the intact cell membrane of living cells and thus accumulates and produces a green cytoplasmatic fluorescence under appropriate excitation conditions. PI is excluded from intact cells and permeates only through the membranes of dead or dying cells where it binds to nucleic acids and produces a bright red nuclear fluorescence.

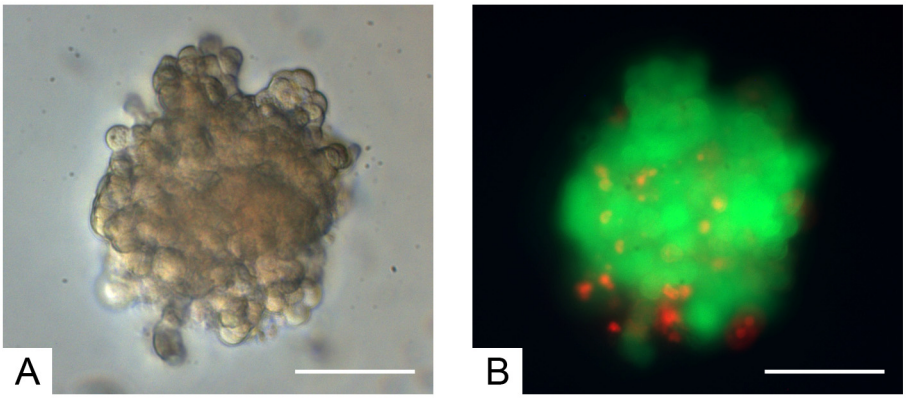

Figure 3.5: Determination of islet vitality by FDA/PI staining

Native **(A)** and FDA/PI stained **(B)** porcine islet of Langerhans after 20 days of in vitro culture; all green stained areas are indicative for viable islet cells while red stained areas show dead islet cells; magnification 40 x; scale bar 200 µm.

3.3.7.4 Production of frozen sections

While detectable antigens are much better conserved in frozen sections compared to paraffin sections, the conservation of morphological details is worse in frozen section. Small sections (0.5 cm in diameter) of the left pancreatic lobe free from fat, connective tissue, blood vessels and lymph nodes were transferred to cryotubes (Brand GmbH; Wertheim), filled with a special cryomedium (Tissue Tek, Sakura Finetek Europe B. V.; Zöterwoude, Holland) and immediately frozen in liquid nitrogen at -196°C to prevent the development of ice crystals. Blocks were stored at

-80°C until further processing. At least one hour prior to the production of frozen sections, tissue blocks were stored in the cryostat (Frigocut-N-2800, Reichert Jung; Bensheim) at -20°C. Subsequently, ~5 µm thick sections were cut in the cryostat using a C-blade (Leica; Nussloch) at -20°C and mounted on silanized glass slides (Histobond™, Marienfeld, Lauda-Königshofen). Sections were then dried for two hours at room temperature and stored at -20°C until further assayed.

3.3.7.4.1 Dithizone staining

Dithizone (diphenylthiocarbazone) is a zinc-specific stain used for the differentiation of islets of Langerhans and exocrine tissue components. While zinc containing β-cells are stained red, exocrine acinous cells remain unstained. Therefore 10 mg Dithizone (Sigma-Aldrich) were dissolved in 1 ml dimethyl sulfoxyd (Sigma Aldrich). Nine ml HBSS were added and the solution was filtered using a 0.2 µm filter. 100 µl of the Dithizone solution were added per frozen section and the immediate staining of the section was analyzed under a light microscope.

3.3.7.4.2 Immunohistochemistry for insulin

At first frozen sections were fixed in acetone for 10 minutes at 4°C and then dried for 15 minutes at RT. Subsequently, endogenous peroxidase was blocked for 15 minutes at RT using a methanol-hydrogen-peroxide mixture (200 ml methanol + 3 ml H_2O_2 30%). After that sections were washed three times with PBS (pH 7.4), followed by saturation of the tissue antigens with a protein block (normal goat serum, BioGenex, San Ramon, USA) in order to prevent nonspecific antibody binding (incubation ten minutes at RT). Incubation of the sections with the primary polyclonal guinea pig-anti-porcine insulin antibody (dilution 1:75) (Dako Cytomation, Hamburg) was carried out overnight in the refrigerator. A background reducing medium was used (Dako Cytomation) to dilute the antibody. Then sections were washed again three times with PBS, followed by an incubation step with a peroxidase conjugated goat-anti-guinea pig secondary antibody (dilution 1:1000); (Rockland; Gilbertsville, USA) in addition to 10% porcine serum (Serotec, Duesseldorf) for 30 minutes at RT. Afterwards, sections were washed three times with PBS. Immunoreactivity was visualized using the Peroxid-Block-Kit (BioGenex, Hamburg). For this, two drops of

3,3´ diaminobenzidine tetrahydrochloride (DAB) as well as one drop of H_2O_2 were added to the prepared substrate buffer according to the manufacturer's instructions, mixed and incubated for approximately three minutes under microscopic control until sufficient dye intensity was reached. Slides were washed with deionized water, counterstained with Mayer's hemalaun solution and washed again before they were dehydrated in an ascending alcohol series, cleared in xylene (Merck, Darmstadt) and mounted under coverslips using Pertex (Medite GmbH, Burgdorf).

All islet isolation procedures as well as preparation and staining of frozen sections were carried out in collaboration with Prof. K. Ulrichs, Dr. I. Chodnevskaja and B. Schneiker (Experimental Transplantation Immunology, Surgical Clinic I, University Hospital of Würzburg, Germany).

3.3.8 Quantitative stereological analyses

3.3.8.1 Pancreas preparation and quantitative stereological analyses

Following prefixation to allow manipulation of the organ without damaging the tissue, the pancreas (without left lobe) was cut into 1 cm thick slices, slices were tilted to their left side and covered by a 1 cm^2 point-counting grid which was used for area-weighted subsampling of pancreas tissue for quantitative stereological analyses. As pancreas slices were of the same thickness this procedure represents volume-weighted subsampling. The total number of points hitting pancreas tissue was determined. One tenth of the total number of points hitting pancreas tissue yielded the total sample number. For determination of the sites of sample collection, a random number (X) between one and the quotient of total hitting points and total sample number (Y) was determined. Pieces with a volume of 0.5 cm^3 were taken at the sites X+Y; X+2*Y; X+3*Y … Selected samples were placed in an embedding cassette with the right cut surface facing downwards, fixed in 10% neutral buffered formalin at room temperature overnight, routinely processed and embedded in paraffin. From half of the paraffin embedded samples a series of sections of approximately 4 µm thickness was cut with a HM 315 microtome (Microm). One section from each series was mounted on a glass slide for hematoxylin and eosin (H&E) staining and the following section was mounted on a 3-aminopropyltriethoxy-

silane-treated glass slide for immunohistochemistry. All H&E stained sections as well as a sheet of millimeter paper for calibration purposes were photocopied at a final magnification of 400% on a commercial photocopier showing the complete cut surface of all pancreas slices. Morphometric evaluation was carried out on a Videoplan® image analysis system (Zeiss-Kontron, Eching, Germany) attached to a microscope by a color video camera. The cross-sectional area of the pancreas was determined planimetrically by circling the cut surfaces on the photocopies. Planimetric measurements of islet profiles were performed on H&E stained sections while β-cell areas were determined on immunohistochemically stained sections (see 3.3.8.3) by circling their outlines with a cursor on a digitizing tablet of the image analysis system. Images were displayed on a color monitor at an 850x final magnification. The volume of the pancreas ($V_{(Pan)}$) before embedding was calculated by the quotient of the pancreas weight and the specific weight of the pig pancreas (1.07 g/cm^3). The specific weight was determined by the submersion method (Scherle 1970). The volume density of the islets in the pancreas ($Vv_{(Islet/Pan)}$) was calculated by dividing the total islet area ($A_{(Islet)}$) by the total pancreas area ($A_{(Pan)}$). The total volume of islets in the pancreas ($V_{(Islet,\ Pan)}$) was determined as the product of $Vv_{(Islet/Pan)}$ and $V_{(Pan)}$. Accordingly, the volume density of β-cells in the pancreas ($Vv_{(β\text{-}cell/Pan)}$) was obtained as the quotient of the total area of β-cells ($A_{(β\text{-}cells)}$) and $A_{(Pan)}$. Here, total area of β-cells included total area of β-cells in the islets and total area of isolated β-cells in the pancreas. Further, the total volume of β-cells in the pancreas was determined as the product of $Vv_{(β\text{-}cell/Pan)}$ and $V_{(Pan)}$. Division of $A_{(β\text{-}cell)}$ by $A_{(Islet)}$ yielded the volume density of the β-cells in the islets ($Vv_{(β\text{-}cell/Islet)}$) and the product of $Vv_{(β\text{-}cell/Islet)}$ and $V_{(Islet,\ Pan)}$ resulted in the total volume of β-cells in the islets ($V_{(β\text{-}cell,\ Islet)}$).

Isolated β-cells (insulin positive single cells and small clusters of insulin positive cells not belonging to established islets) were quantified separately. The volume density of isolated β-cells in the pancreas was obtained by division of the total profile areas of isolated β-cells by $A_{(Pan)}$. The total volume of isolated β-cells was determined as the product of their volume density in the pancreas and the total volume of the pancreas.

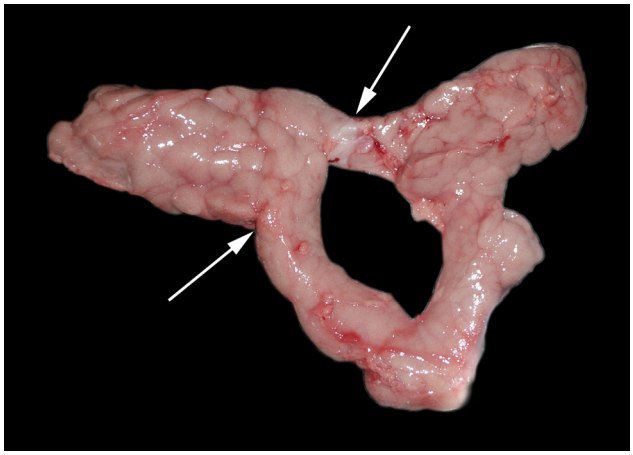

Figure 3.6: Pancreas preparation for islet isolation and quantitative stereological analyses

White arrows indicate the separation site of the left pancreatic lobe from the rest of the organ using the left pancreatic lobe for islet isolation and the remnant organ for quantitative stereological analyses.

3.3.8.2 Hemalaun & Eosin staining

After incubation overnight at 37°C in an incubator, sections were deparaffinized in xylene for 15 minutes, rehydrated in a descending alcohol series and washed in distilled water. Subsequently nuclear staining was carried out by incubation of the slides in Meyer's Hemalaun solution for four minutes. Then tissue sections were washed with tap water for five minutes and dipped four to five times in eosin solution. Sections were dehydrated in an ascending alcohol series, cleared in xylene and mounted under coverslips using Eukitt® (Electron Microscopy Sciences).

3.3.8.3 Immunohistochemistry for insulin

The indirect immunoperoxidase technique was applied to localize insulin containing cells. Sections were deparaffinized in xylene, rehydrated in a descending alcohol series and washed in distilled water. Endogenous peroxidase activity was blocked using 1% hydrogen peroxide in TBS buffer (pH 7.4). After that sections were washed in TBS (pH 7.4) for ten minutes and pre-incubated with normal rabbit serum (MP Biomedicals) for 30 minutes to reduce non-specific binding. Subsequently, slides were incubated for two hours at room temperature with a polyclonal guinea pig anti-

porcine insulin antibody (dilution 1:1000 in TBS) (Dako Cytomation). Thereafter slides were washed in TBS buffer for ten minutes, followed by an incubation step with horseradish peroxidase conjugated polyclonal rabbit anti-guinea pig IgG (dilution 1:50 in TBS buffer containing 5% (vol/vol) porcine serum) for one hour. The slides were washed again in TBS buffer for ten minutes and immunoreactivity was visualized using 3,3´ diaminobenzidine tetrahydrochloride dehydrate (Sigma-Aldrich) as chromogen and 1% hydrogen peroxide as substrate. Mayer's hemalaun solution was used for counterstaining. Tissue sections were then dehydrated in an ascending alcohol series, cleared in xylene and mounted under coverslips using Eukitt®.
Specificity controls included substitution of primary antisera with nonimmune serum and omission of the secondary antiserum.

3.3.9 Statistics

All data are presented as means ± SEM. The statistical significance of differential findings between groups was determined using the Mann-Whitney-U-Test while differential findings within one group (group of control or transgenic animals) were evaluated using the Wilcoxon-Test. Both tests were applied in combination with an exact test procedure because of the small sample size (SPSS 15.0). *P* values less than 0.05 were considered significant.

4 Results

4.1 Generation and genotyping of GIPR^{dn} transgenic pigs

To generate GIPR^{dn} transgenic pigs, a gene transfer technology based on lentiviral vectors was used. The lentiviral construct is composed of the human dominant-negative GIPR under control of the rat insulin 2 (Ins2) gene promoter (RIP2). The dominant-negative GIPR as described in Figure 4.1 has an eight amino acid deletion (amino acid position 319-326/nucleotide position 955-978) and two additional point mutations (amino acid position 340/nucleotide position 1018-1020), leading to an amino acid exchange from alanine to glutamate (Ala → Glu) in the third intracellular loop which is known to be essential for further signal transduction (Harmar 2001; Cypess et al. 1999; Hallbrink et al. 2001; Salapatek et al. 1999; Takhar et al. 1996). This targeted mutation results in a sustained binding affinity of the ligand GIP but a loss of the ligands ability to induce further signal transduction (Herbach et al. 2005, Volz 1997).

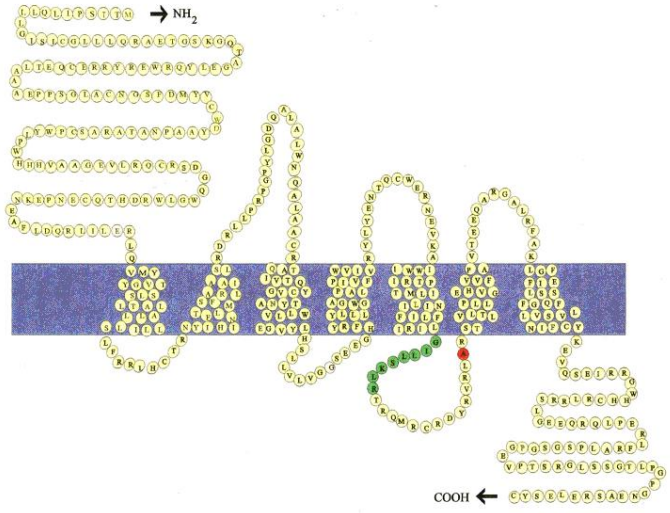

Figure 4.1: Amino acid sequence of the human GIPR

Amino acid sequence of the human seven transmembrane domain G-protein coupled GIPR including marked areas where targeted mutations have been inserted (eight amino acid deletion (green) and an amino acid shift (Ala → Glu, red) (courtesy of Dr. Nadja Herbach).

Lentiviral particles were injected into the perivitelline space of 113 pig zygotes (Figure 4.2), which were then transferred laparoscopically into the oviducts of three cycle synchronized recipient gilts (sow 1: 32 zygotes; sow 2: 31 zygotes, sow 3: 50 zygotes). Nineteen piglets (17% of the transferred zygotes) were born. Genotyping by PCR using DNA obtained from ear punches revealed nine transgenic (47.3%) founder animals (4 female; 5 male) confirming the high efficiency of lentiviral transgenesis in large animals (Hofmann et al. 2003). Southern blot analysis using DNA from EDTA blood and a probe which hybridizes in the region of the rat insulin 2 promoter sequence identified either one or two lentiviral integrants in the previously determined nine founder pigs (Figure 4.3) while no signal was detected in littermate control animals.

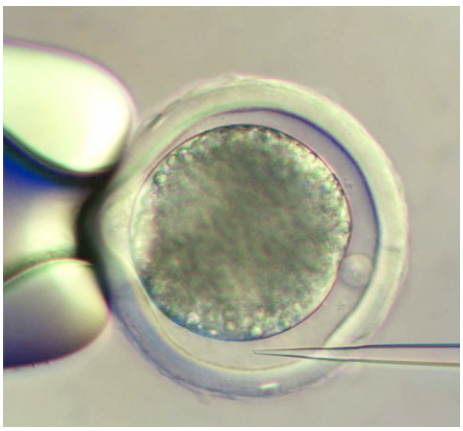

Figure 4.2: Injection of the lentiviral construct into the perivitelline space of a pig zygote (courtesy of Tamara Holy).

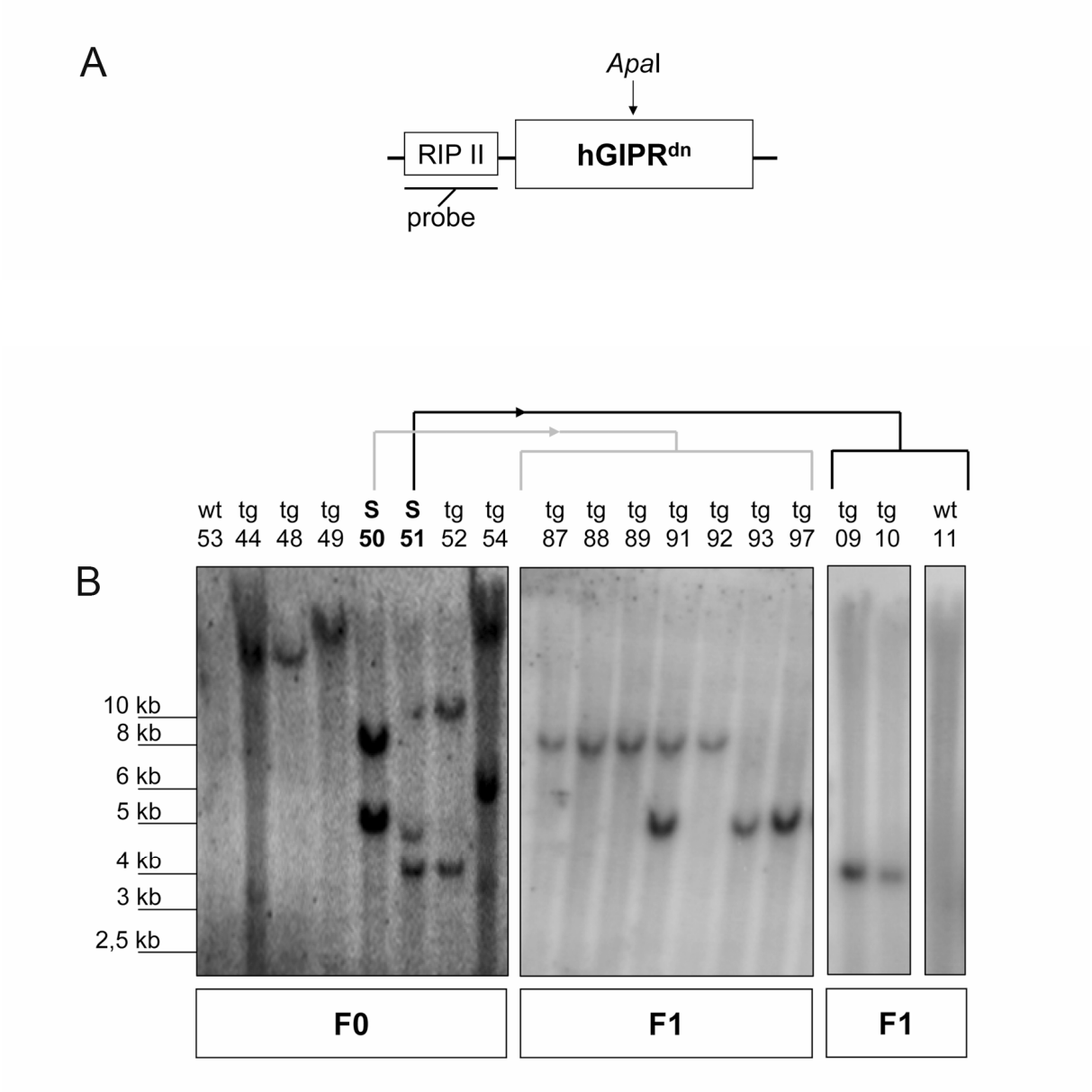

Figure 4.3: Southern Blot analyses of GIPR^{dn} transgenic and control animals of the F0- and F1-generation

(A) Schematic illustration of the transgenic construct consisting of the human dominant-negative GIPR (GIPR^{dn}) under control of the rat insulin 2 gene promoter (RIP2); probe: probe used for southern blot analyses directed towards the RIP2 sequence; *Apa*I: restriction site of *Apa*I; **(B)** Southern blot analyses of *Apa*I digested genomic DNA from EDTA blood of GIPR^{dn} transgenic pigs (tg) and littermate control (wt) animals of the F0- and the F1-generation; S: sire of the piglets shown in the Southern blot of the F1-generation; piglets of the F1-generation show segregation of the two integration sites of their particular sire.

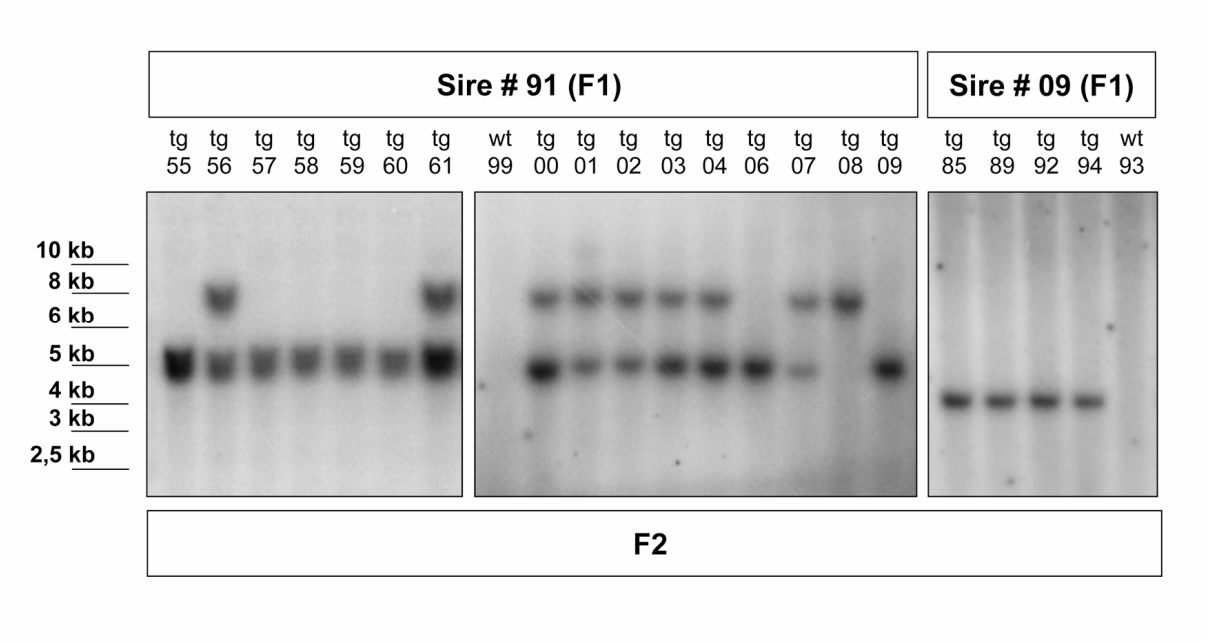

Figure 4.4: Southern Blot analyses of GIPR^{dn} transgenic and control animals of the F2-generation

Southern blot analyses of *Apa*I digested genomic DNA from EDTA blood of all live-born GIPR^{dn} transgenic pigs (tg) and littermate control (wt) animals of the F2-generation; probe used for the analyses is shown in Figure 4.3 A; Southern blot analyses of sire #91 and sire #09 of the F1-generation is shown in Figure 4.3.

For further characterization of germ line transmission and expression of the LV-RIP2-GIPR^{dn} construct, two male founder animals (#50, #51) (see Figure 4.3) were mated to non-transgenic German Landrace-Swabian-Hall crossbred control females, and offspring were genotyped by PCR (Figure 4.5) as well as by Southern blot analysis. Southern blot analysis demonstrated segregation of the integrants according to Mendelian rules (Figure 4.3). To establish a F2-generation of GIPR^{dn} transgenic pigs from both previously selected founder animals, two boars (#91; #09) (see Figure 4.3) of the F1-generation were mated to German Landrace-Swabian-Hall crossbred wild-type sows. Transgenic offspring also were identified by PCR and Southern blot analysis (Figure 4.4).

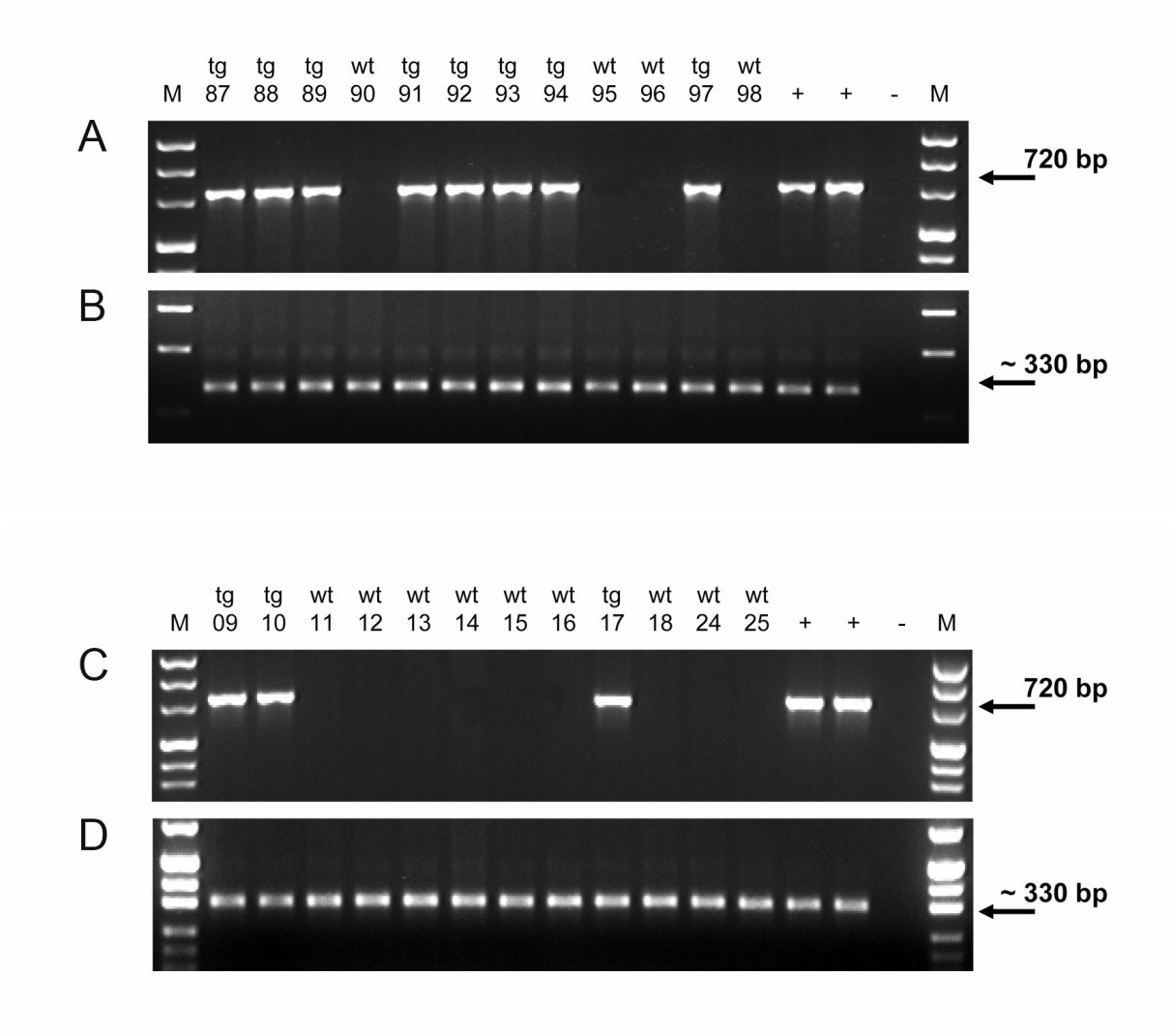

Figure 4.5: PCR analyses for identification of GIPR^{dn} transgenic pigs and littermate control animals of the F1-generation

(A/C) Transgene specific PCR analyses for the GIPR^{dn} transgene of offspring from founder boar #50 **(A)** and founder boar #51 **(C)**; tg: GIPR^{dn} transgenic pigs; wt: littermate non-transgenic control pigs; M: pUC Mix Marker 8; +: positive control (genomic DNA of a previously genotyped pig); -: negative control (aqua bidest.); **(B/D)** PCR using β-actin specific primers was performed of all samples to control DNA integrity; M: pUC Mix Marker 8; +: positive control (genomic DNA of a previously genotyped pig); -: negative control (aqua bidest.).

4.2 Inheritance

Inheritance of the GIPR^{dn} transgene is summarized in the following table:

Table 4.1: Inheritance of the GIPR^{dn} transgene

Generation	Transgenic sire	Number of litters	Offspring				
			m (wt)	m (tg)	f (wt)	f (tg)	Total (tg) %
F1	# 50 (F0)	1	1	6	3	2	66.67
F1	# 51 (F0)	2	11	2	9	2	16.67
F2	# 91 (F1)	2	3	12	3	10	78.57
F2	# 09 (F1)	1	3	2	3	3	45.45

4.3 Expression analysis of the GIPR^{dn} transgene

To demonstrate expression of GIPR^{dn} mRNA, porcine islets of Langerhans were isolated from 12 to 13-month-old transgenic (n=3) and three non-transgenic littermate control animals (offspring of both founder boars) and analyzed by reverse transcriptase polymerase chain reaction (RT-PCR) specific for GIPR^{dn} complementary DNA. For each pig, two RNA samples (400 ng of total RNA each) were reverse transcribed and cDNA was analyzed for the presence of the GIPR^{dn} transcript by PCR. Positive signals were obtained for islets from all transgenic animals, but not for islets from non-transgenic littermates. Signals from cDNA of islets from GIPR^{dn} transgenic pigs #97 and #10 were less intense than signals from pig #91. No signals were obtained from islets of transgenic offspring after omission of the RT step, demonstrating that expressed rather than integrated sequences were detected. In addition, all cDNA samples were analyzed for the presence of mRNA of the housekeeping gene β-actin in order to evaluate efficiency of reverse transcription. Positive signals could be detected for all cDNA samples although signals from the cDNA of islets from GIPR^{dn} transgenic pigs #97 and #10 were less intense than signals from pig #91. This led to the assumption that the weaker signals obtained by amplification of GIPR^{dn} transcripts from islets of pig #97 and #10 may be caused rather by less efficient reverse transcription or differential RNA quality than by different expression levels. Nevertheless differences between expression levels of the GIPR^{dn} transgene of the individual pigs could also have contributed to the

difference in signal intensity because GIPR^{dn} transgenic pigs #97 and #10 have one integration site while pig #91 has two integration sites of the transgene.

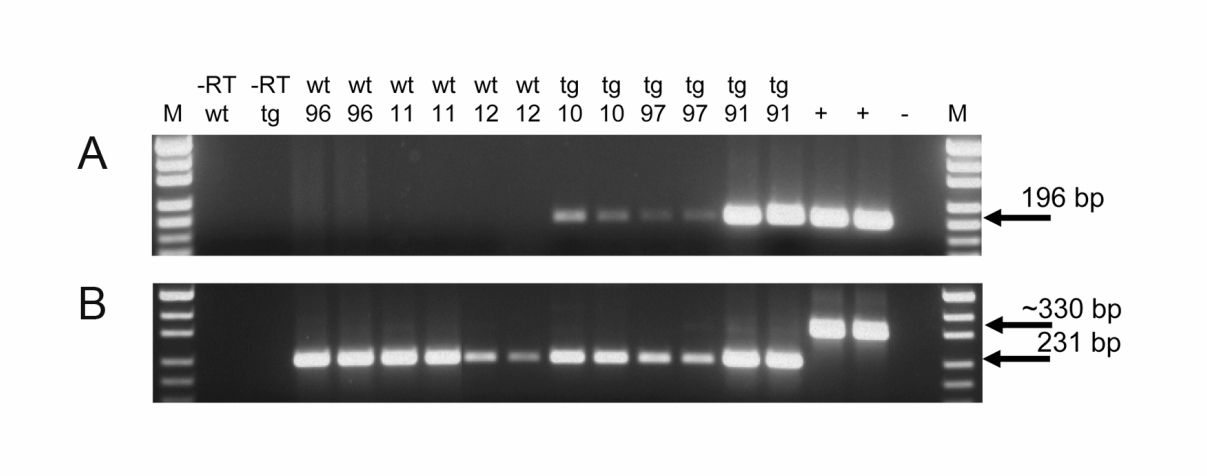

Figure 4.6: Analysis of transgene expression (GIPR^{dn}) in isolated porcine islets of Langerhans by RT-PCR

(A) GIPR^{dn} RT-PCR of transgenic and non-transgenic littermate control animals; **(B)** β-actin RT-PCR used for confirmation of reverse transcription efficiency; M: pUC Mix Marker; -RT wt: minus RT wild-type pigs; -RT tg: minus RT GIPR^{dn} transgenic pigs; wt: wild-type pigs (#96, #11, #12); tg: GIPR^{dn} transgenic pigs (#10, #97, #91) of the F1-generation; +: positive control (genomic DNA of GIPR^{dn} transgenic pig); -: negative control (aqua bidest.).

4.4 Normal blood glucose and serum fructosamine levels in GIPR^{dn} transgenic pigs

To evaluate effects of GIPR^{dn} expression on glucose homeostasis, blood was collected from the ear vein with a small lancet in fed 28-day-old animals (before weaning) and in 18 hours fasted pigs from the age of 35 days up to 84 days on a weekly basis and thereafter in longer intervals until the pigs were 210 days old. No significant differences in blood glucose levels were detected in GIPR^{dn} transgenic pigs compared to their non-transgenic littermate control animals at any point of time investigated (Figure 4.7 A). In both groups of animals, all fasting blood glucose concentrations determined were within or little below the reference range of blood glucose for pigs that ranges, dependent on the laboratory, approximately between 70 and 115 mg/dl.

Serum fructosamine levels were analyzed in fed 20-day-old pigs (before weaning) as well as in fasted animals at 41, 62, 84 and 210 days of age. No obvious difference in serum fructosamine levels was detected between $GIPR^{dn}$ transgenic pigs and their non-transgenic littermate control animals at any point of time evaluated (Figure 4.7 B). Nevertheless a small but constant rise in fructosamine levels with age was seen in both groups as has been previously reported (Larsen et al. 2001).

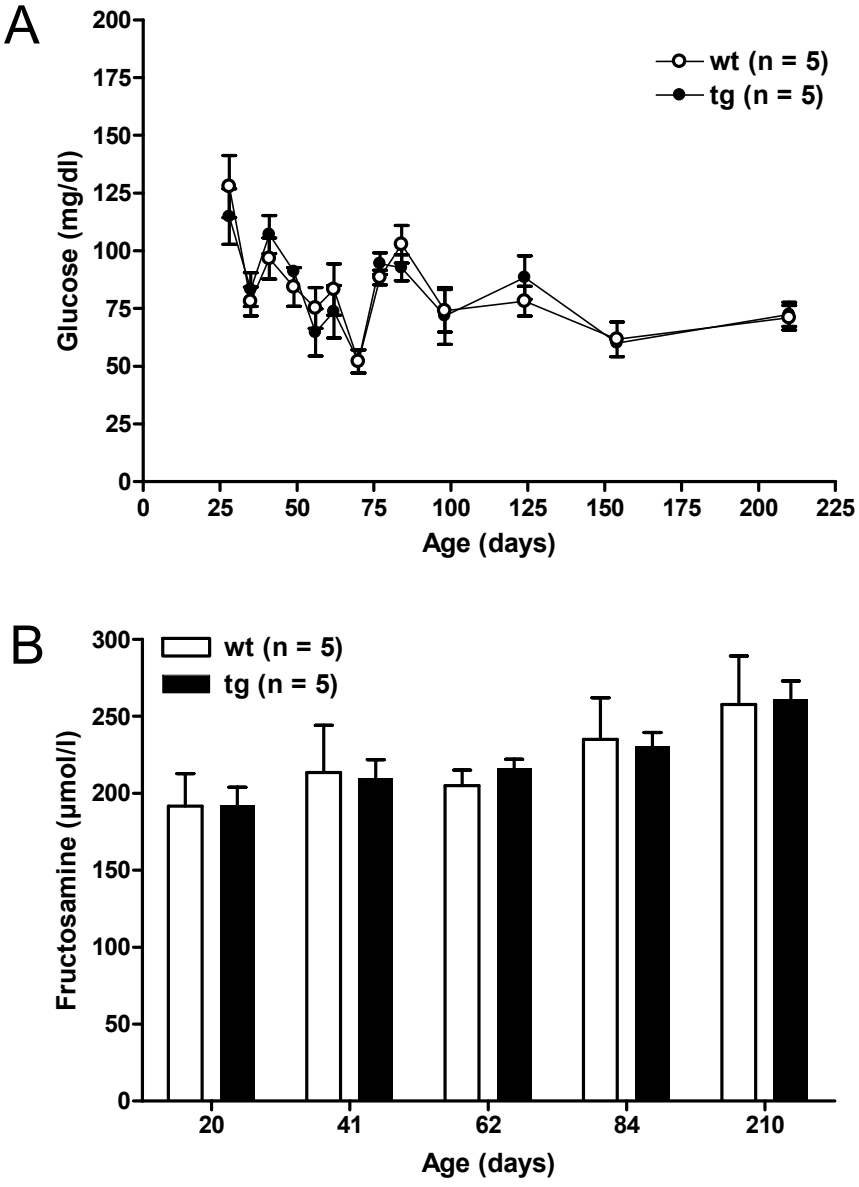

Figure 4.7: Normal blood glucose and serum fructosamine levels in GIPR^{dn} transgenic and non-transgenic littermate control pigs

GIPR^{dn} transgenic pigs (tg) show normal blood glucose and serum fructosamine levels compared to non-transgenic littermate control animals (wt); **(A)** blood glucose concentrations of fed 28-day-old and fasted 35- up to 210-day-old GIPR^{dn} transgenic pigs (tg) and non-transgenic littermate control animals (wt); **(B)** serum fructosamine levels of fed 28-day-old and fasted 41- up to 210-day-old GIPR^{dn} transgenic (tg) and non-transgenic littermate control animals (wt); data are means ± SEM; n: number of animals investigated.

4.5 Impaired oral glucose tolerance in GIPR^{dn} transgenic pigs

The effects of impaired GIP signaling on oral glucose tolerance were evaluated by an oral glucose tolerance test performed in 5-month-old (20 weeks ± 1 week) transgenic pigs (n=5) and five littermate controls originating from founder boar #50 (#91, #93, #97) and #51 (#09, #10). After oral glucose challenge (2 g/kg body weight), transgenic pigs exhibited a distinct reduced insulin secretion as well as elevated glucose levels compared to their non-transgenic littermate controls (Figure 4.8). The decline of blood glucose levels after having reached a peak level was markedly decelerated in GIPR^{dn} transgenic pigs. The area under the curve (AUC) for insulin was reduced to 49% ($p<0.01$) in transgenic pigs as compared to the controls. Furthermore, the AUC for glucose was 26% larger ($p<0.05$) in GIPR^{dn} transgenic pigs than in their non-transgenic littermate controls (Figure 4.8). Thus, these findings clearly demonstrate a reduced oral glucose tolerance in GIPR^{dn} transgenic pigs.

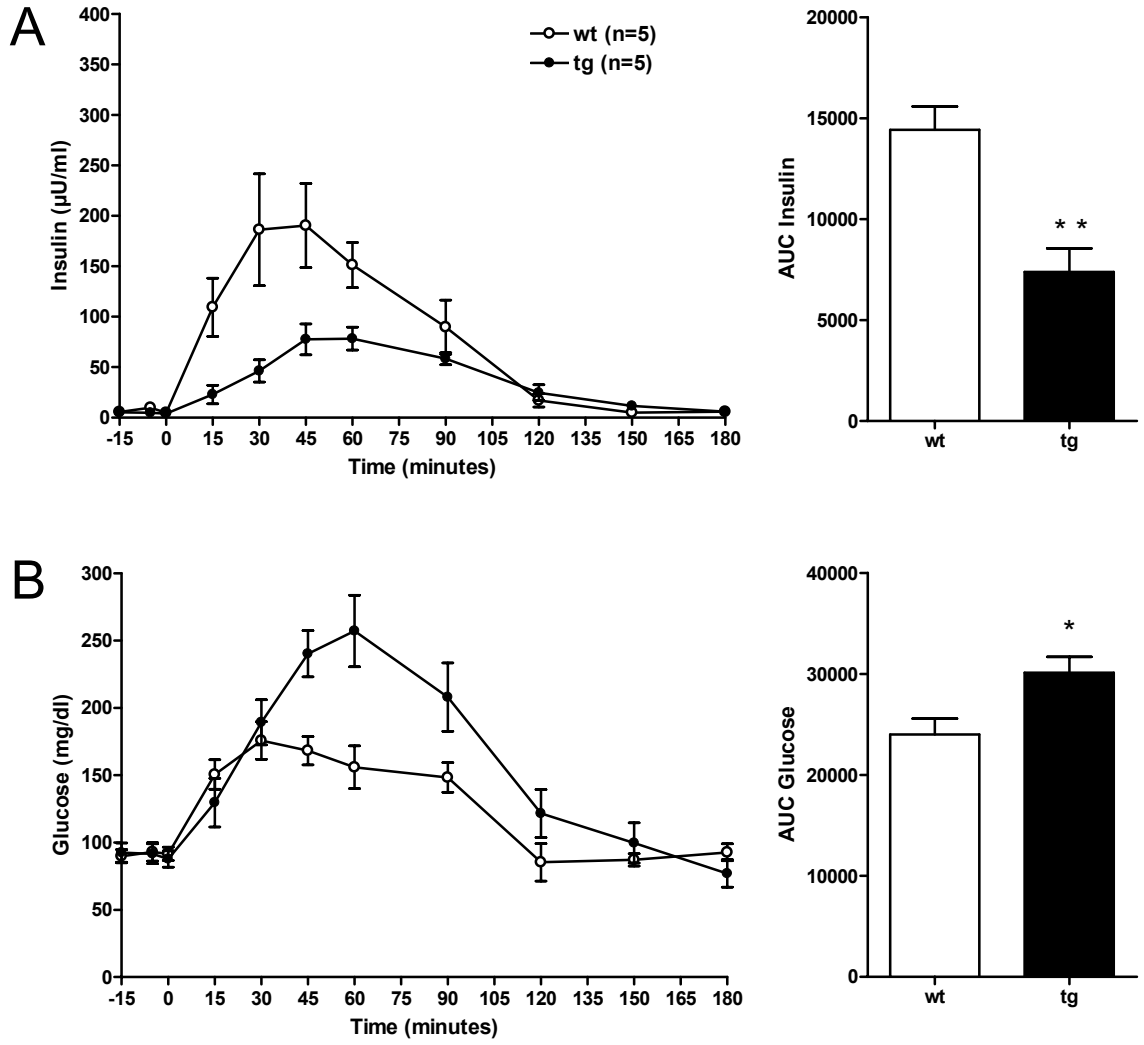

Figure 4.8: Impaired oral glucose tolerance in GIPR^{dn} transgenic pigs

GIPR^{dn} transgenic pigs (tg) show impaired glucose tolerance in an oral glucose tolerance test at 5 months of age versus non-transgenic littermate control animals (wt); **(A)** serum insulin levels; AUC insulin: area under the insulin curve; **(B)** blood glucose levels; AUC glucose: area under the glucose curve; data are means ± SEM; **: $p<0.01$ vs. control; *: $p<0.05$ vs. control; n: number of animals investigated.

4.6 Impaired intravenous glucose tolerance in GIPR^{dn} transgenic pigs

To investigate whether the expression of a GIPR^{dn} not only affects oral glucose tolerance but also general glucose homeostasis, intravenous glucose tolerance tests

were performed in transgenic and control pigs at 10 months (45 weeks ± 2 weeks), 7 months (28-36 weeks), and 8 weeks of age. The group of 10-month-old pigs included five transgenic pigs and four control animals of the F1-generation (originating from founder boars #50 and #51) while intravenous glucose tolerance of five 7-month-old GIPR^{dn} transgenic and four control animals (originating from boar #91 of the F1-generation) of the F2-generation was investigated. In addition, intravenous glucose tolerance of six 8-week-old pigs (3 transgenic pigs originating from boar #91 of the F1-generation and three control pigs) of the F2-generation was analyzed. Concentrated 50% glucose solution (0.5 g/kg body weight (BW)) was infused as a bolus through the jugular vein catheter. 10-month-old GIPR^{dn} transgenic pigs showed considerably reduced insulin release going along with a decelerated decline of blood glucose levels (Figure 4.9). The area under the insulin curve was 52% smaller ($p<0.05$), the AUC for glucose 10% larger ($p<0.05$) in GIPR^{dn} transgenic pigs than in their non-transgenic littermate controls (Figure 4.9). At 7 months of age, GIPR^{dn} transgenic pigs also revealed markedly but not significantly reduced insulin levels as well as a decelerated decline of blood glucose levels (Figure 4.10). Looking at the individual insulin curves of all transgenic animals of this age group, one pig showed exorbitantly higher insulin levels than the rest of the group leading to the assumption that the determined mean as well as AUC for insulin might mask the actual reduction of insulin secretion in transgenic pigs compared to controls (Figure 4.10 B). The area under the insulin curve was 10.2% smaller ($p=0.142$) in transgenic pigs but would have been 43.6% smaller when disregarding the previously mentioned animal. The AUC for glucose was visibly but not significantly larger (21.6%, $p=0.096$) in transgenic pigs compared to controls (Figure 4.10). In contrast, 8-week-old transgenic pigs showed a visible but small reduction of serum insulin levels and almost no difference in serum glucose levels (Figure 4.11). Accordingly, the AUC for insulin was not significantly smaller (39.3%, $p=0.355$) in GIPR^{dn} transgenic pigs compared to controls. The AUC for glucose was 1.7% smaller ($p=0.498$) in transgenic pigs (Figure 4.11).

In summary, GIPR^{dn} transgenic pigs showed an impaired glucose tolerance at 7 and 10 month of age while 8-week-old animals only tended towards this phenotype indicating a progressive deterioration of intravenous glucose tolerance in GIPR^{dn} transgenic pigs. Impaired intravenous glucose tolerance in older GIPR^{dn} transgenic

pigs could not be explained by just a reduced incretin effect initiated by the expression of a GIPR^{dn} because the incretin effect is by-passed when glucose is administered intravenously. This led to the assumption of effects additional to an impaired incretin effect caused by a defective GIPR signaling (see below).

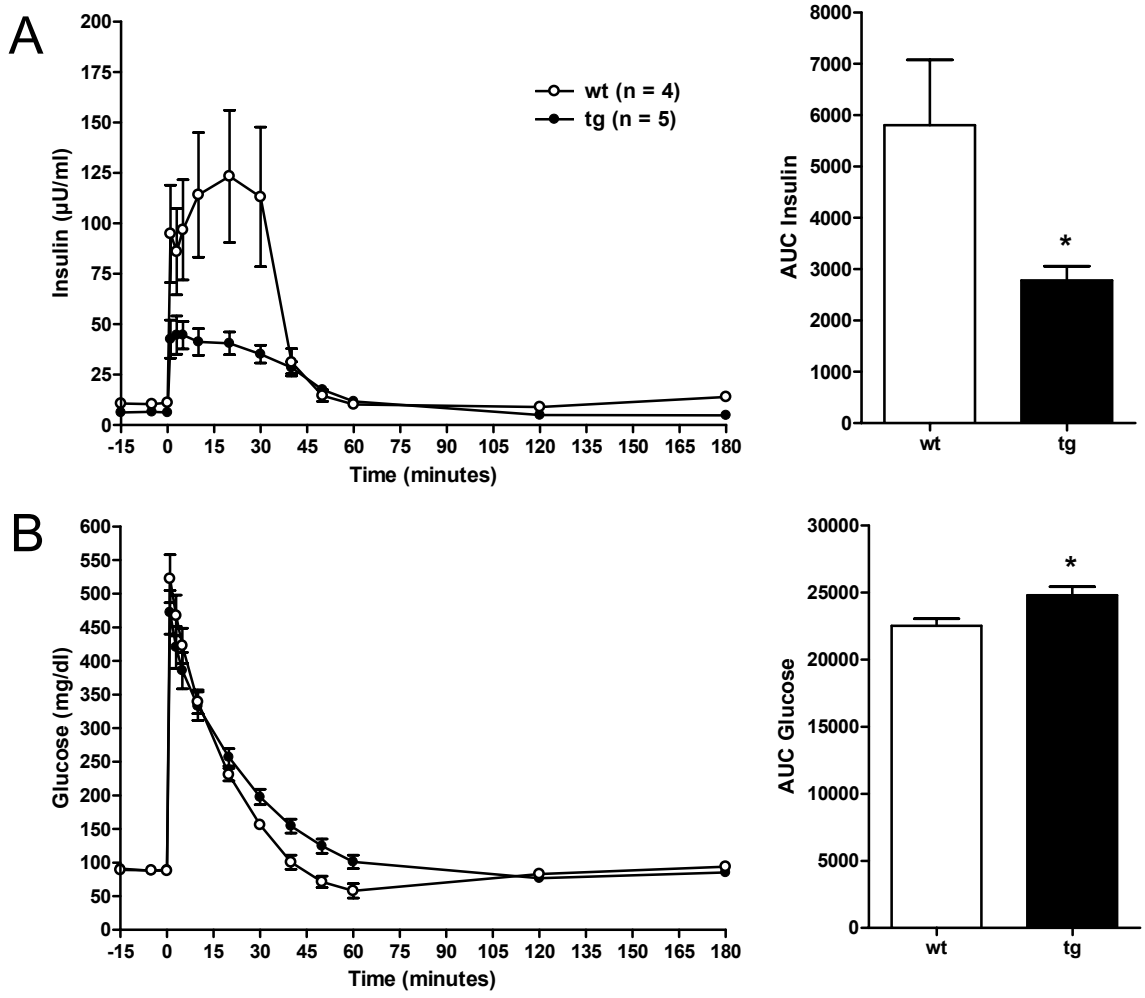

Figure 4.9: Impaired intravenous glucose tolerance in 10-month-old GIPR^{dn} transgenic pigs

Intravenous glucose tolerance test of 10-month-old GIPR^{dn} transgenic pigs (tg) and non-transgenic littermate control animals (wt); **(A)** serum insulin levels; AUC insulin: area under the insulin curve; **(B)** serum glucose levels; AUC glucose: area under the glucose curve; data are means ± SEM; n: number of animals investigated; *: $p<0.05$ vs. control.

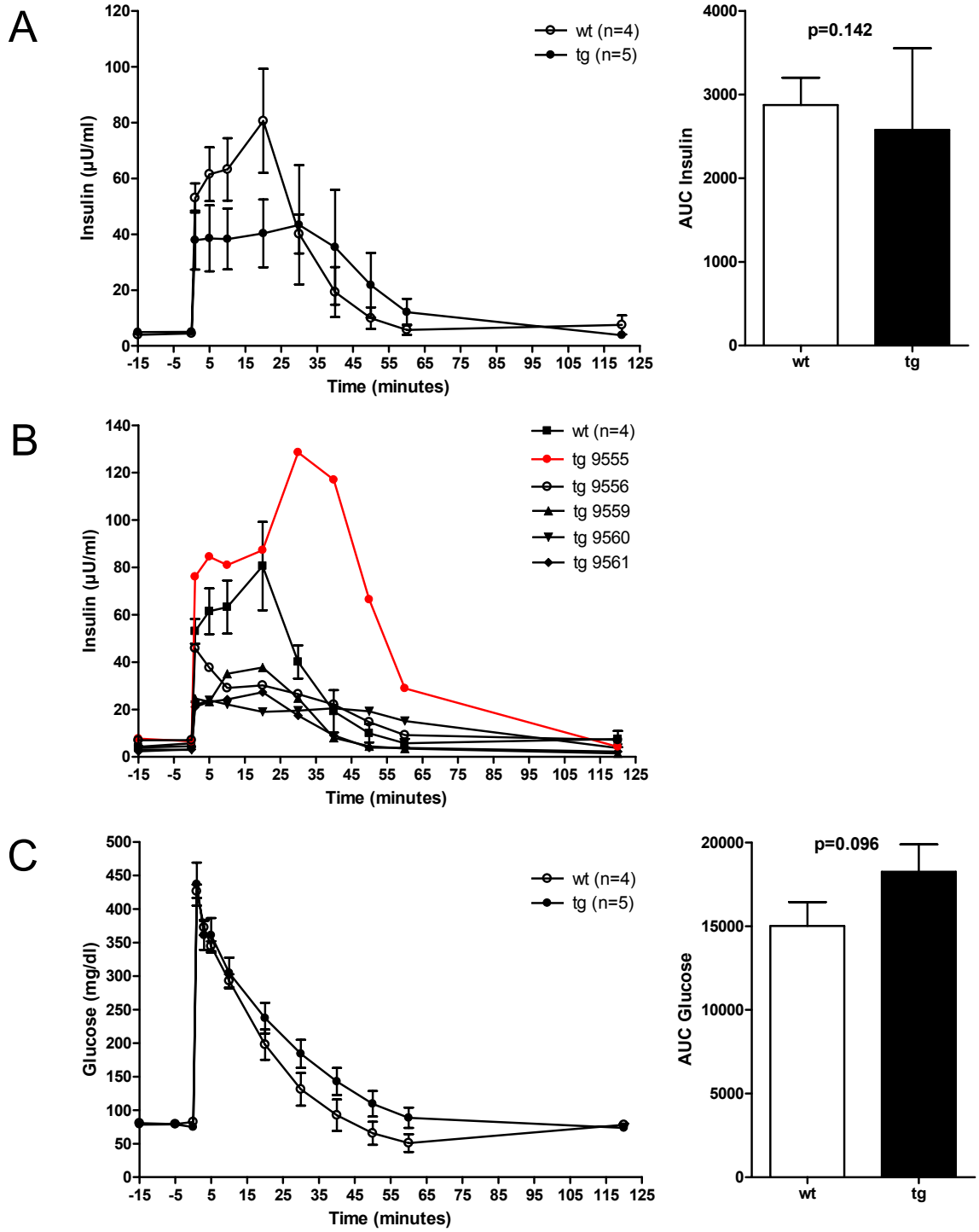

Figure 4.10: Impaired intravenous glucose tolerance in 7-month-old GIPR^{dn} transgenic pigs

Intravenous glucose tolerance test of 7-month-old GIPR^{dn} transgenic pigs (tg) and non-transgenic littermate control animals (wt); **(A)** serum insulin levels; AUC insulin: area under the insulin curve; **(B)** individual insulin curves; **(C)** serum glucose levels; AUC glucose: area under the glucose curve; data are means ± SEM; n: number of animals investigated.

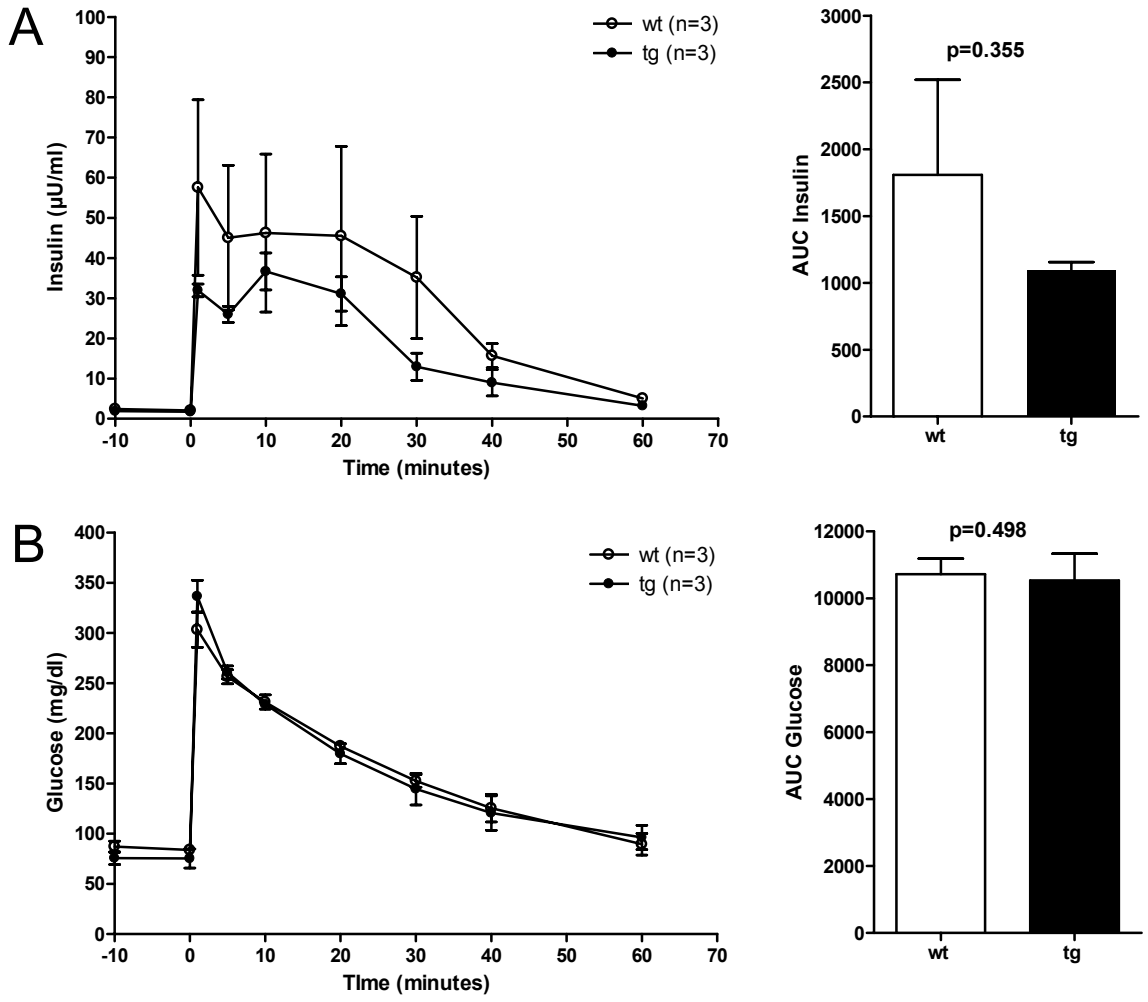

Figure 4.11: Tendency of impaired intravenous glucose tolerance in 8-week-old GIPR^{dn} transgenic pigs

Intravenous glucose tolerance test of 8-week-old GIPR^{dn} transgenic pigs (tg) and non-transgenic littermate control animals (wt); **(A)** serum insulin levels; AUC insulin: area under the insulin curve; **(B)** serum glucose levels; AUC glucose: area under the glucose curve; data are means ± SEM; n: number of animals investigated.

4.7 Reduced insulin secretion capacity in GIPR^{dn} transgenic pigs

The fact that the expression of a dominant-negative GIPR led to impaired intravenous glucose tolerance in older pigs raised the question whether transgenic pigs would also show reduced insulin secretory capacity in response to a challenge with glucagon. This question was addressed by a glucagon stimulation test which is routinely used in human medicine to estimate the need of exogenous insulin in

diabetic patients (Goeke, 2002). In this case, the test was accomplished in five 10-month-old GIPR^{dn} transgenic pigs and four controls analogous to the intravenous glucose tolerance test (IVGTT). In response to the intravenous administration of 1 mg glucagon (GlucaGen®, Novo Nordisk), GIPR^{dn} transgenic pigs exhibited a clearly visible reduction in insulin secretory capacity (Figure 4.12). The course of the glucose curve was slightly lower in GIPR^{dn} transgenic pigs compared to their control group (Figure 4.12). The area under the insulin curve was 51% smaller ($p=0.056$), the AUC for glucose 9% smaller ($p=0.175$) in GIPR^{dn} transgenic pigs than in their non-transgenic littermate controls (Figure 4.12). These results demonstrate a reduced insulin secretion capacity as a consequence of GIPR^{dn} expression in the pancreatic islets of transgenic pigs.

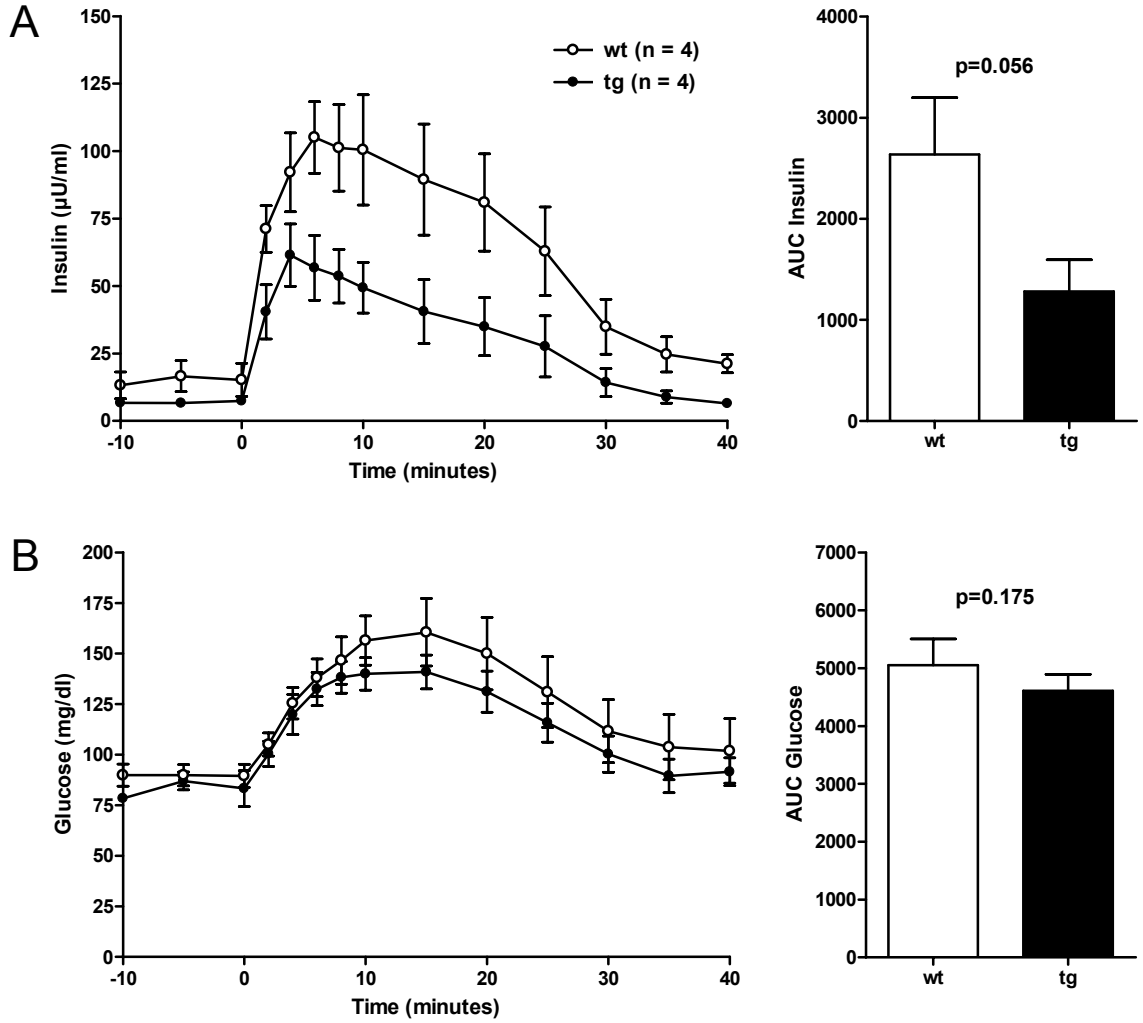

Figure 4.12: Glucagon stimulation test indicating reduced insulin secretion capacity in GIPR^{dn} transgenic pigs

Glucagon stimulation test of 10-month-old GIPR^{dn} transgenic pigs (tg) and non-transgenic littermate control animals (wt); **(A)** serum insulin levels; AUC insulin: area under the insulin curve; **(B)** serum glucose levels; AUC glucose: area under the glucose curve; data are means ± SEM; n: number of animals investigated; AUC insulin: p=0.056 vs. control; AUC glucose: p=0.175 vs. control.

4.8 Impaired insulinotropic action of GIP in GIPR^{dn} transgenic pigs

In order to clarify the effect of porcine GIP on insulin secretion in the presence of the GIPR^{dn}, an intravenous glucose tolerance test (IVGTT) as well as an IVGTT in combination with application of GIP was performed in GIPR^{dn} transgenic pigs and non-transgenic control animals at 7 months (28-36 weeks) and 8 weeks of age (animals originated from F1 boar #91). For this purpose, 20 pmol/kg BW of synthetic porcine GIP were administered intravenously after three minutes relative to a glucose load (0.5 g/kg BW). Seven-month-old GIPR^{dn} transgenic pigs (n=3) revealed a clearly reduced insulin secretion after glucose stimulation (IVGTT) compared to their non-transgenic control animals (n=4); (Figure 4.13 A). In response to stimulation with glucose + GIP, animals of both groups showed increased insulin secretion compared to glucose administration only, although the effect of GIP was considerably more potent in wild-type pigs.

$\Delta Insulin_{(max./1min.)}$ (difference of the maximum insulin level and the insulin level determined at one minute after the intravenous glucose load) following stimulation with glucose and GIP was significantly higher in control animals ($p<0.05$) compared to GIPR^{dn} transgenic pigs, while $\Delta Insulin_{(max./1min.)}$ did not differ significantly between the two groups after stimulation with just glucose ndicating that the insulinotropic action of GIP is impaired in GIPR^{dn} transgenic pigs (Figure 4.13 B). Correspondingly, the decline of glucose levels was delayed in transgenic pigs receiving only glucose compared to controls. GIP was able to reduce the AUC for glucose 20.1% ($p=0.13$) in wild-type pigs but only 12.3% in transgenic pigs ($p=0.127$).

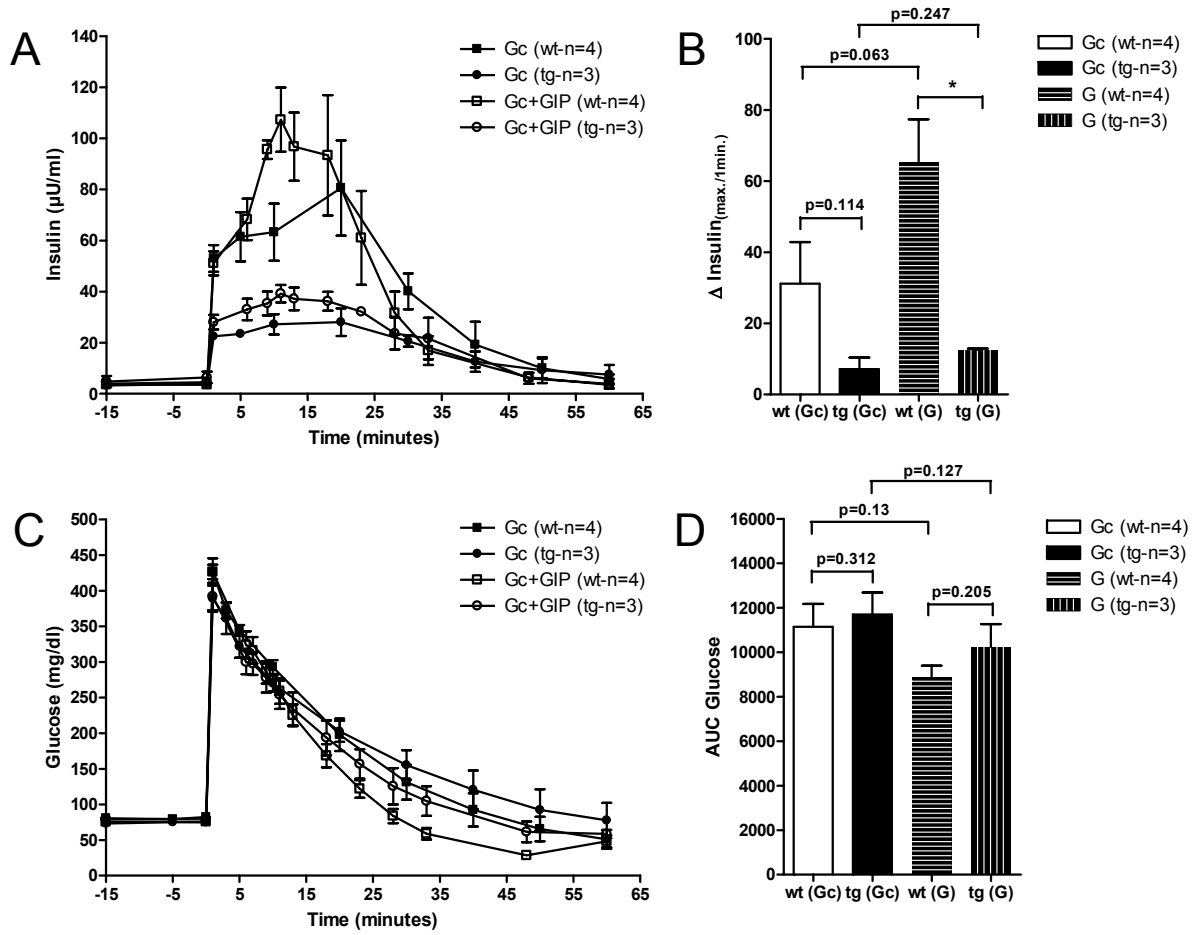

Figure 4.13: Impaired insulinotropic action of GIP in GIPR^{dn} transgenic pigs
Intravenous glucose tolerance test (IVGTT) and IVGTT in combination with application of synthetic porcine GIP in 7-month-old GIPR^{dn} transgenic pigs (tg) and age-matched control animals (wt); **(A)** serum insulin levels **(B)** ΔInsulin$_{(max./1min.)}$ of serum insulin levels; **(C)** serum glucose levels; **(D)** AUC glucose: area under the glucose curve; (Gc) glucose; (G) glucose + GIP; data are means ± SEM; *: p<0.05 vs. control; n: number of animals investigated.

GIPR^{dn} transgenic pigs at 8 weeks of age showed a visible but not significant reduction of insulin secretion following stimulation with glucose compared to controls. The AUC for insulin was diminished 39.3% (p=0.355) in transgenic animals compared to non-transgenic controls (see also Figure 4.11). Exogenous GIP had the ability to enhance insulin secretion of wild-type pigs by 12 µU/ml on average considering ΔInsulin$_{(max./1min.)}$ while it was not able to enhance insulin secretion in GIPR^{dn} transgenic pigs (Figure 4.14 B). However, looking at the insulin curve (Figure 4.14 A) a small increase of insulin levels of transgenic pigs following stimulation with

glucose + GIP could be detected. $\Delta Insulin_{(max./1min.)}$ of wild-type pigs following glucose stimulation was considered zero as all pigs had their maximum insulin level one minute after administration of the glucose load.

The AUC for glucose after glucose stimulation did not show any difference between the two groups (Figure 4.14 C). Exogenous GIP reduced the AUC for glucose 5.4% (p=0.252) in control animals and 8.8% (p=0.247) in transgenic pigs (Figure 4.14 D).

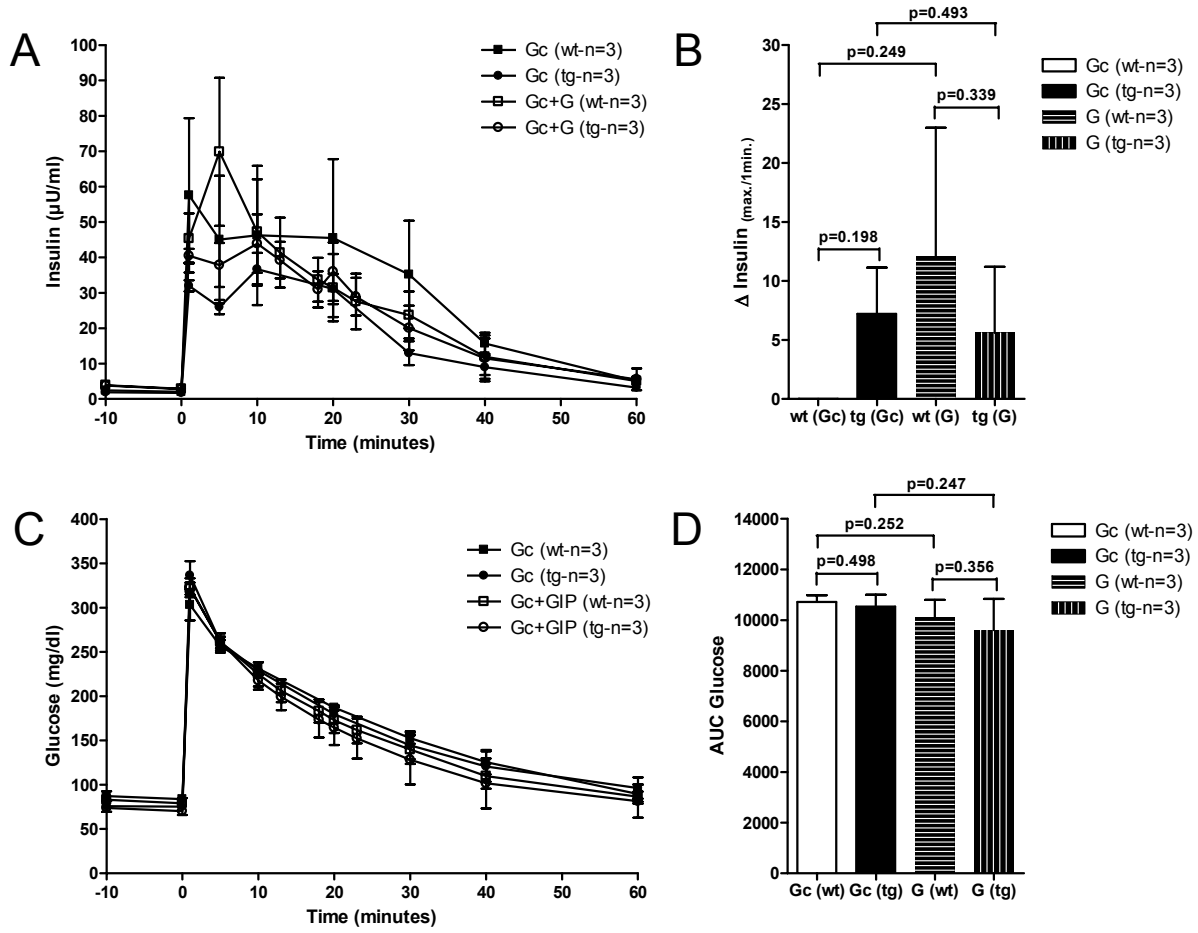

Figure 4.14: Minor impairment of the insulinotropic effect of GIP in GIPR^{dn} transgenic pigs 8 weeks of age

Intravenous glucose tolerance test (IVGTT) and IVGTT in combination with application of porcine GIP in 8-week-old GIPR^{dn} transgenic pigs (tg) and control animals (wt); **(A)** serum insulin levels; **(B)** AUC insulin: area under the insulin curve; **(C)** serum glucose levels; **(D)** AUC glucose: area under the glucose curve; (Gc) glucose; (G) glucose + GIP; data are means ± SEM; n: number of animals investigated.

In conclusion, GIPR^{dn} transgenic pigs show an impaired insulinotropic effect of GIP compared to non-transgenic control animals being more pronounced in 7-month-old pigs compared to animals at 8 weeks of age.

4.9 Reduced insulin secretion in Exendin-4-stimulated older GIPR^{dn} transgenic pigs

The insulinotropic action mediated by the GLP-1 receptor was evaluated by an Exendin-4 stimulation test. Exendin-4 is a naturally occurring, potent GLP-1 receptor agonist due to its resistance against dipeptidyl-peptidase 4 and the resulting long half-life. Glucose (0.5 g/kg BW) was administered intravenously either alone or in combination with synthetic Exendin-4 (10 pmol/kg BW). Following glucose administration, 7-month-old GIPR^{dn} transgenic pigs demonstrated a visible but not significant reduction of insulin secretion compared to non-transgenic control animals which is related to one GIPR^{dn} transgenic pig showing exorbitant higher insulin levels compared to the rest of the transgenic group (Figure 4.15 A; see also Figure 4.10 B). Exendin-4 potentiated insulin secretion in GIPR^{dn} transgenic pigs to a lesser extent than in controls but to a higher extent than after glucose + GIP stimulation (Figure 4.15 A; Figure 4.13 A). Comparison of $\Delta Insulin_{(max./1min.)}$ between GIPR^{dn} transgenic pigs and non-transgenic controls revealed a distinct difference for stimulation with glucose + Exendin-4 ($p=0.052$) but only a minimal difference after having received only glucose (Figure 4.15 B). Additionally, the AUC for glucose following stimulation with glucose + Exendin-4 was significantly larger ($p<0.05$) in transgenic pigs, while no significant difference ($p=0.145$) was observed after glucose stimulation (Figure 4.15 D). Exogenous Exendin-4 had the ability to reduce the AUC for glucose 24.5% in control animals but only 9.3% in GIPR^{dn} transgenic pigs (Figure 4.15 D).

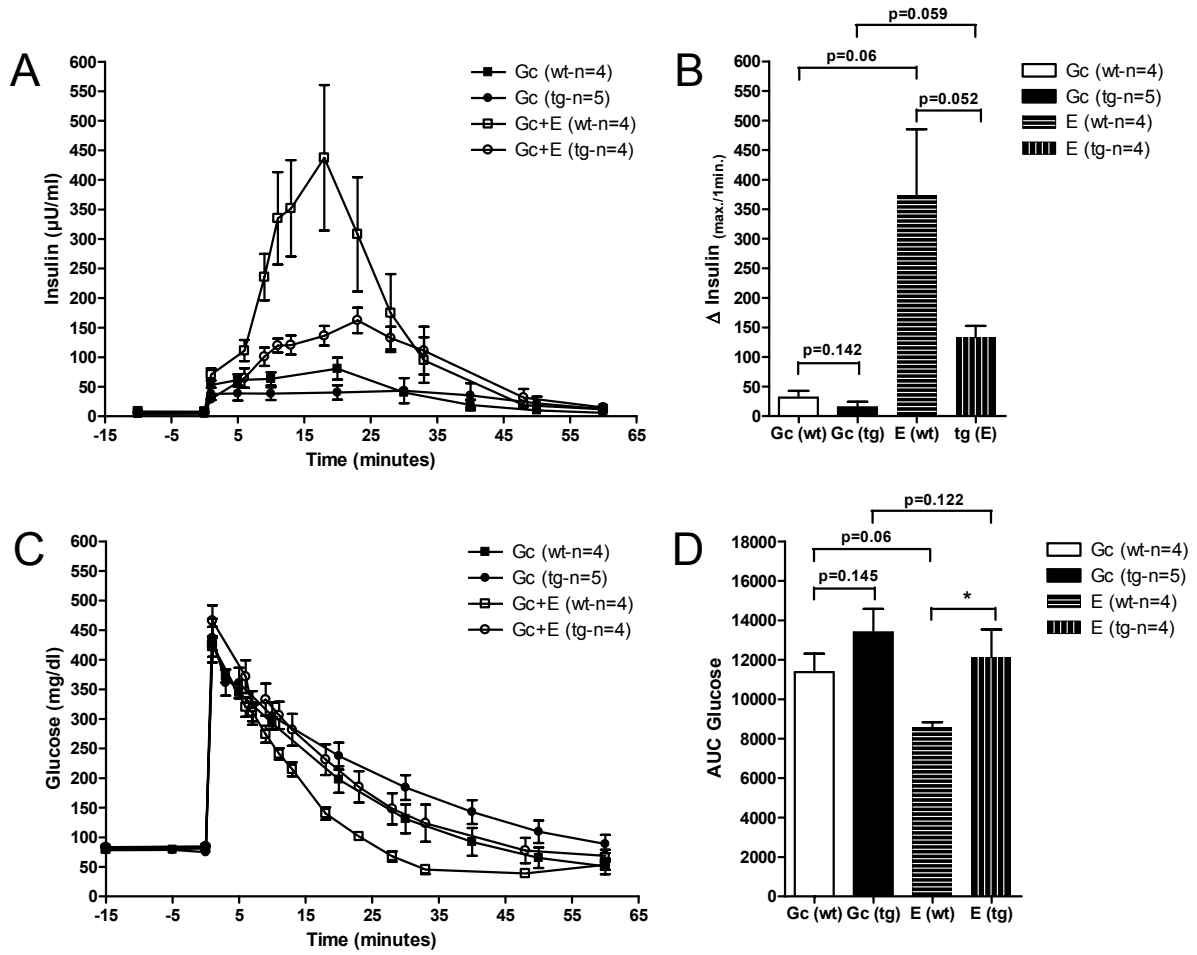

Figure 4.15: Reduced insulin secretion induced by glucose + Exendin-4 application in GIPR^{dn} transgenic pigs

Intravenous glucose tolerance test (IVGTT) and IVGTT in combination with application of synthetic Exendin-4 in 7-month-old GIPR^{dn} transgenic pigs (tg) and control animals (wt); **(A)** serum insulin levels; **(B)** Δ Insulin$_{(max./1min.)}$ of serum insulin levels; **(C)** serum glucose levels; **(D)** AUC glucose: area under the glucose curve; (Gc) glucose; (E) glucose + Exendin-4; data are means ± SEM; *: p<0.05 vs. control; n: number of animals investigated.

In contrast, Exendin-4 potentiated insulin secretion in 8-week-old transgenic pigs to the same extent as in non-transgenic control animals (Figure 4.16 A). Following glucose + Exendin-4 stimulation, Δ Insulin$_{(max./1min.)}$ of transgenic and wild-type pigs rose by 69.9 µU/ml (p=0.124) and 80.5 µU/ml (p=0.249) compared to glucose stimulation, respectively (Figure 4.16 B). Insulin levels after glucose stimulation were visibly but not significantly reduced in GIPR^{dn} transgenic pigs compared to controls

(Figure 4.16 A). Accordingly, serum glucose concentrations were equal between the groups after glucose and glucose + Exendin-4 stimulation (Figure 4.16 C). Exendin-4 was able to reduce the AUC for glucose 13.2% and 14.5% in GIPR^{dn} transgenic pigs and non-transgenic controls, respectively (Figure 4.16 D).

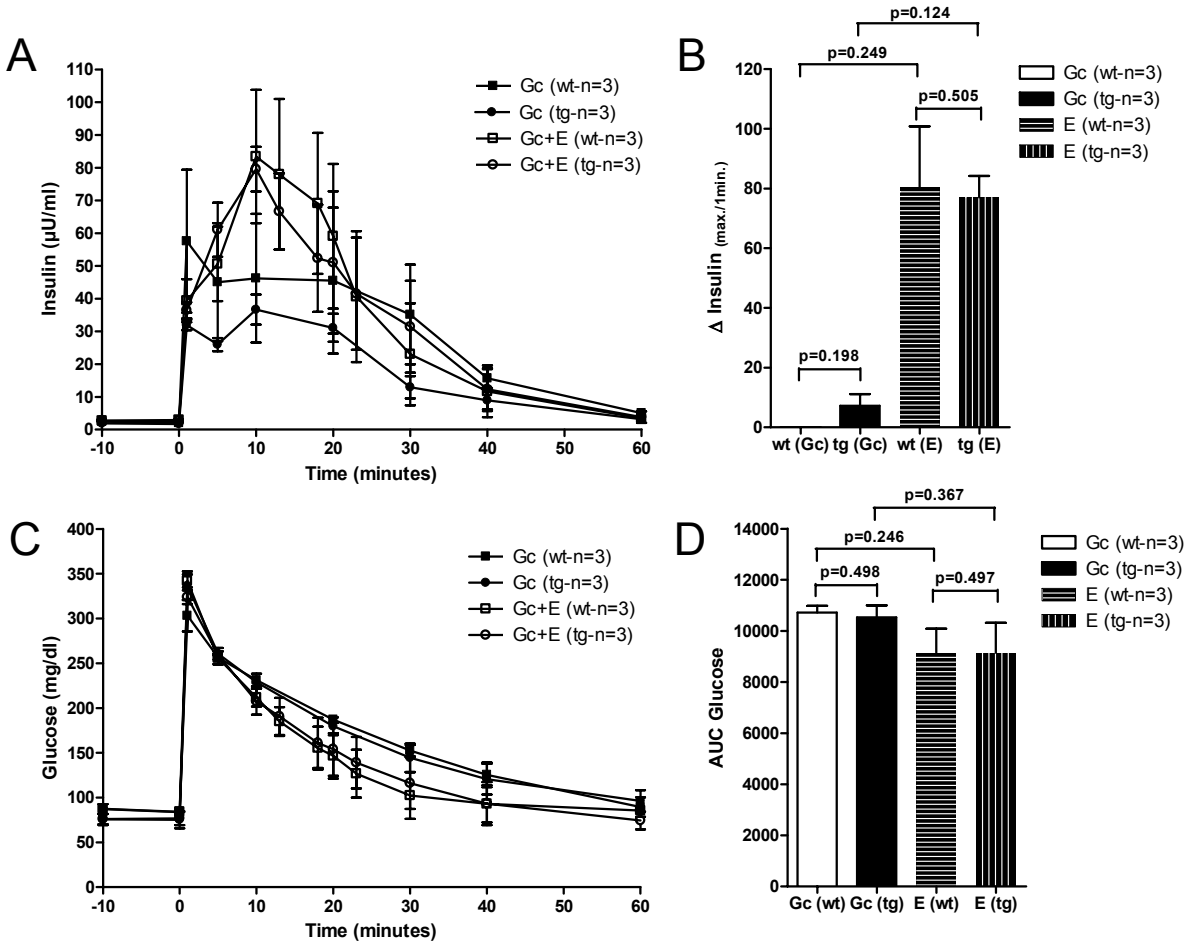

Figure 4.16: Normal insulin secretion following intravenous Exendin-4 application in 8-weeks-old GIPR^{dn} transgenic pigs

Intravenous glucose tolerance test (IVGTT) and IVGTT in combination with application of synthetic Exendin-4 in 8-week-old GIPR^{dn} transgenic pigs (tg) and control animals (wt); **(A)** serum insulin levels; **(B)** Δ Insulin$_{(max./1min.)}$ of serum insulin levels; **(C)** serum glucose levels; **(D)** AUC glucose: area under the glucose curve; (Gc) glucose; (E) glucose + Exendin-4; data are means ± SEM; n: number of animals investigated.

To summarize, insulin secretion following stimulation with glucose + Exendin-4 is equal in GIPR^{dn} transgenic and control pigs at 8 weeks of age but reduced in 7-month-old transgenic animals compared to controls.

4.10 Reduced islet and β-cell mass in older GIPR^{dn} transgenic pigs

In order to clarify whether impaired intravenous glucose tolerance, reduced insulin secretion capacity shown in a glucagon stimulation test as well as reduced insulin secretion following glucose + Exendin-4 stimulation in older GIPR^{dn} transgenic pigs might be caused by alterations in islet structure and/or islet integrity, quantitative islet isolation as well as quantitative stereological analyses were performed in 12 to 13-month-old GIPR^{dn} transgenic pigs (n=3) and three age matched non-transgenic littermate control animals of the F1-generation originating from founder boar #50 and #51. To determine these parameters each organ was divided into two portions along a clearly defined anatomical structure (see Figure 3.6). The left pancreatic lobe was processed for islet isolation using a protocol which is routinely used to isolate pancreatic islets for transplantation purposes (Krickhahn et al. 2001) while the remnant organ was used for quantitative stereological analyses.

4.10.1 Isolation of islets of Langerhans

The six isolations from control and transgenic pancreata were performed without any technical problems. The isolation endpoint in both groups ranged between 20 and 25 minutes, a time frame that was previously determined for the specific batches of collagenase and neutral protease. The results, summarized in Table 4.2, show significant differences in islet numbers, i.e., endocrine cell mass, between the two groups ($p<0.05$). GIPR^{dn} transgenic pigs contained approximately fourteen times less islets in their pancreas compared to the controls. Vitality and purity of islets was identical in both groups (Table 4.2) and islets of both groups showed a tendency to fragment (not documented). Dithizone stained samples (100 µl each) obtained after the digest of the pancreas of each animal were qualitatively assessed and revealed a clearly visible difference between transgenic and non-transgenic pigs regarding islet

size but especially islet number. Samples of GIPR^{dn} transgenic pigs showed fewer islets and islets were smaller in size than samples of control animals.

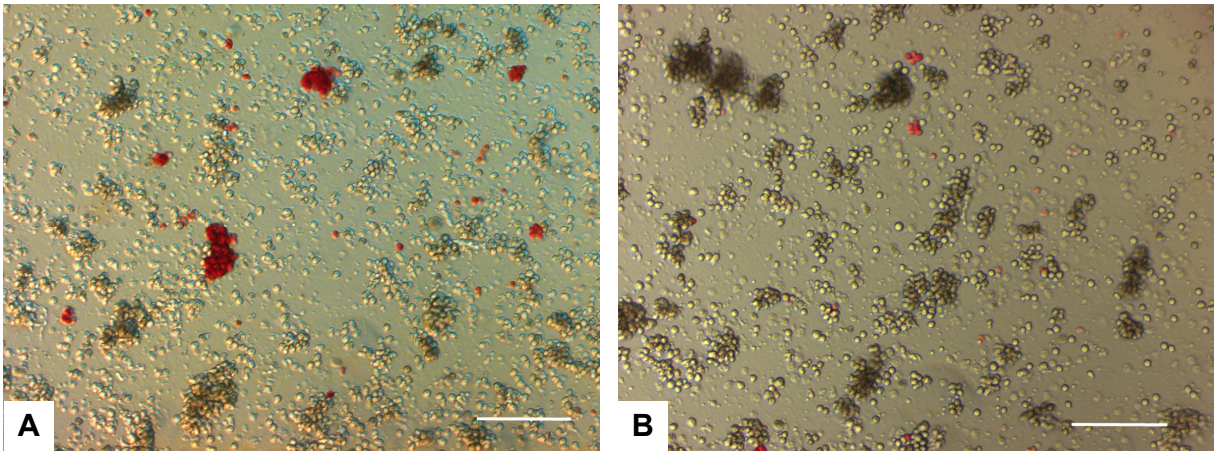

Figure 4.17: Representative dithizone stained samples originating from the left pancreatic lobe of a pancreas from a transgenic and a wild-type pig after completion of the digest

Qualitative assessment of digested samples from the pancreas of control pigs **(A)** show several islets as well as islet fragments per field of view; samples from GIPR^{dn} transgenic pigs **(B)** show few islet fragments per field of view; scale bar 200 µm.

Table 4.2: Islet isolation results using the left pancreatic lobes of non-transgenic (wt) and GIPR^{dn} transgenic pigs (n=3 in each group)

Type of Pig	Total IEQ Purified	Total IEQ/ g Organ	Islet Purity (%)*	Islet Vitality (%)*
wt #1	72,673	889.71	95	95
wt #2	90,260	1519.53	85	80
wt #3	71,658	1119.66	85	80
mean ± SEM	**78,197 ± 6,038**	**1176.23 ± 184**	**88.3 ± 3.33**	**85 ± 5.0**
tg #1	4,053	50.66	85	80
tg #2	6,026	81.76	85	80
tg #3	6,240	89.14	85	80
mean ± SEM	**5,439 ± 696**	**73.85 ± 11.79**	**85**	**80**

IEQ: islet equivalent (islet of 150 µm in size); * estimation by two independent individuals after microscopic inspection.

In addition, qualitative assessment of dithizone stained frozen sections from samples of all left pancreatic lobes used for islet isolation also revealed a clearly visible difference between the two groups (Figure 4.19). While small and medium-sized islets could be detected in great quantities in non-transgenic pigs, dithizone stained frozen sections of transgenic pigs showed only few small and almost none medium-sized islets. Frozen sections immunohistochemically stained for insulin also revealed islets of Langerhans less in number and smaller in size in GIPR^{dn} transgenic animals compared to the control group (Figure 4.18). Thus, these results are consistent with low islet recovery in GIPR^{dn} transgenic pigs.

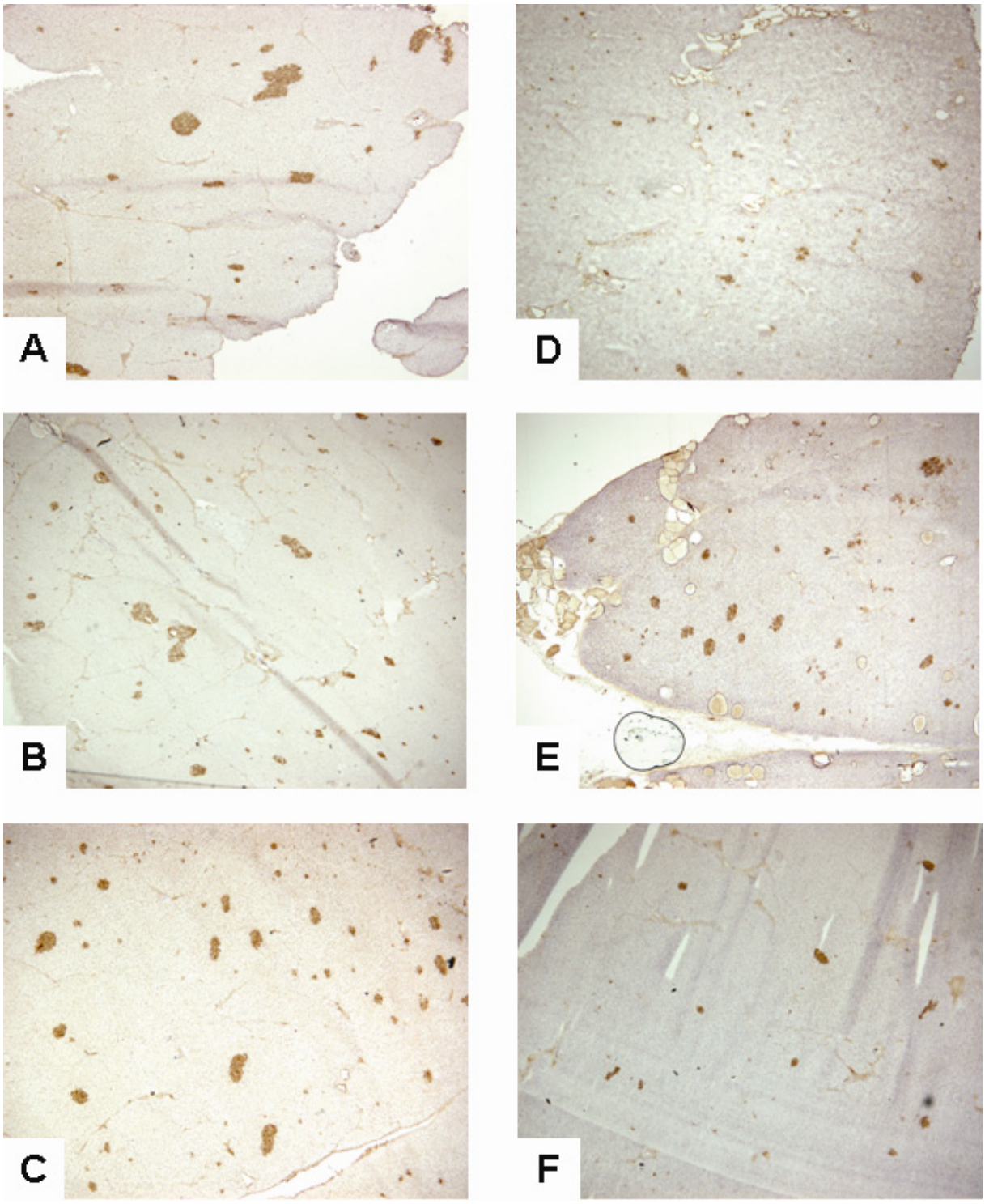

Figure 4.18: Reduced islet number and islet size in GIPR^{dn} transgenic pigs compared to non-transgenic littermate controls

Immunohistochemistry for insulin of frozen sections from tissue samples of the left pancreatic lobe; **(A/B/C)** non-transgenic control pigs #96, #11, #12 of the F1-generation; **(D/E/F)** GIPR^{dn} transgenic pigs #97, #10, #91 of the F1-generation; magnification 4 x.

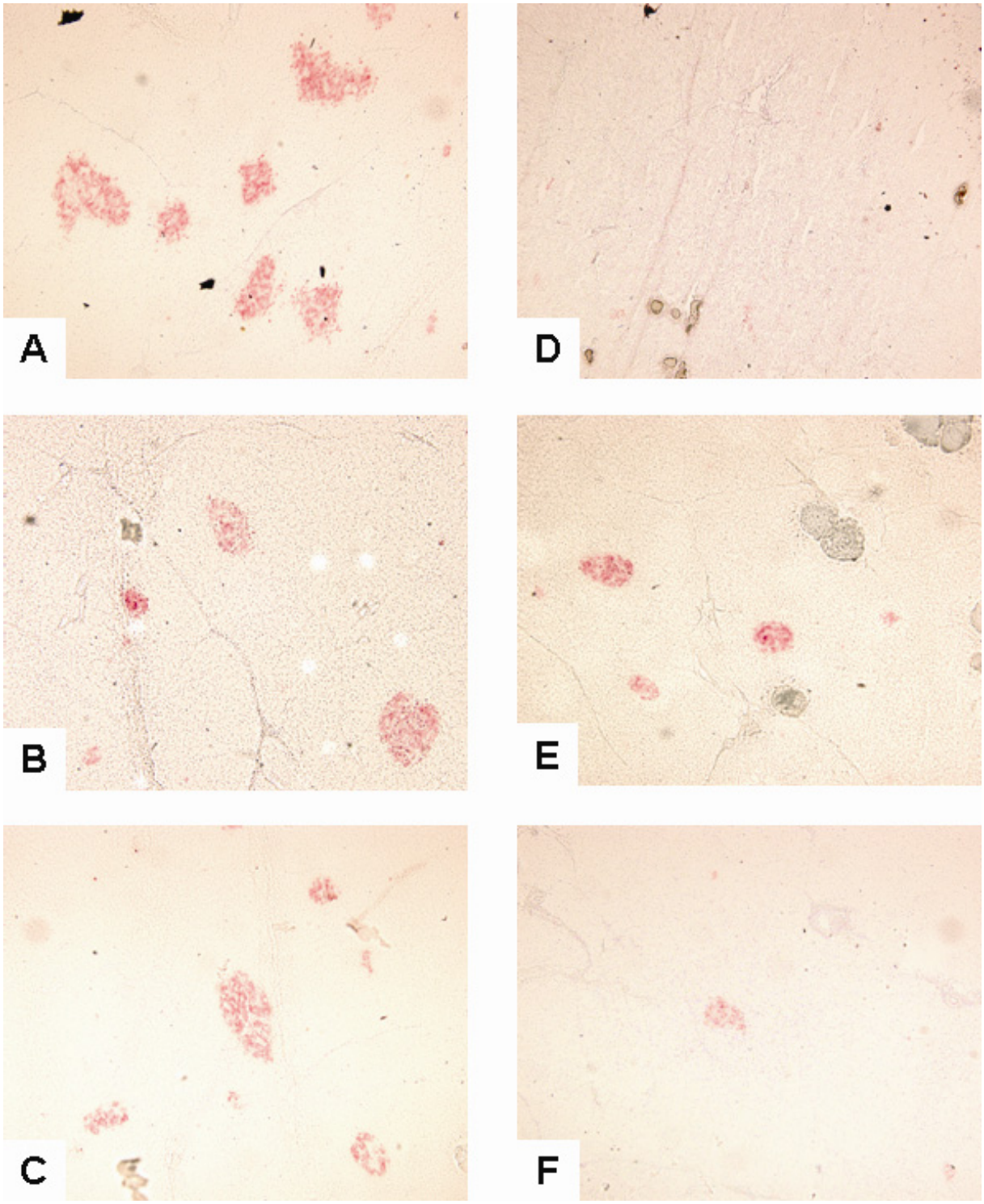

Figure 4.19: Reduced islet number and islet size in GIPR^{dn} transgenic pigs compared to non-transgenic littermate controls

Dithizone stained frozen sections from tissue samples of the left pancreatic lobe; **(A/B/C)** non-transgenic control pigs #96, #11, #12 of the F1-generation; **(D/E/F)** GIPR^{dn} transgenic pigs #97, #10, #91 of the F1-generation; magnification 10 x.

4.10.2 Quantitative stereological analyses

The findings of the quantitative islet isolation procedures were confirmed by quantitative stereological investigations, using the remnant pancreas. Previous qualitative assessment of the organ as well as of H&E stained sections revealed that gross morphology and histological appearance of the exocrine pancreas was unchanged in transgenic pigs. In H&E stained sections, pancreatic islet profiles of $GIPR^{dn}$ transgenic pigs appeared to be smaller in size but especially in number. In addition, distinct differences between the two investigated animal groups were discovered in quantitative stereological parameters. The total islet volume ($V_{(Islet,Pan)}$) was significantly lower (72%; $p<0.05$) in transgenic pigs compared to non-transgenic littermate control animals (Figure 4.20 A). The same was true for the volume density of the islets in the pancreas ($Vv_{(Islet/Pan)}$) (72% reduction in transgenic pigs; $p=0.05$); (Figure 4.20 B). Also, the total volume of "islet-associated" β-cells ($V_{(\beta\text{-cell,Islet})}$) was considerably reduced (75%; $p<0.05$) in transgenic pigs (Figure 4.20 C). The volume density of β-cells in the islets ($Vv_{(\beta\text{-cell/Islet})}$) was diminished by 11% ($p=0.052$) in the group of transgenic pigs compared to the controls (Figure 4.20 D). The total volume of the β-cells including isolated β-cells ($V_{(\beta\text{-cell,Pan})}$) was also significantly reduced (71%, $p<0.05$) in $GIPR^{dn}$ transgenic pigs compared to their non-transgenic littermate controls (Figure 4.20 E). A clear reduction could also be detected for the volume density of the β-cells in the pancreas ($Vv_{(\beta\text{-cell/Pan})}$) of transgenic pigs (71%, $p<0.05$) (Figure 4.20 F). In contrast, the total volume of isolated β-cells (single insulin positive cells and small β-cell clusters) in the pancreas ($V_{(iso\beta\text{-cell,Pan})}$), a parameter indicating islet neogenesis, was not different between the two groups ($p=0.199$) (Figure 4.20 G). According to that, the volume density of isolated β-cells in the pancreas ($Vv_{(iso\beta\text{-cell/Pan})}$) didn't reveal any difference between the two groups ($p=0.198$) (Figure 4.20 H). Representative pancreatic sections from $GIPR^{dn}$ transgenic pigs and control littermates are shown in Figure 4.21 illustrating the morphometric findings. These data demonstrate a marked reduction of pancreatic islet and β-cell mass in transgenic pigs expressing a $GIPR^{dn}$ in their pancreatic islets, however there was no clear evidence for disturbed islet neogenesis.

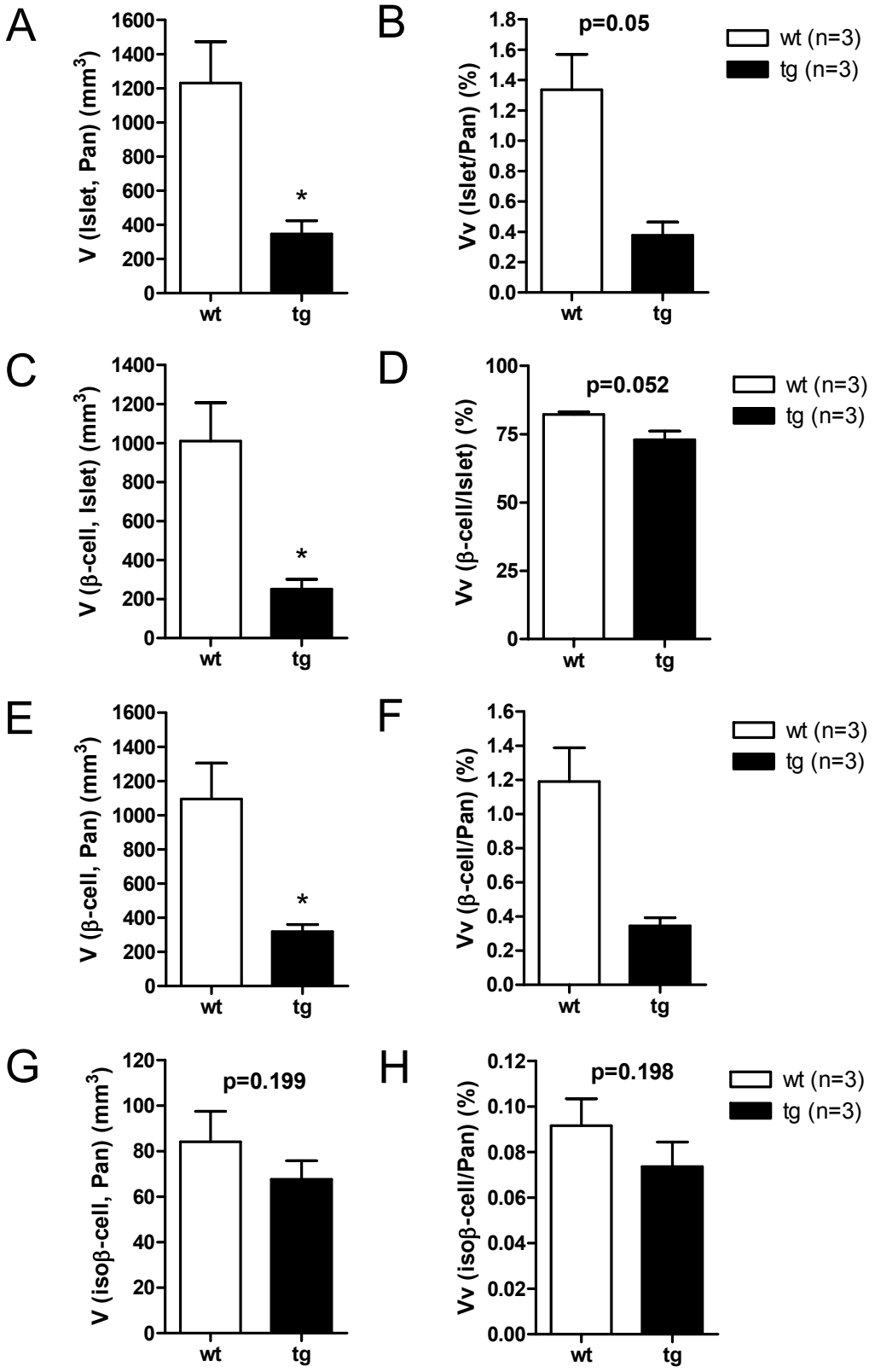

Figure 4.20: Reduced islet and β-cell mass in GIPR^{dn} transgenic pigs

Quantitative stereological analyses of the pancreas of transgenic (tg) and control (wt) pigs; **(A/B)** Total volume ($V_{(Islet,Pan)}$) and volume density ($Vv_{(Islet/Pan)}$) of the islets in the pancreas; **(C/D)** Total volume ($V_{(β\text{-}cell,Islet)}$) and volume density ($Vv_{(β\text{-}cell/Islet)}$) of the β-cells in the islets; **(E/F)** Total volume ($V_{(β\text{-}cell,Pan)}$) and volume density ($Vv_{(β\text{-}cell/Pan)}$) of the β-cells in the pancreas; **(G/H)** Total volume ($V_{(iso\ β\text{-}cell,Pan)}$) and volume density ($Vv_{(iso\ β\text{-}cell/Pan)}$) of isolated β-cells in the pancreas; data are means ± SEM; n: number of animals investigated; *: $p<0.05$ vs. control.

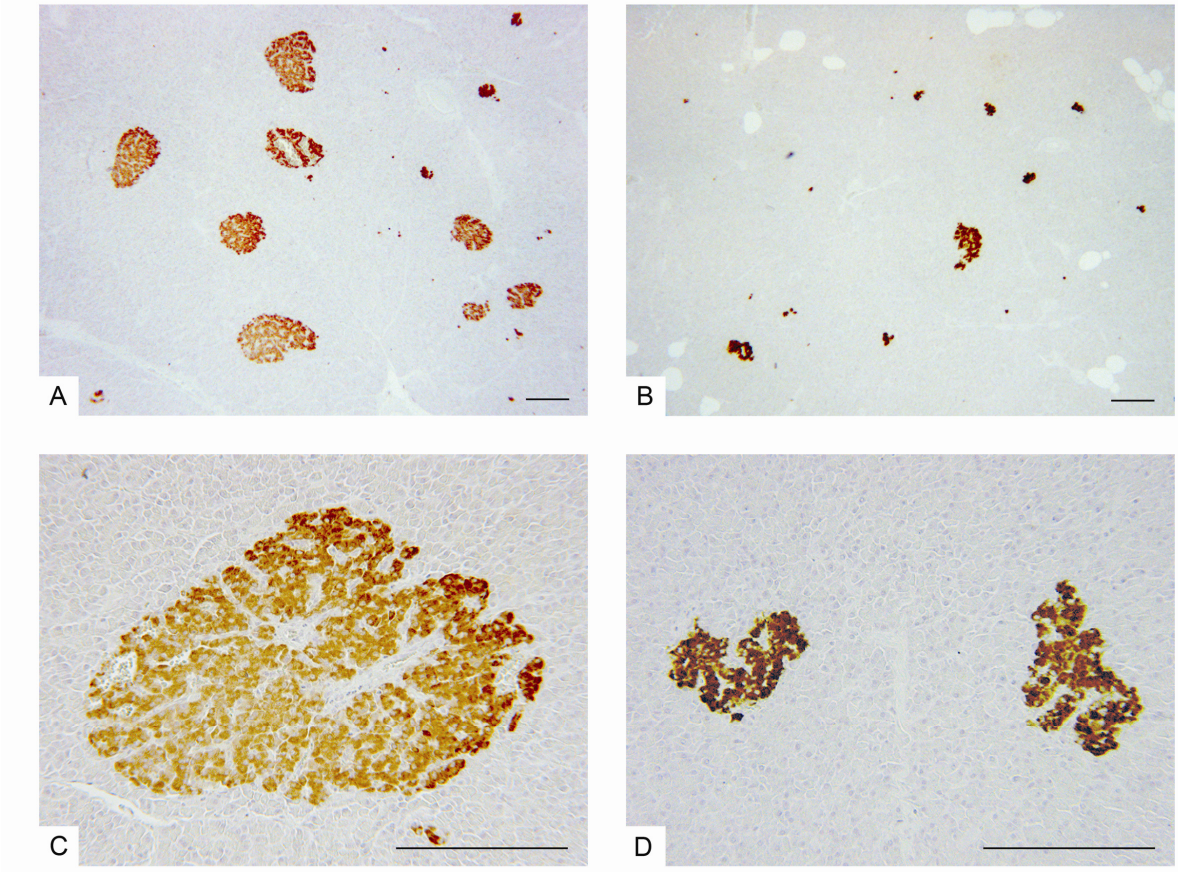

Figure 4.21: Representative pancreatic sections from GIPR^{dn} transgenic pigs and control littermates

Immunohistochemistry for insulin of pancreatic sections from GIPR^{dn} transgenic pigs **(B/D)** and non-transgenic littermate controls **(A/C)** illustrating the morphometric findings: GIPR^{dn} transgenic pigs show islet profiles reduced in numerical area density; **(A/B)** magnification 2.5 x; scale bar 200 µm; **(C/D)** magnification 10 x; scale bar 200 µm.

5 Discussion

This work included the generation and analysis of the first large animal model characterized by a defective GIPR signaling, which is a consistent finding in type 2 diabetic patients with hitherto unclear pathogenetic relevance.

5.1 Generation of GIPR^{dn} transgenic pigs by lentiviral gene transfer

For the generation of this pig model, a gene transfer technology based on lentiviral vectors was used. This technique was chosen since recently a reproducibly high efficiency of lentviral gene transfer into porcine and bovine oocytes and zygotes was shown (Hofmann et al. 2003). In general, the efficiency of DNA microinjection, the most widespread technology to generate transgenic animals (Clark & Whitelaw 2003), is low. In the mouse, approximately 2.6% of transgenic offspring per injected & transferred embryos can be obtained while in the pig the efficiency is even lower ranging at 0.9% (Wall, 1996). In contrast, generation of transgenic pigs carrying the green fluorescent protein (GFP) gene under the control of the ubiquitously expressing phosphoglycerate kinase promoter (PGK) by lentiviral gene transfer revealed 70% of the born animals (13.1% of infected & transferred embryos) being transgenic (Hofmann et al. 2003). Generation of GIPR^{dn} transgenic pigs using the same lentiviral vector backbone based on the human immunodeficiency virus-1 (HIV-1) was little less efficient. Here, 47.3% of all born pigs were transgenic (8% of infected & transferred embryos). Another group that generated transgenic pigs on the basis of an equine infectious anemia virus derived vector achieved 92% of transgenic pigs (31% of the transferred embryos) (Whitelaw et al. 2004). Lentiviral vectors integrate as a single-copy per integration site, however, animals can carry more than one lentiviral integrant. In the two studies previously mentioned, founder pigs revealed one up to twenty (mean 4.6 ± 0.9) lentiviral integrants (Hofmann et al. 2003) or one to five integrants (Whitelaw et al. 2004) by Southern blot analyses. Transgene copy number was determined in seven GIPR^{dn} transgenic founder animals (two animals died shortly after birth and were not analyzed for transgene integration but were determined transgenic by PCR) and revealed either one or two integration sites.

Germline transmission as well as segregation of the integration sites according to the Mendelian rules could be determined by Southern blot analyses of pigs of the F1- and F2-generation originating from two founder boars (#50 and #51).

The transgenesis rate as well as the number of integration sites was lower in GIPR^{dn} transgenic pigs as it has been previously reported for pigs generated by lentiviral gene transfer (Hofmann et al. 2003; Whitelaw et al. 2004). This could be related to a lower virus titer of the LV-RIP2-GIPR^{dn} virus that was used. The yield of different virus preparations is subject to fluctuation and can vary from $5x10^8$ to $2x10^{10}$ infectious units/ml (Hofmann, personal communication). The injection volume that can be transferred into the perivitelline space is limited. Thus, a lower virus titer leads to injection of a lower total number of infectious particles. However, this suspicion cannot be verified or ruled out in this case as the titer of LV-RIP2-GIPR^{dn} was not determined. The biological virus titer of lentiviral vectors carrying the green fluorescent protein can be determined by Fluorescence Activated Cell Sorting (FACS) analyses of infected cells. The virus titer of LV-RIP2-GIPR^{dn} could have been evaluated by quantitative determination of viral proteins like the reverse transcriptase or p24, a major core protein of the HI-virus, using an ELISA. But this technique also accounts for inactive particles leading to a less accurate result.

A lower transgenesis rate with 12% of the born pigs being transgenic (2.3% of the transferred embryos) coming along with a lower virus titer as compared to the lentiviral construct LV-PGK-GFP (described above) was reported in GFP transgenic pigs using the skin-specific human keratin K14 gene promoter (Hofmann et al. 2003; Hofmann 2006a). Another possibility that would explain the reduced integration efficiency of LV-RIP2-GIPR^{dn} is the difficulty to control the volume of virus delivered into the perivitelline space during the injection (Lois et al. 2002). It has been reported in mice, that incubation of denuded embryos in a lentiviral suspension allows better control of the number of proviral integration sites per genome (Lois et al. 2002). However, this method was found to be not practical for the use in pigs due to the high embryonic losses after denudation.

In summary, generation of GIPR^{dn} transgenic pigs by lentiviral gene transfer was 8-fold more efficient as compared to the average success rates of pronuclear DNA microinjection. GIPR^{dn} transgenic founder pigs showed one or two integration sites of the transgene and germline transmission was proven.

5.2 Expression of the GIPR^{dn} transgene

Expression of the transgene was analyzed in isolated porcine islets of Langerhans from GIPR^{dn} transgenic pigs by RT-PCR. Pigs of the F1-generation, 12 to13-months of age, originating from founder boar #50 and #51 and carrying either one or two integration sites were tested. Expression of the GIPR^{dn} transgene could be determined in all transgenic animals although the intensity of the signals was not equal in all three animals evaluated. Signals from cDNA of islets from GIPR^{dn} transgenic pig #97 and #10 were less intense than signals from pig #91. As the same result was obtained for analysis of the presence of β-actin mRNA to control reverse transcription efficiency, it was presumed that the weaker signals obtained by amplification of GIPR^{dn} transcripts from islets of pig #97 and #10 may be caused rather by less efficient reverse transcription or differential RNA quality than by different expression levels. However, a correlation between proviral copy number and transgene expression levels has been reported previously (Hofmann et al. 2003; Lois et al. 2002). Thus, different expression levels of the GIPR^{dn} transgene between the individual pigs could have contributed to the difference in signal intensity because GIPR^{dn} transgenic pigs #97 and #10 have one integration site while pig #91 has two integration sites of the transgene.

However, the presence of GIPR^{dn} transcripts does not necessarily mean that the GIPR^{dn} transgene is expressed on the protein level. Unfortunately, there is no antibody available which can differentiate between the endogenous GIPR and the GIPR^{dn}. However, the phenotypic changes observed in GIPR^{dn} transgenic pigs are indicative of the presence of the GIPR^{dn} protein.

One integration site of founder boar #50 did not result in offspring showing an aberrant phenotype compared to controls although GIPR^{dn} mRNA could be detected in the islets of Langerhans of one 5-month-old animal by RT-PCR (data not shown). This might be related to a low expression level and DNA-hypermethylation as has been previously described (Hofmann et al. 2006).

The results of expression analyses by RT-PCR indicate that the heterologous rat insulin 2 promoter is sufficient to direct the expression of GIPR^{dn} mRNAs in the pancreatic islets of pigs. It was previously shown that expression of the GIPR^{dn}

transgene under control of the rat insulin 2 promoter resulted in a distinct diabetic phenotype and disturbed development of the endocrine pancreas in mice (Herbach et al. 2005); (see below).

5.3 Normal blood glucose and serum fructosamine levels in GIPR^{dn} transgenic pigs

Blood glucose as well as serum fructosamine levels were evaluated to detect the presence of a diabetic phenotype in GIPR^{dn} transgenic pigs. Blood glucose levels were determined in fed 28-day-old animals (before weaning) and in 18 hours fasted pigs from the age of 35 days up to the age of 210 days. Blood was collected from the ear vein in order to reduce the amount of stress associated with the blood collection procedure as blood glucose levels are responsive to stress.

No significant differences in blood glucose levels could be determined in GIPR^{dn} transgenic pigs compared to their non-transgenic littermate control animals at any point of time investigated. Also, fasting blood glucose concentrations were always within or little below the reference range of blood glucose for pigs.

In addition, serum fructosamine levels were determined because this parameter is not responsive to stress and shows long-term glucose control. The analysis of serum fructosamine levels was preferred to the determination of HbA_{1c} because porcine erythrocytes contain only small intracellular glucose concentrations. Thus, porcine hemoglobin contains few glycosylated components (HbA_{1c}) due to a limited permeability of erythrocytes to glucose (Higgins et al. 1982). Therefore HbA_{1c} should not be considered as an appropriate indicator of glycemia in pigs as it is used in humans (Gabbay et al. 1977; Koenig et al. 1976). While fructosamine levels show glycemic control of the previous one to three weeks (dependent on the half-life of albumin), HbA_{1c} levels provide information of glucose control of the past ~120 days (dependent on the half-life of erythrocytes) which means that fructosamine levels are more sensible to changes in glucose control. In GIPR^{dn} transgenic pigs no obvious difference of serum fructosamine levels was detected compared to their non-transgenic littermate control animals at any point of time evaluated. Fructosamine levels were similar to those previously reported for the pig and showed a small but consistent rise with age in both groups (Larsen et al. 2001). At this point it can be

stated that GIPR^{dn} transgenic pigs do not develop an overt diabetic phenotype until an age of at least 15 months.

5.4 Impaired oral glucose tolerance in GIPR^{dn} transgenic pigs

The first important functional consequence of GIPR^{dn} expression in the pancreatic islets of transgenic pigs was reduced oral glucose tolerance associated with reduced initial insulin secretion noted in 5-month-old pigs. This observation is fully in line with the incretin concept. The findings that GIPR^{dn} transgenic pigs exhibit a normal glucose metabolism in the fasting state, indicated by normal fasting blood glucose and serum insulin levels, but abnormal glucose regulation and β-cell function in the postprandial state could also be observed in GIPR$^{-/-}$ mice (Miyawaki et al. 1999). Additionally, administration of a GIPR antibody to healthy mice before oral glucose challenge led to no change in fasting blood glucose showing that the incretin hormone GIP predominantly acts in the postabsorptive state (Baggio et al. 2000). These data are similar to impaired oral glucose tolerance observed in humans. Here, the initial insulin secretion within the first 30 minutes after nutrient ingestion is markedly decreased compared to subjects with normal glucose tolerance which leads to an elevated postprandial rise in glycemia (Leahy 2005). The first phase of insulin secretion seems to play a key role during food ingestion to prime the tissues for the incoming nutrients. It was reported that disruption of the first phase of insulin secretion in healthy humans causes glucose intolerance (Calles-Escandon & Robbins 1987; Luzi & DeFronzo 1989) while in type 2 diabetic patients, the first phase was improved following a period of intense glucose control (Bruce et al. 1988; Vague & Moulin 1982). Considering impaired intravenous glucose tolerance detected in 7-month-old and 10-month-old GIPR^{dn} transgenic pigs (see below), it cannot be excluded that incipient reduction of islet/β-cell mass in 5-month-old transgenic pigs could have contributed to impaired oral glucose tolerance in addition to the impaired incretin effect caused by the expression of a GIPR^{dn} in the islets of Langerhans.

5.5 Impaired intravenous glucose tolerance in older GIPR^{dn} transgenic pigs

Intravenous glucose tolerance tests were performed in pigs of three age groups: 8 weeks, 7 months and 10 months of age. At 10 month of age GIPR^{dn} transgenic pigs showed impaired intravenous glucose tolerance clearly determined by a significantly decelerated decline of glucose levels along with a significantly reduced insulin secretion. Unlike older pigs, 8-week-old animals did not show significant differences in glucose and insulin levels following an intravenous glucose load. Four out of five 7-month-old GIPR^{dn} transgenic pigs revealed significantly reduced insulin levels compared to control pigs, indicating impaired intravenous glucose tolerance. Surprisingly, the fifth transgenic pig showed exorbitantly higher insulin levels than the rest of the group. This observation may be related to individual differences concerning the beginning/progression of the reduction of islet/β-cell mass or glucose tolerance in general. However, this might not explain the large difference in insulin levels. Surprisingly, glucose levels of this pig were higher than glucose levels of the other transgenic pigs.

Irrespective of the results in 7-month-old GIPR^{dn} transgenic pigs, a progressive deterioration of intravenous glucose tolerance with age was detected that may correlate with a progressive decline of islet/β-cell mass. In general, impaired intravenous glucose tolerance cannot be explained by just an impaired incretin effect initiated by the expression of a GIPR^{dn} because the incretin effect is bypassed by intravenous administration of a glucose load.

In contrast, no difference of blood glucose levels of GIPR$^{-/-}$ mice following an intraperitoneal glucose tolerance test which is comparable to an IVGTT was found compared to controls (Miyawaki et al. 1999) (see below). However, release of incretin hormones can be stimulated to some degree due to the rise of glucose levels in the portal vein following an intraperitoneal glucose load (Gallwitz & Schmidt 1997).

5.6 Reduced insulin secretion capacity in GIPR^{dn} transgenic pigs

Glucagon stimulation tests were performed in 10-month-old pigs in order to elucidate a possible impairment of insulin secretion capacity in GIPR^{dn} transgenic pigs. This test has been previously used in diabetic humans to evaluate the remaining function

of the β-cell and therefore estimate the need for exogenous insulin (Faber & Binder 1977; Goeke 2002). GIPR^{dn} transgenic pigs showed a borderline significant reduction of insulin secretion in response to glucagon administration compared to littermate non-transgenic control animals. As the above mentioned impairment in intravenous glucose tolerance, this result points to alterations in islet structure and/or islet integrity, but could also be related to a disturbance of insulin secretion or a combination of both. The application of 1 mg glucagon might not have led to maximal insulin secretion considering the fact that stimulation with Exendin-4 led to notably higher insulin levels in transgenic pigs as well as in controls. Thus, application of more than 1 mg of glucagon might have resulted in an even more pronounced difference in insulin secretion capacity between GIPR^{dn} transgenic pigs and controls. The slightly reduced serum glucose levels of transgenic pigs may be related to less glycogen storage in the liver of transgenic pigs compared to controls. Normally, insulin is a potent suppressor of hepatic glucose production. Thus, insulin deficiency as well as insulin resistance leads to increased glycogenolysis and gluconeogenesis associated with increased hepatic output (Berger, 2000). In GIPR^{dn} transgenic pigs, insulin deficiency can be expected due to defective insulin secretion and/or reduced islet/β-cell mass. This could explain the slightly lower glucose levels in GIPR^{dn} transgenic pigs following stimulation with glucagon.

5.7 GIP/Exendin-4 stimulation test

GIP/Exendin-4 stimulation tests were performed in animals at 7 months and 8 weeks of age to evaluate whether a specific disturbance of GIPR signaling was achieved in transgenic pigs expressing a GIPR^{dn} in their pancreatic islets. Stimulation with only glucose served as a baseline for serum glucose and serum insulin levels. An intravenous glucose load only resulted in impaired insulin secretion of 7-month-old pigs but not of 8-week-old pigs (see intravenous glucose tolerance test). Exogenous GIP was able to stimulate insulin secretion of GIPR^{dn} transgenic and control pigs of both age groups, however this effect was less pronounced in transgenic animals than in controls. The difference of insulin levels following glucose + GIP stimulation between transgenic and control animals turned out to be smaller in the 8-week-old group compared to the 7-month-old group. A functional endogenous GIPR is still

present in GIPR^{dn} transgenic pigs although the endogenous GIPR has to compete with the GIPR^{dn} for the ligand GIP. Therefore a residual function of GIP-related insulin secretion after exogenous GIP stimulation can be expected. This is a different situation than in GIPR$^{-/-}$ mice. According to expectations, in vitro stimulation of isolated islets of Langerhans from GIPR$^{-/-}$ mice did not show residual GIP function (Miyawaki et al. 1999).

In addition, application of supraphysiological GIP levels leads to partial binding of GIP to the GLP-1 receptor that is intact in GIPR^{dn} transgenic pigs resulting in additional insulin secretion following GIP + glucose stimulation (Brubaker & Drucker 2002; Wheeler et al. 1993). Exendin-4, a potent GLP-1 receptor agonist, binds to an intact GLP-1 receptor in controls as well as in transgenic pigs. Normal insulin levels following stimulation with glucose (IVGTT) and glucose + Exendin-4 in 8-week-old transgenic pigs compared to control animals are indicative for a normal insulin secretion capacity and/or islet/β-cell mass. In contrast, stimulation with glucose (IVGTT) and glucose + Exendin-4 led to a diminished insulin secretion in 7-month-old GIPR^{dn} transgenic pigs which is most likely the consequence of an already existing reduction in islet/β-cell mass and/or altered insulin secretion capacity with this age. Thus, potentiation of glucose-stimulated insulin secretion by exogenous GIP administration can yield higher insulin levels in 8-week-old (presumably normal islet/β-cell mass) than in 7-month-old GIPR^{dn} transgenic pigs, explaining the smaller difference of insulin levels in the younger animals compared to controls. Also, Exendin-4 binds the GIPR to some degree following administration of high Exendin-4 concentrations (Gremlich et al. 1995; Brubaker & Drucker 2002). Thus, its effect may be partially reduced by the expression of the GIPR^{dn}. Anyhow, binding of Exendin-4 to the GIPR^{dn} could not visibly reduce insulin secretion because in 8-week-old transgenic pigs, insulin secretion following glucose + Exendin-4 stimulation was preserved. Due to the small number of animals investigated as well as moderate variations of insulin levels in the control group all previously described effects are clearly visible but not all of them reach statistical significance.

In summary, specificity of the dominant-negative approach used for to generate this animal model was proven by both the reduced potentiation of insulin secretion following stimulation with exogenous GIP in transgenic pigs of both age groups and the fully preserved effect of Exendin-4 in GIPR^{dn} transgenic pigs at 8 weeks of age.

However, due to the small number of animals investigated as well as variation of insulin levels of the control group, not all parameters reached statistical significance. Besides the application of a larger animal group, some other methods of resolution might be possible. An option to overcome the short half-life of GIP as well as binding of GIP to the GLP-1 receptor could be the infusion of physiological levels of exogenous GIP over a longer period of time instead of bolus administration. Additionally, stimulation studies with GIP and Exendin-4 using isolated porcine islets of Langerhans might be valuable. That way studies can be performed in a highly standardized manner. Freshly isolated islets in pigs but especially in rodents are commonly used to study the responsiveness of glucose and direct activators of signal transduction cascades. But it has to be taken into account that the acute secretory response may be blunted likely due to receptor damage by collagenase (Siegel & Creutzfeldt 1985). This might be especially problematic in the pig because only 25% of all porcine islets within the pancreas are well capsulated (Ulrichs et al. 1995) making the rest of them more susceptible to damage by collagenase digestion.

5.8 Reduced islet and β-cell mass in GIPR^{dn} transgenic pigs

The suspected reduction of islet/β-cell mass of GIPR^{dn} transgenic pigs was proven by quantitative islet isolation, using the left pancreatic lobe, as well as morphometric analyses of the remnant organ. Recovery of islet equivalents (i.e. islet 150 µm in diameter) in transgenic pigs was fourteen times less than in controls. Some criteria underline the significance of this result. It is well known that the number of islets vary widely between different breeds (Ulrichs et al. 1995). This factor of variance was reduced by the use of littermates for the analyses. The isolation method was highly standardized as it is routinely used for transplantation purposes. This is indicated among other things by the fact that digestion endpoints ranged only between 20-25 minutes, vitality and purity of the isolated islets were identical in both groups and variation of the recovery of total IEQ and accordingly total IEQ/g organ was minimal within one group. Dithizone stained frozen sections as well as sections immunostained for insulin originating from the left pancreatic lobe confirmed the isolation result.

Qualitative assessment of the remnant organ as well as of H&E stained sections revealed no abnormalities of gross morphology and histological appearance of the exocrine pancreas in transgenic pigs. Quantitative stereological analyses of the remnant organ were carried out using unbiased, model-independent stereological methods (Gundersen et al. 1988; Gundersen & Jensen 1987; Kroustrup & Gundersen 1983). The expression of a dominant-negative GIPR in pancreatic islets was found to be associated with a severe reduction of the total volumes as well as volume densities of islets and β-cells within the pancreas. In contrast, no significant difference was seen in the total volume and volume density of isolated β-cells (single insulin positive cells and small β-cell clusters) between $GIPR^{dn}$ transgenic pigs and control animals. Presence of isolated β-cells is indicative for islet neogenesis (Petrik et al. 1999; Xu et al. 1999). Thus, there was no clear evidence for disturbed islet neogenesis in $GIPR^{dn}$ transgenic pigs.

In summary, severe reduction of islet/β-cell mass could be determined by two different approaches, using one organ respectively. In the pig, the β-cell is predominant in both the ventral and the dorsal pancreas while α-cells exist mainly in the dorsal pancreas and pancreatic polypeptide containing cells are almost exclusively located in the ventral pancreas (Wieczorek et al. 1998; Jay et al. 1999). Somatostatin staining cells (δ-cells) also were located in the dorsal and ventral pancreas (Jay et al. 1999).

5.9 Concluding remarks showing $GIPR^{dn}$ transgenic pigs in the context of incretin hormone based mouse models

In summary, impaired intravenous glucose tolerance, reduced insulin secretion capacity in a GST as well as reduced insulin secretion following Exendin-4 stimulation in older $GIPR^{dn}$ transgenic pigs originally led to the suspicion of the presence of alterations in islet structure and/or islet integrity induced by the expression of a $GIPR^{dn}$ in the pancreatic islets. Quantitative islet isolation together with quantitative stereological analyses proved this suspicion by revealing a marked reduction of pancreatic islet and β-cell mass in $GIPR^{dn}$ transgenic pigs. These results are in line with previous evidence for a trophic action of GIP on β-cells in vitro. Proliferative as well as anti-apoptotic actions of GIP have been evaluated by the use

of heterologous cells transfected with the GIPR, β-cell lines, or murine islets and include activation of cAMP/PKA, PKA/CREB, MAPK and PI3K/Akt-PKB signaling modules, reductions in caspase-3 activity, and down-regulation of *Bax* gene transcription (Kim et al. 2005b; Ehses et al. 2003; Trumper et al. 2002; Trumper et al. 2001). Also, GIP was found to reduce biochemical markers associated with endoplasmatic reticulum (ER) stress in islet cell lines after induction of ER stress in vitro (Yusta et al. 2006). In vivo, infusion of GIP via a micro-osmotic pump into Vancouver diabetic fatty Zucker rats for two weeks led to down-regulation of the pro-apoptotic *Bax* gene and up-regulation of the anti-apoptotic *Bcl-2* gene (Kim et al. 2005b). GIPR knockout mice provided no evidence that GIPR action is required for the maintenance of islet and β-cell integrity in vivo (Hansotia & Drucker 2005; Pamir et al. 2003; Brubaker & Drucker 2004). Findings on islet morphology of $GIPR^{-/-}$ mice are quite controversial. $GIPR^{-/-}$ mice were shown to exhibit a paradoxical increase in relative β-cell area (referring to pancreas area) of ~45% (Pamir et al. 2003), whereas the total insulin content of pancreata and insulin mRNA levels in the fed state were significantly reduced compared to controls (Pamir et al. 2003). Elsewhere, no histological abnormalities were found in the pancreas of $GIPR^{-/-}$ mice (Miyawaki et al. 1999). Also, $GIPR^{-/-}$ mice showed no changes in islet-cell distribution (Pamir et al. 2003) and normal glucose tolerance in an intraperitoneal glucose tolerance test considering glucose and insulin levels (Miyawaki et al. 1999; Hansotia et al. 2004). These findings led to the conclusion that in vivo, the function of GIP is primarily restricted to that of an incretin (Hansotia et al. 2004).

It has been suggested that the relatively mild phenotype of $GIPR^{-/-}$ mice may result from compensatory mechanisms, e.g. the up-regulation of the GLP-1 system (Hansotia & Drucker 2005). Islets from $GIPR^{-/-}$ mice were shown to exhibit increased sensitivity to exogenous GLP-1 (Pamir et al. 2003). Compensatory mechanisms may also preserve the integrity of pancreatic islets in $GIPR^{-/-}$ mice. In $GLP\text{-}1R^{-/-}$ mice compensatory mechanisms are also present and might serve to enhance β-cell function in the absence of GLP-1 signaling. Mice lacking a functional GLP-1R exhibit increased GIP secretion following glucose challenge and increased GIP stimulated insulin release from the perfused pancreas or isolated islets (Flamez et al. 1999; Pederson et al. 1998). Thus, phenotypical characteristics of $GIPR^{-/-}$ and $GLP\text{-}1R^{-/-}$ mice might not reflect all essential functions of GIP and GLP-1. $GLP\text{-}1R^{-/-}$ mice

showed no aberrant total β-cell volume and numbers as well as similar insulin and glucagon content compared to controls. However, alterations in islet topography with α–cells being more centrally located than in controls (Ling et al. 2001) as well as abnormal glycemic excursion but no difference in insulin levels in an intraperitoneal glucose tolerance test were found (Hansotia et al. 2004; Scrocchi et al. 1996).

The functional overlap of the GIP and GLP-1 systems was demonstrated by the fact that double mutant mice (DIRKO) lacking functional expression of both the GIPR and the GLP-1R exhibited more severe glucose intolerance than the individual mutants following oral glucose challenge (Hansotia et al. 2004; Preitner et al. 2004).

However, also these double mutant animals did not develop diabetes mellitus indicated by normal fasting blood glucose levels. This was in accordance with findings that total pancreatic insulin content in the fasted state was normal and no apparent difference could be detected in the number and size of islets of DIRKO mice compared to controls.

In contrast, two lines of $GIPR^{dn}$ transgenic mice were characterized by early-onset diabetes mellitus (three weeks of age) indicated by severe glucosuria and fasting hyperglycemia (Volz 1997) coming along with disturbed development of the endocrine pancreas. Results obtained from $GIPR^{dn}$ transgenic mice are indicative for an essential role of the GIP/GIPR axis in the development of the endocrine pancreas. $GIPR^{dn}$ transgenic mice display a large reduction in islet and beta cell mass, and clear reduction of islet neogenesis at 10 days of age, a time point when incretin hormones are not yet essential for glucose homeostasis, and thus transgenic mice did not display hyperglycemia (Herbach et al. 2005).

However, the massive changes detected were unexpected especially in the context that a third line of $GIPR^{dn}$ transgenic mice showed reduced oral glucose tolerance, but neither a full-blown diabetes mellitus nor structural (islet cell distribution and composition) changes of the pancreatic islets.

The difference between diabetic $GIPR^{dn}$ transgenic mouse lines and the pig lines may be related to differences in expression levels of the transgene, possibly originating from species-dependent promoter activity. Moreover, proximity of the transgene integration site as well as the integrated copy number of the transgene could also influence transgene expression level. A high level of overexpression of a dominant-negative receptor may cause - in part - nonspecific effects, e.g. by

squelching of G proteins. It is possible that signal transduction pathways are disturbed in general in GIPR^{dn} transgenic mice, leading to a failure to increase intracellular cAMP levels. This may not only affect the GIP/GIPR axis but also the GLP-1/GLP-1R axis and maybe other components being involved in insulin secretion. Most likely due to the severe changes of the endocrine pancreas, neither stimulation with glucose nor glucose + GIP or glucose + GLP-1 was able to augment serum insulin levels in diabetic GIPR^{dn} transgenic mice in a subcutaneous glucose tolerance test. However, GLP-1 but not GIP was capable to reduce the AUC for glucose, which is most likely related to inhibitory effects of GLP-1 on glucagon secretion from the α-cells as has been shown in these mice (Herbach et al. 2005). In vitro signal transduction studies using isolated islets from diabetic GIPR^{dn} transgenic mice could not be performed so far since it was not possible to isolate intact islets from these mice. Thus, specific relation of the diabetic phenotype to the expression of the GIPR^{dn} transgene or possible differences concerning signal transduction between the 2 diabetic mouse lines and the glucose intolerant mouse line could not be proven so far. There is evidence that diabetic GIPR^{dn} mouse lines have more integrated copies of the transgene compared to the glucose intolerant mouse line which could have resulted in the phenotypic differences (Volz unpublished data).

It can be expected that GIPR^{dn} transgenic pigs exhibit some degree of insulin deficiency due to reduced islet/β-cell mass. In general, insulin deficiency has impact on various organs. The glucose uptake in adipose tissue is reduced. Thus, lipogenesis is low and lipolysis increased. Also, the uptake of glucose into skeletal muscle tissue is reduced. Further, disturbed amino acid uptake and thus protein synthesis as well as increased proteolysis leads to catabolism in muscular tissues. Also, glycogen synthase in the skeletal muscle being stimulated by insulin is less active. Increased glycogenolysis and gluconeogenesis are present in the liver (Berger 2000).

However, GIPR^{dn} transgenic pigs have not deteriorated to a full-blown diabetic phenotype so far, indicated by normal fasting blood glucose and serum fructosamine levels. There is no direct evidence for insulin resistance in GIPR^{dn} transgenic pigs. Neither fasting hyperinsulinemia nor hyperinsulinema following an oral glucose load are present. Although absolute insulin deficiency due to reduced β-cell mass might mask insulin resistance, presence of insulin resistance seems not likely because

GIPR^{dn} transgenic pigs have not developed a diabetic phenotype so far. The fact that transgenic pigs stay normoglycemic despite a distinct reduction of β-cell mass could even be related to an increased sensitivity of peripheral tissues to insulin (fat, skeletal muscle, liver).

Relative β-cell volume (β-cell area/exocrine area) of weight-matched type 2 diabetic patients was found to be decreased by 40-60% compared to controls. Interestingly, also subjects in a prediabetic state showed a 40% decrease in relative β-cell volume (Butler et al. 2003; Yoon et al. 2003). Evaluation of glucose metabolism of 60% pancreatectomized rats following a short period of regeneration for the β-cells (loss of β-cell mass was estimated 40% following the regeneration phase) revealed normoglycmia indicating that normal β-cell mass is more than adequate (Leahy et al. 1988). Thus, pigs might be able to tolerate a distinct loss of β-cell mass without developing a diabetic phenotype.

In summary, GIPR^{dn} transgenic pigs proved an essential role of the GIP/GIPR axis for the maintenance of long-term pancreatic islet integrity. Possible compensatory mechanisms might not be triggered because the endogenous GIPR is still present in GIPR^{dn} transgenic pigs as compared to single incretin receptor knockout mice. Even in DIRKO mice possible compensatory mechanisms of functionally related peptides to enhance β-cell function cannot be excluded (Hansotia et al. 2004). For example, PACAP receptors are known to be expressed on β-cells. Mice lacking a functional PAC 1 receptor revealed a reduced glucose-stimulated insulin secretion in vivo and in vitro (Jamen et al. 2000). Additionally, long-term glucose toxicity is absent in GIPR^{dn} transgenic pigs because they exhibit normal fasting glucose levels until at least 15 months of age. Importantly, a direct coherence that GIPR action is required for the maintenance of islet and β-cell mass has not been determined so far in a large animal model. The pig was chosen to generate this animal model because many physiological characteristics of the pig are more similar to the human than those of the mouse especially considering the gastrointestinal tract. Furthermore, the large size of a pig model facilitates a plethora of physiological and molecular studies as well as therapeutic trials that cannot be performed in the small rodent models.

6 Perspectives

GIPR^{dn} transgenic pigs seem to be a very valuable animal model for numerous further investigations. First, islet and β-cell mass should be determined in different age groups to narrow down the onset of the alterations within the endocrine pancreas. Additionally, a detailed characterization of the mechanisms by which GIP supports islet maintenance as well as the search for targets to bypass or overcome the GIPR signaling defect would be of great interest. This could be accomplished by quantitative evaluation of mitotic (for example by determination of the rate of DNA synthesis by enzyme-linked detection of 5-bromo-deoxyuridine (BrdU) incorporation or detection of Ki67-antigen via immunohistochemistry) and apoptotic indices (for example immunohistochemical detection of caspases, especially caspase-3, or TUNEL assay). Qualitative assessment of several test slides immunohistochemically stained for caspase-3 from pancreatic tissue of one GIPR^{dn} transgenic and one control pig did not show a visible striking difference between the two animals, although a greater number of samples and animals has to be evaluated quantitatively to obtain a definitive result. Second, it might be helpful to explore signaling pathway modules known to be involved in proliferative and anti-apoptotic actions of GIP on the RNA and protein level. In this context, holistic transcriptome and proteome analyses might be useful. As the expression of a dominant-negative GIPR mimics the situation in human type 2 diabetic patients whose insulinotropic action of GIP was found to be greatly reduced up to almost absent, findings from GIPR^{dn} transgenic pigs may give new insights into the pathogenetic consequences of impaired GIP action. Yet another interesting question this animal model could be used for would be the development of in vivo imaging techniques to assess the total islet cell mass of type 2 diabetic patients (Gotthardt et al. 2006). This would be very useful for evaluation of the etiopathology and response to therapeutics in type 2 diabetic patients as increased apoptosis coming along with reduced proliferation of β-cells plays an important pathogenetic role in type 2 diabetes mellitus. Additionally, GIPR^{dn} transgenic pigs might be very valuable for the development and preclinical evaluation of incretin modulatory therapies. Especially interesting is the question whether incretin hormone based therapeutics (incretin mimetics like Exendin-4; GLP-1 analogues; DPP-4-

inhibitors) are able to stimulate β-cell proliferation and –neogenesis and inhibit β-cell apoptosis in human type 2 diabetic patients as has been shown in rodents (Gallwitz 2006a; Mu et al. 2006). Proof of this suspicion in therapeutic trials using $GIPR^{dn}$ transgenic pigs would be especially valuable and therapeutic dosages could be evaluated in an animal species closely related to the human. Last, it will be interesting to see whether $GIPR^{dn}$ transgenic pigs develop diabetes with increasing age.

7 Summary

Transgenic pigs expressing a dominant-negative glucose-dependent insulinotropic polypeptide receptor – a novel animal model for studying the consequences of impaired incretin hormone function

The incretin hormones glucose-dependent insulinotropic polypeptide (GIP) and glucagon-like peptide-1 (GLP-1) are secreted by enteroendocrine cells in response to nutrients like fat and glucose and mediate the incretin effect. The incretin effect describes the phenomenon that an oral glucose load elicits a higher insulin response than an intravenous glucose infusion. In patients with type 2 diabetes mellitus, the overall incretin effect is reduced. This fact is mostly put down to an obviously lowered insulinotropic effect of GIP, while the effect of GLP-1 is vastly preserved. In order to better understand the consequences of an impaired function of GIP, knockout mice lacking a functional GIP receptor ($GIPR^{-/-}$) as well as transgenic mice expressing a dominant-negative GIPR ($GIPR^{dn}$) were established. While $GIPR^{-/-}$ mice show only relatively mild changes in glucose homeostasis, $GIPR^{dn}$ mice display a distinct diabetic phenotype due to disturbed development of the endocrine pancreas. To further clarify the underlying mechanisms we used an efficient gene transfer technology based on lentiviral vectors to generate transgenic pigs expressing a $GIPR^{dn}$ under the control of the rat insulin 2 gene promoter (RIP2). Expression of the $GIPR^{dn}$ transgene could be determined in isolated porcine islets of Langerhans by RT-PCR. As expected, the insulin release in response to intravenous administration of porcine GIP, which was evaluated in two age groups, turned out to be smaller in transgenic pigs compared to controls although the difference did not reach statistical significance in the younger animals. $GIPR^{dn}$ transgenic pigs develop normally and do not display diabetes mellitus up to at least 15 month of age. Weekly measured fasting blood glucose levels in transgenic animals did not show a significant difference compared to control pigs. The same was true for monthly determined fructosamine levels. However, $GIPR^{dn}$ transgenic pigs at 5 month of age exhibited a reduced initial insulin release and higher glucose levels in an oral glucose tolerance test than non-transgenic littermate controls. Intravenous glucose tolerance as well as

insulin secretion following intravenous injection of Exendin-4, a GLP-1 receptor agonist was preserved in younger GIPR^{dn} transgenic pigs, but impaired in older ones compared to non-transgenic controls. Impaired intravenous glucose tolerance, reduced glucagon-induced insulin secretion capacity and impaired insulin secretion following stimulation with Exendin-4 in older GIPR^{dn} transgenic pigs led to the assumption that expression of a GIPR^{dn} in the pancreatic islets might cause alterations in islet composition and/or islet integrity. Quantitative islet isolation as well as quantitative stereological analyses of the pancreas proved this assumption. Significantly diminished islet recovery in transgenic pigs compared to their non-transgenic littermate controls was determined by quantitative islet isolation. Quantitative stereological analyses of the pancreas revealed a marked reduction in islet and β-cell mass of GIPR^{dn} transgenic pigs, but no difference in isolated β-cells within the exocrine pancreas which is an indicator for islet neogenesis compared to controls.

These findings demonstrate for the first time that impaired GIPR function is sufficient to cause the loss of β-cell mass in a large animal model. Importantly, many physiological characteristics of the pig are more similar to the human than those of the mouse. Moreover, the large size of a pig model facilitates a plethora of physiological and molecular studies as well as therapeutic trials that cannot be performed in the small rodent models. Thus, the GIPR^{dn} transgenic pig is a novel, clinically relevant animal model for type 2 diabetes mellitus research.

8 Zusammenfassung

Expression eines dominant-negativen Rezeptors für das Glukose-abhängige insulinotrope Polypeptid in transgenen Schweinen – ein neues Tiermodell zur Untersuchung der Auswirkungen einer verminderten Inkretinhormonfunktion

Die Inkretinhormone glucose-dependent insulinotropic polypeptide (GIP) und glucagon-like peptide-1 werden infolge von Nahrungsreizen wie Glukose oder Fett von enteroendokrinen Zellen aus dem Darm ausgeschüttet und vermitteln den Inkretineffekt. Der Inkretineffekt beschreibt das Phänomen, dass eine orale Glukosegabe im Vergleich zu einer intravenösen Glukoseinfusion einen stärkeren Konzentrationsanstieg von Insulin im Blut auslöst. Bei Patienten mit Typ 2 Diabetes mellitus konnte eine deutlich reduzierte insulinotrope Wirkung von GIP detektiert werden, während die Wirkung von GLP-1 weitgehend erhalten bleibt. Um die Folgen einer gestörten Funktion von GIP besser zu verstehen, wurden GIP Rezeptor knockout Mäuse ($GIPR^{-/-}$) sowie transgene Mäuse, die einen dominant-negativen GIPR ($GIPR^{dn}$) exprimieren, erstellt. Während $GIPR^{-/-}$ Mäuse nur relativ geringe Veränderungen im Glukosemetabolismus zeigen, entwickeln $GIPR^{dn}$ transgene Mäuse einen ausgeprägten diabetischen Phänotyp infolge einer gestörten postnatalen Ausbildung des endokrinen Pankreas. Um ein Großtiermodell mit gestörter GIP-Funktion zu generieren, wurde eine hocheffiziente, auf lentiviralen Vektoren basierende Gentransfertechnologie verwendet. Transgene Schweine, die den $GIPR^{dn}$ unter der Kontrolle des Ratten Insulin 2 Promotors (RIP2) exprimieren, entwickeln sich normal. Mittels RT-PCR Analysen von RNA aus isolierten Langerhansschen Inseln konnte gezeigt werden, dass die mRNA für den mutierten GIPR im endokrinen Pankreas exprimiert wird. Erwartungsgemäß konnte bei $GIPR^{dn}$ transgenen Tieren zweier Altersgruppen im Vergleich zu nicht transgenen, gleich alten Kontrolltieren eine verminderte Insulinsekretion nach intravenöser Applikation von porcinem GIP festgestellt werden, wenn auch der Unterschied bei den jüngeren Tieren keine statistische Signifikanz erreichte. Anhand der Nüchternblutglukose- und Fruktosaminkonzentration konnte gezeigt werden, dass transgene Schweine bis zu

einem Alter von mindestens 15 Monaten keinen diabetischen Phänotyp entwickeln. Im oralen Glukosetoleranztest hingegen zeigten GIPR^{dn} transgene Schweine im Alter von fünf Monaten eine verminderte initiale Insulinfreisetzung sowie erhöhte Blutglukosespiegel. Die intravenöse Glukosetoleranz sowie die Insulinsekretion nach intravenöser Applikation von Exendin-4, einem GLP-1R Agonisten, war normal bei jüngeren transgenen Tieren und vermindert bei älteren GIPR^{dn} transgenen Schweinen im Vergleich zu gleich alten Kontrolltieren.

Aufgrund verminderter intravenöser Glukosetoleranz, reduzierter Glukagon-induzierter Insulinsekretionskapazität, sowie einer verminderten Insulinsekretion nach Stimulation mit Exendin-4 bei älteren GIPR^{dn} transgenen Schweinen im Vergleich zu gleich alten Kontrolltieren, wurde eine mögliche Auswirkung der Expression eines GIPR^{dn} in den Langerhansschen Inseln auf die Morphologie und/oder die Integrität der Langerhansschen Inseln vermutet. Eine quantitative Inselisolation sowie quantitativ-stereologische Untersuchungen des Pankreas konnten diesen Verdacht bestätigen. Aus Pancreata von GIPR^{dn} transgenen Schweinen konnten signifikant weniger Langerhanssche Inseln isoliert werden. Die quantitativ-stereologischen Untersuchungen zeigten signifikant geringere Gesamtinselvolumina sowie Gesamtbetazellvolumina bei transgenen Schweinen im Vergleich zu Kontrolltieren. Kein Unterschied ergab sich im Gesamtvolumen der isolierten β-Zellen im Pankreas, einem Indikator für Inselneogenese.

Diese Ergebnisse zeigen zum ersten Mal in einem Großtiermodell, dass die Expression eines GIPR^{dn} in den Langerhansschen Inseln ausreicht, um eine Verminderung der β-Zellmasse zu verursachen. Das Schwein als Modelltier ist von großem Vorteil, da physiologische Charakteristika vieler Organsysteme des Schweines dem Menschen ähnlicher sind als die der Maus. Das Modelltier Schwein erleichtert bzw. ermöglicht zudem zahlreiche physiologische, molekularbiologische sowie klinische Untersuchungen inklusive Therapiestudien. Somit kann das GIPR^{dn} transgene Schwein als ein klinisch relevantes Tiermodell für die Typ 2 Diabetesforschung gesehen werden.

9 Index of figures

10 Index of tables

11 Index of abbreviations

ATP	adenosine triphosphate
BMD	bone mineral density
BW	body weight
cAMP	cyclic adenosine monophosphate
CCK	cholecystokinin
CNS	central nervous system
cpm	counts per minute
CV	coefficient of variance
DAB	3,3´ diaminobenzidine tetrahydrochloride
DIRKO	double incretin receptor knockout
DPP-4	dipeptidyl peptidase 4
ds	double-stranded
DTZ	dithizone (diphenylthiocarbazone)
EIAV	equine infectious anemia virus
ELISA	enzyme-linked immunosorbent assay
ER	endoplasmatic reticulum
FACS	fluorescence activated cell sorting
FCS	fetal calf serum
FDA	fluorescein diacetate
FIV	feline immunodeficiency virus
GEFII/Epac2	guanine nucleotide exchange factor
GFP	green fluorescent protein
GH	growth hormone
GHRH	growth hormone releasing hormone
GIP	glucose-dependent insulinotropic polypeptide
$GIPR^{dn}$	dominant-negative glucose-dependent insulinotropic polypeptide receptor
GIPR	glucose-dependent-insulinotropic polypeptide receptor
$GIPR^{-/-}$	GIPR knockout
GLP-1	glucagon-like peptide-1

GLP-2	glucagon-like peptide-2
GLP-1R	glucagon-like peptide-1 receptor
GLP-1R$^{-/-}$	GLP-1R knockout
GST	glucagon stimulation test
HBSS	hanks balanced salt solution
hCG	human chorionic gonadotropin
H&E	hematoxylin and eosin
HIV-1	human immunodeficiency virus-1
H_2O_2	hydrogen peroxide
HP	horseradish peroxidase
IAPP	islet amyloid polypeptide
IEQ	islet equivalents
IPTT	intraperitoneal glucose tolerance test
IVGTT	intravenous glucose tolerance test
K_{ATP}	ATP-dependent potassium channel
kb	kilobase
K_{Ca}	calcium sensitive potassium channel
KO	knockout
K_v	voltage-dependent potassium channel
LDL	low-density lipoprotein
LTR	long terminal repeat
LV	lentivirus
MAPK	mitogen-activated protein kinase
mg	milligram
ml	milliliter
MLV	murine leukemia virus
NTC	non-template control
OGTT	oral glucose tolerance test
p.a.	pro analysis
PACAP	pituitary adenylyl cyclase – activating polypeptide
PBS	phosphate buffered saline
PC	prohormone convertase
PCR	polymerase chain reaction

PGK	phosphoglycerate kinase
PI	propidium iodide
PI3-kinase	phosphatidylinositol 3-kinase
PKA	protein kinase A
PKB	protein kinase B
PLA	phospholipase A
PMSG	pregnant mare serum gonadotropin
ppt	polypurine tract
RIA	radioimmunoassay
RIP2	rat insulin 2 promoter
RNase	ribonuclease
RRE	*rev* responsive element
RT	room temperature
RT-PCR	reverse transcription PCR
SDS	sodium dodecyl sulphate
SIN	self-inactivating mutation
SIRKO	single incretin receptor knockout
STZ	streptozotocin
TAE	tris-acetate-EDTA
TBS	tris-buffered saline
Tris	tris-(hydroxymethyl)-aminomethan
TNF α/β	tumor necrosis factor α/β
UV	ultraviolet
UWS	University of Wisconsin solution
VIP	vasoactive intestinal polypeptide
VSV	vesiculostomatitis virus

12 Reference List

Aiken, C. 1997. Pseudotyping human immunodeficiency virus type 1 (HIV-1) by the glycoprotein of vesicular stomatitis virus targets HIV-1 entry to an endocytic pathway and suppresses both the requirement for Nef and the sensitivity to cyclosporin A. *J Virol* 71: 5871-7.

Akkina, R. K., Walton, R. M., Chen, M. L., Li, Q. X., Planelles, V. & Chen, I. S. 1996. High-efficiency gene transfer into CD34+ cells with a human immunodeficiency virus type 1-based retroviral vector pseudotyped with vesicular stomatitis virus envelope glycoprotein G. *J Virol* 70: 2581-5.

Almind, K., Ambye, L., Urhammer, S. A., Hansen, T., Echwald, S. M., Holst, J. J., Gromada, J., Thorens, B. & Pedersen, O. 1998. Discovery of amino acid variants in the human glucose-dependent insulinotropic polypeptide (GIP) receptor: the impact on the pancreatic beta cell responses and functional expression studies in Chinese hamster fibroblast cells. *Diabetologia* 41: 1194-8.

Amland, P. F., Jorde, R., Aanderud, S., Burhol, P. G. & Giercksky, K. E. 1985. Effects of intravenously infused porcine GIP on serum insulin, plasma C-peptide, and pancreatic polypeptide in non-insulin-dependent diabetes in the fasting state. *Scand J Gastroenterol* 20: 315-20.

Andersen, D. K., Elahi, D., Brown, J. C., Tobin, J. D. & Andres, R. 1978. Oral glucose augmentation of insulin secretion. Interactions of gastric inhibitory polypeptide with ambient glucose and insulin levels. *J Clin Invest* 62: 152-61.

Baggio, L., Kieffer, T. J. & Drucker, D. J. 2000. Glucagon-like peptide-1, but not glucose-dependent insulinotropic peptide, regulates fasting glycemia and nonenteral glucose clearance in mice. *Endocrinology* 141: 3703-9.

Baggio, L. L. & Drucker, D. J. 2007. Biology of incretins: GLP-1 and GIP. *Gastroenterology* 132: 2131-57.

Beck, B. & Max, J. P. 1983. Gastric inhibitory polypeptide enhancement of the insulin effect on fatty acid incorporation into adipose tissue in the rat. *Regul Pept* 7: 3-8.

Beck, B. & Max, J. P. 1987. Hypersensitivity of adipose tissue to gastric inhibitory polypeptide action in the obese Zucker rat. *Cell Mol Biol* 33: 555-62.

Benech-Kieffer, F., Wegrich, P., Schwarzenbach, R., Klecak, G., Weber, T., Leclaire, J. & Schaefer, H. 2000. Percutaneous absorption of sunscreens in vitro: interspecies comparison, skin models and reproducibility aspects. *Skin Pharmacol Appl Skin Physiol* 13: 324-35.

Berger, M. (2000). Diabetes mellitus; Second Edition; Munich; Jena: Urban & Fischer Press. Ref Type: Serial (Book, Monograph).

Berglund, J. A., Charpentier, B. & Rosbash, M. 1997. A high affinity binding site for the HIV-1 nucleocapsid protein. *Nucleic Acids Res* 25: 1042-9.

Berkowitz, R. D., Ilves, H., Plavec, I. & Veres, G. 2001. Gene transfer systems derived from Visna virus: analysis of virus production and infectivity. *Virology* 279: 116-29.

Besenfelder, U., Modl, J., Muller, M. & Brem, G. 1997. Endoscopic embryo collection and embryo transfer into the oviduct and the uterus of pigs. *Theriogenology* 47: 1051-60.

Bollag, R. J., Zhong, Q., Ding, K. H., Phillips, P., Zhong, L., Qin, F., Cranford, J., Mulloy, A. L., Cameron, R. & Isales, C. M. 2001. Glucose-dependent insulinotropic peptide is an integrative hormone with osteotropic effects. *Mol Cell Endocrinol* 177: 35-41.

Bollag, R. J., Zhong, Q., Phillips, P., Min, L., Zhong, L., Cameron, R., Mulloy, A. L., Rasmussen, H., Qin, F., Ding, K. H. & Isales, C. M. 2000. Osteoblast-derived cells express functional glucose-dependent insulinotropic peptide receptors. *Endocrinology* 141: 1228-35.

Brodala, N., Merricks, E. P., Bellinger, D. A., Damrongsri, D., Offenbacher, S., Beck, J., Madianos, P., Sotres, D., Chang, Y. L., Koch, G. & Nichols, T. C. 2005. Porphyromonas gingivalis bacteremia induces coronary and aortic atherosclerosis in normocholesterolemic and hypercholesterolemic pigs. *Arterioscler Thromb Vasc Biol* 25: 1446-51.

Bromberg, J. S. & LeRoith, D. 2006. Diabetes cure--is the glass half full? *N Engl J Med* 355: 1372-4.

Brown, J. C. & Dryburgh, J. R. 1971. A gastric inhibitory polypeptide. II. The complete amino acid sequence. *Can J Biochem* 49: 867-72.

Brown, J. C., Mutt, V. & Pederson, R. A. 1970. Further purification of a polypeptide demonstrating enterogastrone activity. *J Physiol* 209: 57-64.

Brubaker, P. L. & Drucker, D. J. 2002. Structure-function of the glucagon receptor family of G protein-coupled receptors: the glucagon, GIP, GLP-1, and GLP-2 receptors. *Receptors Channels* 8: 179-88.

Brubaker, P. L. & Drucker, D. J. 2004. Minireview: Glucagon-like peptides regulate cell proliferation and apoptosis in the pancreas, gut, and central nervous system. *Endocrinology* 145: 2653-9.

Bruce, D. G., Chisholm, D. J., Storlien, L. H. & Kraegen, E. W. 1988. Physiological importance of deficiency in early prandial insulin secretion in non-insulin-dependent diabetes. *Diabetes* 37: 736-44.

Buchan, A. M., Polak, J. M., Capella, C., Solcia, E. & Pearse, A. G. 1978. Electronimmunocytochemical evidence for the K cell localization of gastric inhibitory polypeptide (GIP) in man. *Histochemistry* 56: 37-44.

Buffa, R., Polak, J. M., Pearse, A. G., Solcia, E., Grimelius, L. & Capella, C. 1975. Identification of the intestinal cell storing gastric inhibitory peptide. *Histochemistry* 43: 249-55.

Bundesministerium für Ernährung, Landwirtschaft und Verbraucherschutz. Tierversuchszahlen 2005. www.bmelv.de .2006. Ref Type: Internet Communication.

Buteau, J., El-Assaad, W., Rhodes, C. J., Rosenberg, L., Joly, E. & Prentki, M. 2004. Glucagon-like peptide-1 prevents beta cell glucolipotoxicity. *Diabetologia* 47: 806-15.

Butler, A. E., Janson, J., Bonner-Weir, S., Ritzel, R., Rizza, R. A. & Butler, P. C. 2003. Beta-cell deficit and increased beta-cell apoptosis in humans with type 2 diabetes. *Diabetes* 52: 102-10.

Calles-Escandon, J. & Robbins, D. C. 1987. Loss of early phase of insulin release in humans impairs glucose tolerance and blunts thermic effect of glucose. *Diabetes* 36: 1167-72.

Cataland, S., Crockett, S. E., Brown, J. C. & Mazzaferri, E. L. 1974. Gastric inhibitory polypeptide (GIP) stimulation by oral glucose in man. *J Clin Endocrinol Metab* 39: 223-8.

Cheung, A. T., Dayanandan, B., Lewis, J. T., Korbutt, G. S., Rajotte, R. V., Bryer-Ash, M., Boylan, M. O., Wolfe, M. M. & Kieffer, T. J. 2000. Glucose-dependent insulin release from genetically engineered K cells. *Science* 290: 1959-62.

Clark, J. & Whitelaw, B. 2003. A future for transgenic livestock. *Nat Rev Genet* 4: 825-33.

Clever, J. L., Taplitz, R. A., Lochrie, M. A., Polisky, B. & Parslow, T. G. 2000. A heterologous, high-affinity RNA ligand for human immunodeficiency virus Gag protein has RNA packaging activity. *J Virol* 74: 541-6.

Coffin, J.M. (1992). Structure and classification of retroviruses. In The Retroviridae, Levy, J.A. (ed.), Volume 1, New York: Plenum Press, pp. 19–49. Ref Type: Serial (Book, Monograph).

Creutzfeldt, W. 1979. The incretin concept today. *Diabetologia* 16: 75-85.

Creutzfeldt, W. 2005. The (pre-) history of the incretin concept. *Regul Pept* 128: 87-91.

Cypess, A. M., Unson, C. G., Wu, C. R. & Sakmar, T. P. 1999. Two cytoplasmic loops of the glucagon receptor are required to elevate cAMP or intracellular calcium. *J Biol Chem* 274: 19455-64.

Deacon, C. F., Danielsen, P., Klarskov, L., Olesen, M. & Holst, J. J. 2001. Dipeptidyl peptidase IV inhibition reduces the degradation and clearance of GIP and potentiates its insulinotropic and antihyperglycemic effects in anesthetized pigs. *Diabetes* 50: 1588-97.

Deacon, C. F., Johnsen, A. H. & Holst, J. J. 1995. Degradation of glucagon-like peptide-1 by human plasma in vitro yields an N-terminally truncated peptide that is a major endogenous metabolite in vivo. *J Clin Endocrinol Metab* 80: 952-7.

Deacon, C. F., Nauck, M. A., Meier, J., Hucking, K. & Holst, J. J. 2000. Degradation of endogenous and exogenous gastric inhibitory polypeptide in healthy and in type 2 diabetic subjects as revealed using a new assay for the intact peptide. *J Clin Endocrinol Metab* 85: 3575-81.

Delenda, C. 2004. Lentiviral vectors: optimization of packaging, transduction and gene expression. *J Gene Med* 6 Suppl 1: S125-38.

Ding, K. H., Zhong, Q., Xie, D., Chen, H. X., Della-Fera, M. A., Bollag, R. J., Bollag, W. B., Gujral, R., Kang, B., Sridhar, S., Baile, C., Curl, W. & Isales, C. M. 2006. Effects of glucose-dependent insulinotropic peptide on behavior. *Peptides* 27: 2750-5.

Ding, W. G. & Gromada, J. 1997. Protein kinase A-dependent stimulation of exocytosis in mouse pancreatic beta-cells by glucose-dependent insulinotropic polypeptide. *Diabetes* 46: 615-21.

Dixon, J. L., Stoops, J. D., Parker, J. L., Laughlin, M. H., Weisman, G. A. & Sturek, M. 1999. Dyslipidemia and vascular dysfunction in diabetic pigs fed an atherogenic diet. *Arterioscler Thromb Vasc Biol* 19: 2981-92.

Dull, T., Zufferey, R., Kelly, M., Mandel, R. J., Nguyen, M., Trono, D. & Naldini, L. 1998. A third-generation lentivirus vector with a conditional packaging system. *J Virol* 72: 8463-71.

Dupre, J., Greenidge, N., McDonald, T. J., Ross, S. A. & Rubinstein, D. 1976. Inhibition of actions of glucagon in adipocytes by gastric inhibitory polypeptide. *Metabolism* 25: 1197-9.

Dupre, J., Ross, S. A., Watson, D. & Brown, J. C. 1973. Stimulation of insulin secretion by gastric inhibitory polypeptide in man. *J Clin Endocrinol Metab* 37: 826-8.

Dyson, M. C., Alloosh, M., Vuchetich, J. P., Mokelke, E. A. & Sturek, M. 2006. Components of metabolic syndrome and coronary artery disease in female Ossabaw swine fed excess atherogenic diet. *Comp Med* 56: 35-45.

Ebert, R. & Creutzfeldt, W. 1982. Influence of gastric inhibitory polypeptide antiserum on glucose-induced insulin secretion in rats. *Endocrinology* 111: 1601-6.

Ebert, R. & Creutzfeldt, W. 1987. Gastrointestinal peptides and insulin secretion. *Diabetes Metab Rev* 3: 1-26.

Ebert, R., Unger, H. & Creutzfeldt, W. 1983. Preservation of incretin activity after removal of gastric inhibitory polypeptide (GIP) from rat gut extracts by immunoadsorption. *Diabetologia* 24: 449-54.

Eckel, R. H., Fujimoto, W. Y. & Brunzell, J. D. 1979. Gastric inhibitory polypeptide enhanced lipoprotein lipase activity in cultured preadipocytes. *Diabetes* 28: 1141-2.

Ehses, J. A., Casilla, V. R., Doty, T., Pospisilik, J. A., Winter, K. D., Demuth, H. U., Pederson, R. A. & McIntosh, C. H. 2003. Glucose-dependent insulinotropic polypeptide promotes beta-(INS-1) cell survival via cyclic adenosine monophosphate-mediated caspase-3 inhibition and regulation of p38 mitogen-activated protein kinase. *Endocrinology* 144: 4433-45.

Ehses, J. A., Lee, S. S., Pederson, R. A. & McIntosh, C. H. 2001. A new pathway for glucose-dependent insulinotropic polypeptide (GIP) receptor signaling: evidence for the involvement of phospholipase A2 in GIP-stimulated insulin secretion. *J Biol Chem* 276: 23667-73.

Ehses, J. A., Pelech, S. L., Pederson, R. A. & McIntosh, C. H. 2002. Glucose-dependent insulinotropic polypeptide activates the Raf-Mek1/2-ERK1/2 module via a cyclic AMP/cAMP-dependent protein kinase/Rap1-mediated pathway. *J Biol Chem* 277: 37088-97.

Elahi, D., Andersen, D. K., Brown, J. C., Debas, H. T., Hershcopf, R. J., Raizes, G. S., Tobin, J. D. & Andres, R. 1979. Pancreatic alpha- and beta-cell responses to GIP infusion in normal man. *Am J Physiol* 237: E185-91.

Elahi, D., McAloon-Dyke, M., Fukagawa, N. K., Meneilly, G. S., Sclater, A. L., Minaker, K. L., Habener, J. F. & Andersen, D. K. 1994. The insulinotropic actions of glucose-dependent insulinotropic polypeptide (GIP) and glucagon-like peptide-1 (7-37) in normal and diabetic subjects. *Regul Pept* 51: 63-74.

Elrick, H., Stimmler, L., Hlad, C. J. Jr & Arai, Y. 1964. Plasma insulin response to oral and intravenous glucose administration. *J Clin Endocrinol Metab* 24: 1076-82.

Faber, O. K. & Binder, C. 1977. C-peptide response to glucagon. A test for the residual beta-cell function in diabetes mellitus. *Diabetes* 26: 605-10.

Falko, J. M., Crockett, S. E., Cataland, S. & Mazzaferri, E. L. 1975. Gastric inhibitory polypeptide (GIP) stimulated by fat ingestion in man. *J Clin Endocrinol Metab* 41: 260-5.

Farilla, L., Bulotta, A., Hirshberg, B., Li Calzi, S., Khoury, N., Noushmehr, H., Bertolotto, C., Di Mario, U., Harlan, D. M. & Perfetti, R. 2003. Glucagon-like peptide 1 inhibits cell apoptosis and improves glucose responsiveness of freshly isolated human islets. *Endocrinology* 144: 5149-58.

Farilla, L., Hui, H., Bertolotto, C., Kang, E., Bulotta, A., Di Mario, U. & Perfetti, R. 2002. Glucagon-like peptide-1 promotes islet cell growth and inhibits apoptosis in Zucker diabetic rats. *Endocrinology* 143: 4397-408.

Fassler, R. 2004. Lentiviral transgene vectors. *EMBO Rep* 5: 28-9.

Fehmann, H. C., Goke, R. & Goke, B. 1995. Cell and molecular biology of the incretin hormones glucagon-like peptide-I and glucose-dependent insulin releasing polypeptide. *Endocr Rev* 16: 390-410.

Flamez, D., Gilon, P., Moens, K., Van Breusegem, A., Delmeire, D., Scrocchi, L. A., Henquin, J. C., Drucker, D. J. & Schuit, F. 1999. Altered cAMP and Ca2+ signaling in mouse pancreatic islets with glucagon-like peptide-1 receptor null phenotype. *Diabetes* 48: 1979-86.

Flint, A., Raben, A., Astrup, A. & Holst, J. J. 1998. Glucagon-like peptide 1 promotes satiety and suppresses energy intake in humans. *J Clin Invest* 101: 515-20.

Follenzi, A., Ailles, L. E., Bakovic, S., Geuna, M. & Naldini, L. 2000. Gene transfer by lentiviral vectors is limited by nuclear translocation and rescued by HIV-1 pol sequences. *Nat Genet* 25: 217-22.

Gabbay, K. H., Hasty, K., Breslow, J. L., Ellison, R. C., Bunn, H. F. & Gallop, P. M. 1977. Glycosylated hemoglobins and long-term blood glucose control in diabetes mellitus. *J Clin Endocrinol Metab* 44: 859-64.

Gallwitz, B. 2006a. Exenatide in type 2 diabetes: treatment effects in clinical studies and animal study data. *Int J Clin Pract* 60: 1654-61.

Gallwitz, B. & Schmidt, W. E. 1997. [GLP-1 receptor gen "knock out" causes glucose intolerance, but no alterations of eating behavior]. *Z Gastroenterol* 35: 655-8.

Gallwitz, B. (2006). GLP-1 als Therapieprinzip bei Typ 2-Diabetes: Inkretin-Mimetika und DPP-4-Inhibitoren; Second Edition; Bremen: UNI-MED press. Ref Type: Serial (Book, Monograph).

Gasmi, M., Glynn, J., Jin, M. J., Jolly, D. J., Yee, J. K. & Chen, S. T. 1999. Requirements for efficient production and transduction of human immunodeficiency virus type 1-based vectors. *J Virol* 73: 1828-34.

Gelling, R. W., Coy, D. H., Pederson, R. A., Wheeler, M. B., Hinke, S., Kwan, T. & McIntosh, C. H. 1997a. GIP(6-30amide) contains the high affinity binding region of GIP and is a potent inhibitor of GIP1-42 action in vitro. *Regul Pept* 69: 151-4.

Gelling, R. W., Wheeler, M. B., Xue, J., Gyomorey, S., Nian, C., Pederson, R. A. & McIntosh, C. H. 1997b. Localization of the domains involved in ligand binding and activation of the glucose-dependent insulinotropic polypeptide receptor. *Endocrinology* 138: 2640-3.

Gerrity, R. G., Natarajan, R., Nadler, J. L. & Kimsey, T. 2001. Diabetes-induced accelerated atherosclerosis in swine. *Diabetes* 50: 1654-65.

Goeke, B., Parhofer, K.G., Otto, C. (2002). Diabetes mellitus; First Edition; Munich; Jena: Urban & Fischer Press. Ref Type: Serial (Book, Monograph).

Goff, S.P. (2001). Retroviridae: The retroviruses and their replication. In: Howley, P.M., Knipe, D.M., Griffin, D., Lamb, R.A., Martin, A., Roizman, B., and Straus, S.E. (eds.) Fields Virology, Philadelphia, Lippincott-Raven Publishers, pp 1871-1939. Ref Type: Serial (Book, Monograph).

Gotthardt, M., Lalyko, G., van Eerd-Vismale, J., Keil, B., Schurrat, T., Hower, M., Laverman, P., Behr, T. M., Boerman, O. C., Goke, B. & Behe, M. 2006. A new technique for in vivo imaging of specific GLP-1 binding sites: first results in small rodents. *Regul Pept* 137: 162-7.

Gremlich, S., Porret, A., Hani, E. H., Cherif, D., Vionnet, N., Froguel, P. & Thorens, B. 1995. Cloning, functional expression, and chromosomal localization of the human pancreatic islet glucose-dependent insulinotropic polypeptide receptor. *Diabetes* 44: 1202-8.

Gundersen, H. J., Bendtsen, T. F., Korbo, L., Marcussen, N., Moller, A., Nielsen, K., Nyengaard, J. R., Pakkenberg, B., Sorensen, F. B., Vesterby, A. & et, a. l. 1988. Some new, simple and efficient stereological methods and their use in pathological research and diagnosis. *APMIS* 96: 379-94.

Gundersen, H. J. & Jensen, E. B. 1987. The efficiency of systematic sampling in stereology and its prediction. *J Microsc* 147: 229-63.

Hallbrink, M., Holmqvist, T., Olsson, M., Ostenson, C. G., Efendic, S. & Langel, U. 2001. Different domains in the third intracellular loop of the GLP-1 receptor are responsible for Galpha(s) and Galpha(i)/Galpha(o) activation. *Biochim Biophys Acta* 1546: 79-86.

Hansotia, T., Baggio, L. L., Delmeire, D., Hinke, S. A., Yamada, Y., Tsukiyama, K., Seino, Y., Holst, J. J., Schuit, F. & Drucker, D. J. 2004. Double incretin receptor knockout (DIRKO) mice reveal an essential role for the enteroinsular axis in transducing the glucoregulatory actions of DPP-IV inhibitors. *Diabetes* 53: 1326-35.

Hansotia, T. & Drucker, D. J. 2005. GIP and GLP-1 as incretin hormones: lessons from single and double incretin receptor knockout mice. *Regul Pept* 128: 125-34.

Harmar, A. J. 2001. Family-B G-protein-coupled receptors. *Genome Biol* 2: REVIEWS3013.

Hasler-Rapacz, J. O., Nichols, T. C., Griggs, T. R., Bellinger, D. A. & Rapacz, J. 1994. Familial and diet-induced hypercholesterolemia in swine. Lipid, ApoB, and ApoA-I concentrations and distributions in plasma and lipoprotein subfractions. *Arterioscler Thromb* 14: 923-30.

Hauner, H., Glatting, G., Kaminska, D. & Pfeiffer, E. F. 1988. Effects of gastric inhibitory polypeptide on glucose and lipid metabolism of isolated rat adipocytes. *Ann Nutr Metab* 32: 282-8.

He, J., Yang, Q. & Chang, L. J. 2005. Dynamic DNA methylation and histone modifications contribute to lentiviral transgene silencing in murine embryonic carcinoma cells. *J Virol* 79: 13497-508.

Heiser, A., Ulrichs, K. & Muller-Ruchholtz, W. 1994. Isolation of porcine pancreatic islets: low trypsin activity during the isolation procedure guarantees reproducible high islet yields. *J Clin Lab Anal* 8: 407-11.

Henriksen, D. B., Alexandersen, P., Bjarnason, N. H., Vilsboll, T., Hartmann, B., Henriksen, E. E., Byrjalsen, I., Krarup, T., Holst, J. J. & Christiansen, C. 2003. Role of gastrointestinal hormones in postprandial reduction of bone resorption. *J Bone Miner Res* 18: 2180-9.

Herbach, N., Goeke, B., Schneider, M., Hermanns, W., Wolf, E. & Wanke, R. 2005. Overexpression of a dominant negative GIP receptor in transgenic mice results in disturbed postnatal pancreatic islet and beta-cell development. *Regul Pept* 125: 103-17.

Herbach, N. (2002). Clinical and pathological characterization of a novel transgenic animal model of diabetes mellitus expressing a dominant-negative glucose-dependent insulinotropic polypeptide receptor ($GIPR^{dn}$). Thesis for the attainment of the title Doctor in Veterinary Medicine; Ludwig-Maximilians University Munich; p 1-167.

Herrmann, C., Goke, R., Richter, G., Fehmann, H. C., Arnold, R. & Goke, B. 1995. Glucagon-like peptide-1 and glucose-dependent insulin-releasing polypeptide plasma levels in response to nutrients. *Digestion* 56: 117-26.

Herrmann-Rinke, C., Voge, A., Hess, M. & Goke, B. 1995. Regulation of glucagon-like peptide-1 secretion from rat ileum by neurotransmitters and peptides. *J Endocrinol* 147: 25-31.

Higgins, P. J., Garlick, R. L. & Bunn, H. F. 1982. Glycosylated hemoglobin in human and animal red cells. Role of glucose permeability. *Diabetes* 31: 743-8.

Hofmann, A., Kessler, B., Ewerling, S., Kabermann, A., Brem, G., Wolf, E. & Pfeifer, A. 2006. Epigenetic regulation of lentiviral transgene vectors in a large animal model. *Mol Ther* 13: 59-66.

Hofmann, A., Kessler, B., Ewerling, S., Weppert, M., Vogg, B., Ludwig, H., Stojkovic, M., Boelhauve, M., Brem, G., Wolf, E. & Pfeifer, A. 2003. Efficient transgenesis in farm animals by lentiviral vectors. *EMBO Rep* 4: 1054-60.

Hofmann, A. (2006a). Entwicklung lentiviraler Transgenese in höheren Säugetieren. Thesis for the attainment of the degree of doctor of the faculty for chemistry and pharmacy; Ludwig-Maximilians University Munich; p 1-123.

Hogan, P., Dall, T. & Nikolov, P. 2003. Economic costs of diabetes in the US in 2002. *Diabetes Care* 26: 917-32.

Holst, J. J. 1994. Glucagonlike peptide 1: a newly discovered gastrointestinal hormone. *Gastroenterology* 107: 1848-55.

Jaenisch, R. 1976. Germ line integration and Mendelian transmission of the exogenous Moloney leukemia virus. *Proc Natl Acad Sci U S A* 73: 1260-4.

Jaenisch, R., Fan, H. & Croker, B. 1975. Infection of preimplantation mouse embryos and of newborn mice with leukemia virus: tissue distribution of viral DNA and RNA and leukemogenesis in the adult animal. *Proc Natl Acad Sci U S A* 72: 4008-12.

Jamen, F., Persson, K., Bertrand, G., Rodriguez-Henche, N., Puech, R., Bockaert, J., Ahren, B. & Brabet, P. 2000. PAC1 receptor-deficient mice display impaired insulinotropic response to glucose and reduced glucose tolerance. *J Clin Invest* 105: 1307-15.

Jay, T. R., Heald, K. A., Carless, N. J., Topham, D. E. & Downing, R. 1999. The distribution of porcine pancreatic beta-cells at ages 5, 12 and 24 weeks. *Xenotransplantation* 6: 131-40.

Johansen, T., Hansen, H. S., Richelsen, B. & Malmlof, R. 2001. The obese Gottingen minipig as a model of the metabolic syndrome: dietary effects on obesity, insulin sensitivity, and growth hormone profile. *Comp Med* 51: 150-5.

Jones, I. R., Owens, D. R., Moody, A. J., Luzio, S. D., Morris, T. & Hayes, T. M. 1987. The effects of glucose-dependent insulinotropic polypeptide infused at physiological concentrations in normal subjects and type 2 (non-insulin-dependent) diabetic patients on glucose tolerance and B-cell secretion. *Diabetologia* 30: 707-12.

Jorde, R., Burhol, P. G., Gunnes, P. & Schulz, T. B. 1981. Removal of IR-GIP by the kidneys in man, and the effect of acute nephrectomy on plasma GIP in rats. *Scand J Gastroenterol* 16: 469-71.

Jornvall, H., Carlquist, M., Kwauk, S., Otte, S. C., McIntosh, C. H., Brown, J. C. & Mutt, V. 1981. Amino acid sequence and heterogeneity of gastric inhibitory polypeptide (GIP). *FEBS Lett* 123: 205-10.

Kahn, S. E., Hull, R. L. & Utzschneider, K. M. 2006. Mechanisms linking obesity to insulin resistance and type 2 diabetes. *Nature* 444: 840-6.

Kao, S. Y., Calman, A. F., Luciw, P. A. & Peterlin, B. M. 1987. Anti-termination of transcription within the long terminal repeat of HIV-1 by tat gene product. *Nature* 330: 489-93.

Kashima, Y., Miki, T., Shibasaki, T., Ozaki, N., Miyazaki, M., Yano, H. & Seino, S. 2001. Critical role of cAMP-GEFII--Rim2 complex in incretin-potentiated insulin secretion. *J Biol Chem* 276: 46046-53.

Kieffer, T. J., McIntosh, C. H. & Pederson, R. A. 1995. Degradation of glucose-dependent insulinotropic polypeptide and truncated glucagon-like peptide 1 in vitro and in vivo by dipeptidyl peptidase IV. *Endocrinology* 136: 3585-96.

Kim, S. J., Choi, W. S., Han, J. S., Warnock, G., Fedida, D. & McIntosh, C. H. 2005a. A novel mechanism for the suppression of a voltage-gated potassium channel by glucose-dependent insulinotropic polypeptide: protein kinase A-dependent endocytosis. *J Biol Chem* 280: 28692-700.

Kim, S. J., Winter, K., Nian, C., Tsuneoka, M., Koda, Y. & McIntosh, C. H. 2005b. Glucose-dependent insulinotropic polypeptide (GIP) stimulation of pancreatic beta-cell survival is dependent upon phosphatidylinositol 3-kinase (PI3K)/protein kinase B (PKB) signaling, inactivation of the forkhead transcription factor Foxo1, and down-regulation of bax expression. *J Biol Chem* 280: 22297-307.

Kjems, L. L., Kirby, B. M., Welsh, E. M., Veldhuis, J. D., Straume, M., McIntyre, S. S., Yang, D., Lefebvre, P. & Butler, P. C. 2001. Decrease in beta-cell mass leads to impaired pulsatile insulin secretion, reduced postprandial hepatic insulin clearance, and relative hyperglucagonemia in the minipig. *Diabetes* 50: 2001-12.

Kobayashi, K., Kobayashi, N., Okitsu, T., Yong, C., Fukazawa, T., Ikeda, H., Kosaka, Y., Narushima, M., Arata, T. & Tanaka, N. 2004. Development of a porcine model of type 1 diabetes by total pancreatectomy and establishment of a glucose tolerance evaluation method. *Artif Organs* 28: 1035-42.

Koenig, R. J., Peterson, C. M., Jones, R. L., Saudek, C., Lehrman, M. & Cerami, A. 1976. Correlation of glucose regulation and hemoglobin AIc in diabetes mellitus. *N Engl J Med* 295: 417-20.

Kolakowski, L. F. Jr 1994. GCRDb: a G-protein-coupled receptor database. *Receptors Channels* 2: 1-7.

Kraft, W., Dürr U.M. (1999). Klinische Labordiagnostik in der Tiermedizin. Fifth edition, Stuttgart; New York: Schattauer Press. Ref Type: Serial (Book, Monograph).

Krarup, T., Saurbrey, N., Moody, A. J., Kuhl, C. & Madsbad, S. 1987. Effect of porcine gastric inhibitory polypeptide on beta-cell function in type I and type II diabetes mellitus. *Metabolism* 36: 677-82.

Kreymann, B., Williams, G., Ghatei, M. A. & Bloom, S. R. 1987. Glucagon-like peptide-1 7-36: a physiological incretin in man. *Lancet* 2: 1300-4.

Krickhahn, M., Meyer, T., Buhler, C., Thiede, A. & Ulrichs, K. 2001. Highly efficient isolation of porcine islets of Langerhans for xenotransplantation: numbers, purity, yield and in vitro function. *Ann Transplant* 6: 48-54.

Kroustrup, J. P. & Gundersen, H. J. 1983. Sampling problems in an heterogeneous organ: quantitation of relative and total volume of pancreatic islets by light microscopy. *J Microsc* 132: 43-55.

Kubota, A., Yamada, Y., Hayami, T., Yasuda, K., Someya, Y., Ihara, Y., Kagimoto, S., Watanabe, R., Taminato, T., Tsuda, K. & Seino, Y. 1996. Identification of two missense mutations in the GIP receptor gene: a functional study and association analysis with NIDDM: no evidence of association with Japanese NIDDM subjects. *Diabetes* 45: 1701-5.

Larsen, M. O. & Rolin, B. 2004. Use of the Gottingen minipig as a model of diabetes, with special focus on type 1 diabetes research. *ILAR J* 45: 303-13.

Larsen, M. O., Rolin, B., Wilken, M., Carr, R. D. & Gotfredsen, C. F. 2003. Measurements of insulin secretory capacity and glucose tolerance to predict pancreatic beta-cell mass in vivo in the nicotinamide/streptozotocin Gottingen minipig, a model of moderate insulin deficiency and diabetes. *Diabetes* 52: 118-23.

Larsen, M. O., Rolin, B., Wilken, M., Carr, R. D., Svendsen, O. & Bollen, P. 2001. Parameters of glucose and lipid metabolism in the male Gottingen minipig: influence of age, body weight, and breeding family. *Comp Med* 51: 436-42.

Latif, Z. A., Noel, J. & Alejandro, R. 1988. A simple method of staining fresh and cultured islets. *Transplantation* 45: 827-30.

Lauritsen, K. B., Moody, A. J., Christensen, K. C. & Lindkaer Jensen, S. 1980. Gastric inhibitory polypeptide (GIP) and insulin release after small-bowel resection in man. *Scand J Gastroenterol* 15: 833-40.

Leahy, J. L. 2005. Pathogenesis of type 2 diabetes mellitus. *Arch Med Res* 36: 197-209.

Leahy, J. L., Bonner-Weir, S. & Weir, G. C. 1988. Minimal chronic hyperglycemia is a critical determinant of impaired insulin secretion after an incomplete pancreatectomy. *J Clin Invest* 81: 1407-14.

Lever, A. M., Strappe, P. M. & Zhao, J. 2004. Lentiviral vectors. *J Biomed Sci* 11: 439-49.

Levin, S. R., Pehlevanian, M. Z., Lavee, A. E. & Adachi, R. I. 1979. Secretion of an insulinotropic factor from isolated, perfused rat intestine. *Am J Physiol* 236: E710-20.

Ling, Z., Wu, D., Zambre, Y., Flamez, D., Drucker, D. J., Pipeleers, D. G. & Schuit, F. C. 2001. Glucagon-like peptide 1 receptor signaling influences topography of islet cells in mice. *Virchows Arch* 438: 382-7.

Lois, C., Hong, E. J., Pease, S., Brown, E. J. & Baltimore, D. 2002. Germline transmission and tissue-specific expression of transgenes delivered by lentiviral vectors. *Science* 295: 868-72.

Lukinius, A., Korsgren, O., Grimelius, L. & Wilander, E. 1996. Expression of islet amyloid polypeptide in fetal and adult porcine and human pancreatic islet cells. *Endocrinology* 137: 5319-25.

Luzi, L. & DeFronzo, R. A. 1989. Effect of loss of first-phase insulin secretion on hepatic glucose production and tissue glucose disposal in humans. *Am J Physiol* 257: E241-6.

Lynn, F. C., Pamir, N., Ng, E. H., McIntosh, C. H., Kieffer, T. J. & Pederson, R. A. 2001. Defective glucose-dependent insulinotropic polypeptide receptor expression in diabetic fatty Zucker rats. *Diabetes* 50: 1004-11.

Lynn, F. C., Thompson, S. A., Pospisilik, J. A., Ehses, J. A., Hinke, S. A., Pamir, N., McIntosh, C. H. & Pederson, R. A. 2003. A novel pathway for regulation of glucose-dependent insulinotropic polypeptide (GIP) receptor expression in beta cells. *FASEB J* 17: 91-3.

Mangeot, P. E., Negre, D., Dubois, B., Winter, A. J., Leissner, P., Mehtali, M., Kaiserlian, D., Cosset, F. L. & Darlix, J. L. 2000. Development of minimal lentivirus vectors derived from simian immunodeficiency virus (SIVmac251) and their use for gene transfer into human dendritic cells. *J Virol* 74: 8307-15.

Matte, J. J. 1999. A rapid and non-surgical procedure for jugular catheterization of pigs. *Lab Anim* 33: 258-64.

McIntyre, N., Holdsworth, C. D. & Turner, D. S. 1964. New interpretation of oral glucose tolerance. *Lancet* 2: 20-1.

Meier, J. J., Hucking, K., Holst, J. J., Deacon, C. F., Schmiegel, W. H. & Nauck, M. A. 2001. Reduced insulinotropic effect of gastric inhibitory polypeptide in first-degree relatives of patients with type 2 diabetes. *Diabetes* 50: 2497-504.

Meier, J. J., Nauck, M. A., Kranz, D., Holst, J. J., Deacon, C. F., Gaeckler, D., Schmidt, W. E. & Gallwitz, B. 2004. Secretion, degradation, and elimination of glucagon-like peptide 1 and gastric inhibitory polypeptide in patients with chronic renal insufficiency and healthy control subjects. *Diabetes* 53: 654-62.

Meier, J. J., Nauck, M. A., Schmidt, W. E. & Gallwitz, B. 2002. Gastric inhibitory polypeptide: the neglected incretin revisited. *Regul Pept* 107: 1-13.

Mentlein, R. 1999. Dipeptidyl-peptidase IV (CD26)--role in the inactivation of regulatory peptides. *Regul Pept* 85: 9-24.

Meyer, W. 1996. [Comments on the suitability of swine skin as a biological model for human skin]. *Hautarzt* 47: 178-82.

Miller, D. G., Adam, M. A. & Miller, A. D. 1990. Gene transfer by retrovirus vectors occurs only in cells that are actively replicating at the time of infection. *Mol Cell Biol* 10: 4239-42.

Miller, E. R. & Ullrey, D. E. 1987. The pig as a model for human nutrition. *Annu Rev Nutr* 7: 361-82.

Miyawaki, K., Yamada, Y., Ban, N., Ihara, Y., Tsukiyama, K., Zhou, H., Fujimoto, S., Oku, A., Tsuda, K., Toyokuni, S., Hiai, H., Mizunoya, W., Fushiki, T., Holst, J. J., Makino, M., Tashita, A., Kobara, Y., Tsubamoto, Y., Jinnouchi, T., Jomori, T. & Seino, Y. 2002. Inhibition of gastric inhibitory polypeptide signaling prevents obesity. *Nat Med* 8: 738-42.

Miyawaki, K., Yamada, Y., Yano, H., Niwa, H., Ban, N., Ihara, Y., Kubota, A., Fujimoto, S., Kajikawa, M., Kuroe, A., Tsuda, K., Hashimoto, H., Yamashita, T., Jomori, T., Tashiro, F., Miyazaki, J. & Seino, Y. 1999. Glucose intolerance caused by a defect in the entero-insular axis: a study in gastric inhibitory polypeptide receptor knockout mice. *Proc Natl Acad Sci U S A* 96: 14843-7.

Miyoshi, H., Blomer, U., Takahashi, M., Gage, F. H. & Verma, I. M. 1998. Development of a self-inactivating lentivirus vector. *J Virol* 72: 8150-7.

Modrow, S., Falke, D., Truyen, U. (2003). Molekulare Virologie; Second Edition; Heidelberg; Berlin: Spektrum press. Ref Type: Serial (Book, Monograph).

Mojsov, S., Weir, G. C. & Habener, J. F. 1987. Insulinotropin: glucagon-like peptide I (7-37) co-encoded in the glucagon gene is a potent stimulator of insulin release in the perfused rat pancreas. *J Clin Invest* 79: 616-9.

Moody, A. J., Thim, L. & Valverde, I. 1984. The isolation and sequencing of human gastric inhibitory peptide (GIP). *FEBS Lett* 172: 142-8.

Mortensen, K., Christensen, L. L., Holst, J. J. & Orskov, C. 2003. GLP-1 and GIP are colocalized in a subset of endocrine cells in the small intestine. *Regul Pept* 114: 189-96.

Mortensen, K., Petersen, L. L. & Orskov, C. 2000. Colocalization of GLP-1 and GIP in human and porcine intestine. *Ann N Y Acad Sci* 921: 469-72.

Mu, J., Woods, J., Zhou, Y. P., Roy, R. S., Li, Z., Zycband, E., Feng, Y., Zhu, L., Li, C., Howard, A. D., Moller, D. E., Thornberry, N. A. & Zhang, B. B. 2006. Chronic inhibition of dipeptidyl peptidase-4 with a sitagliptin analog preserves pancreatic beta-cell mass and function in a rodent model of type 2 diabetes. *Diabetes* 55: 1695-704.

Muscelli, E., Mari, A., Natali, A., Astiarraga, B. D., Camastra, S., Frascerra, S., Holst, J. J. & Ferrannini, E. 2006. Impact of incretin hormones on beta-cell function in subjects with normal or impaired glucose tolerance. *Am J Physiol Endocrinol Metab* 291: E1144-50.

Naldini, L., Blomer, U., Gallay, P., Ory, D., Mulligan, R., Gage, F. H., Verma, I. M. & Trono, D. 1996. In vivo gene delivery and stable transduction of nondividing cells by a lentiviral vector. *Science* 272: 263-7.

Nauck, M., Stockmann, F., Ebert, R. & Creutzfeldt, W. 1986a. Reduced incretin effect in type 2 (non-insulin-dependent) diabetes. *Diabetologia* 29: 46-52.

Nauck, M. A. 1999. Is glucagon-like peptide 1 an incretin hormone? *Diabetologia* 42: 373-9.

Nauck, M. A., Baller, B. & Meier, J. J. 2004. Gastric inhibitory polypeptide and glucagon-like peptide-1 in the pathogenesis of type 2 diabetes. *Diabetes* 53 Suppl 3: S190-6.

Nauck, M. A., Bartels, E., Orskov, C., Ebert, R. & Creutzfeldt, W. 1993a. Additive insulinotropic effects of exogenous synthetic human gastric inhibitory polypeptide and glucagon-like peptide-1-(7-36) amide infused at near-physiological insulinotropic hormone and glucose concentrations. *J Clin Endocrinol Metab* 76: 912-7.

Nauck, M. A., Busing, M., Orskov, C., Siegel, E. G., Talartschik, J., Baartz, A., Baartz, T., Hopt, U. T., Becker, H. D. & Creutzfeldt, W. 1993b. Preserved incretin effect in type 1 diabetic patients with end-stage nephropathy treated by combined heterotopic pancreas and kidney transplantation. *Acta Diabetol* 30: 39-45.

Nauck, M. A., Heimesaat, M. M., Behle, K., Holst, J. J., Nauck, M. S., Ritzel, R., Hufner, M. & Schmiegel, W. H. 2002. Effects of glucagon-like peptide 1 on counterregulatory hormone responses, cognitive functions, and insulin secretion during hyperinsulinemic, stepped hypoglycemic clamp experiments in healthy volunteers. *J Clin Endocrinol Metab* 87: 1239-46.

Nauck, M. A., Heimesaat, M. M., Orskov, C., Holst, J. J., Ebert, R. & Creutzfeldt, W. 1993. Preserved incretin activity of glucagon-like peptide 1 but not of synthetic human gastric inhibitory polypeptide in patients with type-2 diabetes mellitus. *J Clin Invest* 91: 301-7.

Nauck, M. A., Homberger, E., Siegel, E. G., Allen, R. C., Eaton, R. P., Ebert, R. & Creutzfeldt, W. 1986b. Incretin effects of increasing glucose loads in man calculated from venous insulin and C-peptide responses. *J Clin Endocrinol Metab* 63: 492-8.

Nauck, M. A., Niedereichholz, U., Ettler, R., Holst, J. J., Orskov, C., Ritzel, R. & Schmiegel, W. H. 1997. Glucagon-like peptide 1 inhibition of gastric emptying outweighs its insulinotropic effects in healthy humans. *Am J Physiol* 273: E981-8.

Nichols, T. C., Bellinger, D. A., Davis, K. E., Koch, G. G., Reddick, R. L., Read, M. S., Rapacz, J., Hasler-Rapacz, J., Brinkhous, K. M. & Griggs, T. R. 1992. Porcine von Willebrand disease and atherosclerosis. Influence of polymorphism in apolipoprotein B100 genotype. *Am J Pathol* 140: 403-15.

Nyberg, J., Anderson, M. F., Meister, B., Alborn, A. M., Strom, A. K., Brederlau, A., Illerskog, A. C., Nilsson, O., Kieffer, T. J., Hietala, M. A., Ricksten, A. & Eriksson, P. S. 2005. Glucose-dependent insulinotropic polypeptide is expressed in adult hippocampus and induces progenitor cell proliferation. *J Neurosci* 25: 1816-25.

Oben, J., Morgan, L., Fletcher, J. & Marks, V. 1991. Effect of the entero-pancreatic hormones, gastric inhibitory polypeptide and glucagon-like polypeptide-1(7-36) amide, on fatty acid synthesis in explants of rat adipose tissue. *J Endocrinol* 130: 267-72.

Olsen, J. C. 1998. Gene transfer vectors derived from equine infectious anemia virus. *Gene Ther* 5: 1481-7.

Orskov, C. 1992. Glucagon-like peptide-1, a new hormone of the entero-insular axis. *Diabetologia* 35: 701-11.

Orskov, C., Rabenhoj, L., Wettergren, A., Kofod, H. & Holst, J. J. 1994. Tissue and plasma concentrations of amidated and glycine-extended glucagon-like peptide I in humans. *Diabetes* 43: 535-9.

Orskov, C., Wettergren, A. & Holst, J. J. 1996. Secretion of the incretin hormones glucagon-like peptide-1 and gastric inhibitory polypeptide correlates with insulin secretion in normal man throughout the day. *Scand J Gastroenterol* 31: 665-70.

Palmiter, R. D., Sandgren, E. P., Koeller, D. M. & Brinster, R. L. 1993. Distal regulatory elements from the mouse metallothionein locus stimulate gene expression in transgenic mice. *Mol Cell Biol* 13: 5266-75.

Pamir, N., Lynn, F. C., Buchan, A. M., Ehses, J., Hinke, S. A., Pospisilik, J. A., Miyawaki, K., Yamada, Y., Seino, Y., McIntosh, C. H. & Pederson, R. A. 2003. Glucose-dependent insulinotropic polypeptide receptor null mice exhibit compensatory changes in the enteroinsular axis. *Am J Physiol Endocrinol Metab* 284: E931-9.

Pederson, R. A. & Brown, J. C. 1978. Interaction of gastric inhibitory polypeptide, glucose, and arginine on insulin and glucagon secretion from the perfused rat pancreas. *Endocrinology* 103: 610-5.

Pederson, R. A., Satkunarajah, M., McIntosh, C. H., Scrocchi, L. A., Flamez, D., Schuit, F., Drucker, D. J. & Wheeler, M. B. 1998. Enhanced glucose-dependent insulinotropic polypeptide secretion and insulinotropic action in glucagon-like peptide 1 receptor -/- mice. *Diabetes* 47: 1046-52.

Pederson, R. A., Schubert, H. E. & Brown, J. C. 1975. Gastric inhibitory polypeptide. Its physiologic release and insulinotropic action in the dog. *Diabetes* 24: 1050-6.

Petrik, J., Pell, J. M., Arany, E., McDonald, T. J., Dean, W. L., Reik, W. & Hill, D. J. 1999. Overexpression of insulin-like growth factor-II in transgenic mice is associated with pancreatic islet cell hyperplasia. *Endocrinology* 140: 2353-63.

Pfeifer, A. 2004. Lentiviral transgenesis. *Transgenic Res* 13: 513-22.

Pfeifer, A., Ikawa, M., Dayn, Y. & Verma, I. M. 2002. Transgenesis by lentiviral vectors: lack of gene silencing in mammalian embryonic stem cells and preimplantation embryos. *Proc Natl Acad Sci U S A* 99: 2140-5.

Pfeifer, A. & Verma, I. M. 2001. Gene therapy: promises and problems. *Annu Rev Genomics Hum Genet* 2: 177-211.

Phillips, R. W., Panepinto, L. M., Spangler, R. & Westmoreland, N. 1982. Yucatan miniature swine as a model for the study of human diabetes mellitus. *Diabetes* 31: 30-6.

Poeschla, E., Gilbert, J., Li, X., Huang, S., Ho, A. & Wong-Staal, F. 1998a. Identification of a human immunodeficiency virus type 2 (HIV-2) encapsidation determinant and transduction of nondividing human cells by HIV-2-based lentivirus vectors. *J Virol* 72: 6527-36.

Poeschla, E. M., Wong-Staal, F. & Looney, D. J. 1998b. Efficient transduction of nondividing human cells by feline immunodeficiency virus lentiviral vectors. *Nat Med* 4: 354-7.

Preitner, F., Ibberson, M., Franklin, I., Binnert, C., Pende, M., Gjinovci, A., Hansotia, T., Drucker, D. J., Wollheim, C., Burcelin, R. & Thorens, B. 2004. Gluco-incretins control insulin secretion at multiple levels as revealed in mice lacking GLP-1 and GIP receptors. *J Clin Invest* 113: 635-45.

Prescott, M. F., Hasler-Rapacz, J., von Linden-Reed, J. & Rapacz, J. 1995. Familial hypercholesterolemia associated with coronary atherosclerosis in swine bearing different alleles for apolipoprotein B. *Ann N Y Acad Sci* 748: 283-92; discussion 292-3.

Prescott, M. F., McBride, C. H., Hasler-Rapacz, J., Von Linden, J. & Rapacz, J. 1991. Development of complex atherosclerotic lesions in pigs with inherited hyper-LDL cholesterolemia bearing mutant alleles for apolipoprotein B. *Am J Pathol* 139: 139-47.

Qvist, M. H., Hoeck, U., Kreilgaard, B., Madsen, F. & Frokjaer, S. 2000. Evaluation of Gottingen minipig skin for transdermal in vitro permeation studies. *Eur J Pharm Sci* 11: 59-68.

Ricordi, C., Socci, C., Davalli, A. M., Staudacher, C., Baro, P., Vertova, A., Sassi, I., Gavazzi, F., Pozza, G. & Di Carlo, V. 1990. Isolation of the elusive pig islet. *Surgery* 107: 688-94.

Rood, P. P. & Cooper, D. K. 2006. Islet xenotransplantation: are we really ready for clinical trials? *Am J Transplant* 6: 1269-74.

Ross, S. A., Brown, J. C. & Dupre, J. 1977. Hypersecretion of gastric inhibitory polypeptide following oral glucose in diabetes mellitus. *Diabetes* 26: 525-9.

Ross, S. A. & Dupre, J. 1978. Effects of ingestion of triglyceride or galactose on secretion of gastric inhibitory polypeptide and on responses to intravenous glucose in normal and diabetic subjects. *Diabetes* 27: 327-33.

Sakuraba, H., Mizukami, H., Yagihashi, N., Wada, R., Hanyu, C. & Yagihashi, S. 2002. Reduced beta-cell mass and expression of oxidative stress-related DNA damage in the islet of Japanese Type II diabetic patients. *Diabetologia* 45: 85-96.

Salapatek, A. M., MacDonald, P. E., Gaisano, H. Y. & Wheeler, M. B. 1999. Mutations to the third cytoplasmic domain of the glucagon-like peptide 1 (GLP-1) receptor can functionally uncouple GLP-1-stimulated insulin secretion in HIT-T15 cells. *Mol Endocrinol* 13: 1305-17.

Scherle, W. 1970. A simple method for volumetry of organs in quantitative stereology. *Mikroskopie* 26: 57-60.

Schmidt, W. E., Siegel, E. G. & Creutzfeldt, W. 1985. Glucagon-like peptide-1 but not glucagon-like peptide-2 stimulates insulin release from isolated rat pancreatic islets. *Diabetologia* 28: 704-7.

Schroder, A. R., Shinn, P., Chen, H., Berry, C., Ecker, J. R. & Bushman, F. 2002. HIV-1 integration in the human genome favors active genes and local hotspots. *Cell* 110: 521-9.

Scrocchi, L. A., Brown, T. J., MaClusky, N., Brubaker, P. L., Auerbach, A. B., Joyner, A. L. & Drucker, D. J. 1996. Glucose intolerance but normal satiety in mice with a null mutation in the glucagon-like peptide 1 receptor gene. *Nat Med* 2: 1254-8.

Siegel, E. G. & Creutzfeldt, W. 1985. Stimulation of insulin release in isolated rat islets by GIP in physiological concentrations and its relation to islet cyclic AMP content. *Diabetologia* 28: 857-61.

Starcich, B., Ratner, L., Josephs, S. F., Okamoto, T., Gallo, R. C. & Wong-Staal, F. 1985. Characterization of long terminal repeat sequences of HTLV-III. *Science* 227: 538-40.

Swindle, M. (2007). Swine in the laboratory, surgery, anesthesia, imaging, and experimental techniques; Second Edition; CRC press. Ref Type: Serial (Book, Monograph).

Takhar, S., Gyomorey, S., Su, R. C., Mathi, S. K., Li, X. & Wheeler, M. B. 1996. The third cytoplasmic domain of the GLP-1[7-36 amide] receptor is required for coupling to the adenylyl cyclase system. *Endocrinology* 137: 2175-8.

Theodorakis, M. J., Carlson, O., Michopoulos, S., Doyle, M. E., Juhaszova, M., Petraki, K. & Egan, J. M. 2006. Human duodenal enteroendocrine cells: source of both incretin peptides, GLP-1 and GIP. *Am J Physiol Endocrinol Metab* 290: E550-9.

Thomas, F. B., Shook, D. F., O'Dorisio, T. M., Cataland, S., Mekhjian, H. S., Caldwell, J. H. & Mazzaferri, E. L. 1977. Localization of gastric inhibitory polypeptide release by intestinal glucose perfusion in man. *Gastroenterology* 72: 49-54.

Toft-Nielsen, M. B., Damholt, M. B., Madsbad, S., Hilsted, L. M., Hughes, T. E., Michelsen, B. K. & Holst, J. J. 2001. Determinants of the impaired secretion of glucagon-like peptide-1 in type 2 diabetic patients. *J Clin Endocrinol Metab* 86: 3717-23.

Trumper, A., Trumper, K. & Horsch, D. 2002. Mechanisms of mitogenic and anti-apoptotic signaling by glucose-dependent insulinotropic polypeptide in beta(INS-1)-cells. *J Endocrinol* 174: 233-46.

Trumper, A., Trumper, K., Trusheim, H., Arnold, R., Goke, B. & Horsch, D. 2001. Glucose-dependent insulinotropic polypeptide is a growth factor for beta (INS-1) cells by pleiotropic signaling. *Mol Endocrinol* 15: 1559-70.

Tseng, C. C., Boylan, M. O., Jarboe, L. A., Usdin, T. B. & Wolfe, M. M. 1996a. Chronic desensitization of the glucose-dependent insulinotropic polypeptide receptor in diabetic rats. *Am J Physiol* 270: E661-6.

Tseng, C. C., Kieffer, T. J., Jarboe, L. A., Usdin, T. B. & Wolfe, M. M. 1996b. Postprandial stimulation of insulin release by glucose-dependent insulinotropic polypeptide (GIP). Effect of a specific glucose-dependent insulinotropic polypeptide receptor antagonist in the rat. *J Clin Invest* 98: 2440-5.

Tseng, C. C., Zhang, X. Y. & Wolfe, M. M. 1999. Effect of GIP and GLP-1 antagonists on insulin release in the rat. *Am J Physiol* 276: E1049-54.

Turton, M. D., O'Shea, D., Gunn, I., Beak, S. A., Edwards, C. M., Meeran, K., Choi, S. J., Taylor, G. M., Heath, M. M., Lambert, P. D., Wilding, J. P., Smith, D. M., Ghatei, M. A., Herbert, J. & Bloom, S. R. 1996. A role for glucagon-like peptide-1 in the central regulation of feeding. *Nature* 379: 69-72.

Ugleholdt, R., Poulsen, M. L., Holst, P. J., Irminger, J. C., Orskov, C., Pedersen, J., Rosenkilde, M. M., Zhu, X., Steiner, D. F. & Holst, J. J. 2006. Prohormone convertase 1/3 is essential for processing of the glucose-dependent insulinotropic polypeptide precursor. *J Biol Chem* 281: 11050-7.

Ulrichs, K., Bosse, M., Heiser, A., Eckstein, V., Wacker, H., Thiede, A., Mueller Ruchholtz, W. (1995). Histomorphologcal characteristics of the pancreas as a basis for the isolation of islets of Langerhans. *Xenotransplantation* 2: 167-187.

Unger, R. H. & Eisentraut, A. M. 1969. Entero-insular axis. *Arch Intern Med* 123: 261-6.

Usdin, T. B., Mezey, E., Button, D. C., Brownstein, M. J. & Bonner, T. I. 1993. Gastric inhibitory polypeptide receptor, a member of the secretin-vasoactive intestinal peptide receptor family, is widely distributed in peripheral organs and the brain. *Endocrinology* 133: 2861-70.

Vague, P. & Moulin, J. P. 1982. The defective glucose sensitivity of the B cell in non insulin dependent diabetes. Improvement after twenty hours of normoglycaemia. *Metabolism* 31: 139-42.

van Deijnen, J. H., Hulstaert, C. E., Wolters, G. H. & van Schilfgaarde, R. 1992. Significance of the peri-insular extracellular matrix for islet isolation from the pancreas of rat, dog, pig, and man. *Cell Tissue Res* 267: 139-46.

van der Burg, M. P. & Graham, J. M. 2003. Iodixanol density gradient preparation in university of wisconsin solution for porcine islet purification. *ScientificWorldJournal* 3: 1154-9.

Vilsboll, T., Agerso, H., Lauritsen, T., Deacon, C. F., Aaboe, K., Madsbad, S., Krarup, T. & Holst, J. J. 2006. The elimination rates of intact GIP as well as its primary metabolite, GIP 3-42, are similar in type 2 diabetic patients and healthy subjects. *Regul Pept* 137: 168-72.

Vilsboll, T., Krarup, T., Deacon, C. F., Madsbad, S. & Holst, J. J. 2001. Reduced postprandial concentrations of intact biologically active glucagon-like peptide 1 in type 2 diabetic patients. *Diabetes* 50: 609-13.

Vilsboll, T., Krarup, T., Madsbad, S. & Holst, J. J. 2002. Defective amplification of the late phase insulin response to glucose by GIP in obese Type II diabetic patients. *Diabetologia* 45: 1111-9.

Volz, A., Goke, R., Lankat-Buttgereit, B., Fehmann, H. C., Bode, H. P. & Goke, B. 1995. Molecular cloning, functional expression, and signal transduction of the GIP-receptor cloned from a human insulinoma. *FEBS Lett* 373: 23-9.

Volz, A. (1997). Klonierung und funktionelle Charakterisierung des humanen GIP-Rezeptors. Thesis for the attainment of the title Doctor in natural sciences, University of Marburg, p 1-159.

Wacker, T., Jahr, H., Weinand, S., Brandhorst, H., Brandhorst, D., Lau, D., Hering, B. J., Federlin, K. & Bretzel, R. G. 1995. Different toxic effects of hydrogen peroxide, nitric oxide, and superoxide on human, pig, and rat islets of Langerhans. *Exp Clin Endocrinol Diabetes* 103 Suppl 2: 133-35.

Wall, R.J. (1996). Transgenic livestock: progress and prospects for the future. *Theriogenology* 45: 57-68.

Wang, Y., Montrose-Rafizadeh, C., Adams, L., Raygada, M., Nadiv, O. & Egan, J. M. 1996. GIP regulates glucose transporters, hexokinases, and glucose-induced insulin secretion in RIN 1046-38 cells. *Mol Cell Endocrinol* 116: 81-7.

Wang, Z., Wang, R. M., Owji, A. A., Smith, D. M., Ghatei, M. A. & Bloom, S. R. 1995. Glucagon-like peptide-1 is a physiological incretin in rat. *J Clin Invest* 95: 417-21.

Wheeler, M. B., Gelling, R. W., Hinke, S. A., Tu, B., Pederson, R. A., Lynn, F., Ehses, J. & McIntosh, C. H. 1999. Characterization of the carboxyl-terminal domain of the rat glucose-dependent insulinotropic polypeptide (GIP) receptor. A role for serines 426 and 427 in regulating the rate of internalization. *J Biol Chem* 274: 24593-601.

Wheeler, M. B., Gelling, R. W., McIntosh, C. H., Georgiou, J., Brown, J. C. & Pederson, R. A. 1995. Functional expression of the rat pancreatic islet glucose-dependent insulinotropic polypeptide receptor: ligand binding and intracellular signaling properties. *Endocrinology* 136: 4629-39.

Wheeler, M. B., Lu, M., Dillon, J. S., Leng, X. H., Chen, C. & Boyd, A. E. 3rd 1993. Functional expression of the rat glucagon-like peptide-I receptor, evidence for coupling to both adenylyl cyclase and phospholipase-C. *Endocrinology* 133: 57-62.

Whitelaw, C. B., Radcliffe, P. A., Ritchie, W. A., Carlisle, A., Ellard, F. M., Pena, R. N., Rowe, J., Clark, A. J., King, T. J. & Mitrophanous, K. A. 2004. Efficient generation of transgenic pigs using equine infectious anaemia virus (EIAV) derived vector. *FEBS Lett* 571: 233-6.

Wieczorek, G., Pospischil, A. & Perentes, E. 1998. A comparative immunohistochemical study of pancreatic islets in laboratory animals (rats, dogs, minipigs, nonhuman primates). *Exp Toxicol Pathol* 50: 151-72.

Wild, S., Roglic, G., Green, A., Sicree, R. & King, H. 2004. Global prevalence of diabetes: estimates for the year 2000 and projections for 2030. *Diabetes Care* 27: 1047-53.

Wu, X. & Burgess, S. M. 2004. Integration target site selection for retroviruses and transposable elements. *Cell Mol Life Sci* 61: 2588-96.

Wu, X., Li, Y., Crise, B. & Burgess, S. M. 2003. Transcription start regions in the human genome are favored targets for MLV integration. *Science* 300: 1749-51.

Xi, S., Yin, W., Wang, Z., Kusunoki, M., Lian, X., Koike, T., Fan, J. & Zhang, Q. 2004. A minipig model of high-fat/high-sucrose diet-induced diabetes and atherosclerosis. *Int J Exp Pathol* 85: 223-31.

Xie, D., Cheng, H., Hamrick, M., Zhong, Q., Ding, K. H., Correa, D., Williams, S., Mulloy, A., Bollag, W., Bollag, R. J., Runner, R. R., McPherson, J. C., Insogna, K. & Isales, C. M. 2005. Glucose-dependent insulinotropic polypeptide receptor knockout mice have altered bone turnover. *Bone* 37: 759-69.

Xie, D., Zhong, Q., Ding, K. H., Cheng, H., Williams, S., Correa, D., Bollag, W. B., Bollag, R. J., Insogna, K., Troiano, N., Coady, C., Hamrick, M. & Isales, C. M. 2007. Glucose-dependent insulinotropic peptide-overexpressing transgenic mice have increased bone mass. *Bone* 40: 1352-60.

Xu, G., Kaneto, H., Laybutt, D. R., Duvivier-Kali, V. F., Trivedi, N., Suzuma, K., King, G. L., Weir, G. C. & Bonner-Weir, S. 2007. Downregulation of GLP-1 and GIP receptor expression by hyperglycemia: possible contribution to impaired incretin effects in diabetes. *Diabetes* 56: 1551-8.

Xu, G., Stoffers, D. A., Habener, J. F. & Bonner-Weir, S. 1999. Exendin-4 stimulates both beta-cell replication and neogenesis, resulting in increased beta-cell mass and improved glucose tolerance in diabetic rats. *Diabetes* 48: 2270-6.

Yamada, Y., Hayami, T., Nakamura, K., Kaisaki, P. J., Someya, Y., Wang, C. Z., Seino, S. & Seino, Y. 1995. Human gastric inhibitory polypeptide receptor: cloning of the gene (GIPR) and cDNA. *Genomics* 29: 773-6.

Yamamoto, H., Uchigata, Y. & Okamoto, H. 1981. Streptozotocin and alloxan induce DNA strand breaks and poly(ADP-ribose) synthetase in pancreatic islets. *Nature* 294: 284-6.

Yasuda, K., Inagaki, N., Yamada, Y., Kubota, A., Seino, S. & Seino, Y. 1994. Hamster gastric inhibitory polypeptide receptor expressed in pancreatic islets and clonal insulin-secreting cells: its structure and functional properties. *Biochem Biophys Res Commun* 205: 1556-62.

Yip, R. G., Boylan, M. O., Kieffer, T. J. & Wolfe, M. M. 1998. Functional GIP receptors are present on adipocytes. *Endocrinology* 139: 4004-7.

Yip, R. G. & Wolfe, M. M. 2000. GIP biology and fat metabolism. *Life Sci* 66: 91-103.

Yoon, K. H., Ko, S. H., Cho, J. H., Lee, J. M., Ahn, Y. B., Song, K. H., Yoo, S. J., Kang, M. I., Cha, B. Y., Lee, K. W., Son, H. Y., Kang, S. K., Kim, H. S., Lee, I. K. & Bonner-Weir, S. 2003. Selective beta-cell loss and alpha-cell expansion in patients with type 2 diabetes mellitus in Korea. *J Clin Endocrinol Metab* 88: 2300-8.

Yusta, B., Baggio, L. L., Estall, J. L., Koehler, J. A., Holland, D. P., Li, H., Pipeleers, D., Ling, Z. & Drucker, D. J. 2006. GLP-1 receptor activation improves beta cell function and survival following induction of endoplasmic reticulum stress. *Cell Metab* 4: 391-406.

Zennou, V., Petit, C., Guetard, D., Nerhbass, U., Montagnier, L. & Charneau, P. 2000. HIV-1 genome nuclear import is mediated by a central DNA flap. *Cell* 101: 173-85.

Zhong, Q., Itokawa, T., Sridhar, S., Ding, K. H., Xie, D., Kang, B., Bollag, W. B., Bollag, R. J., Hamrick, M., Insogna, K. & Isales, C. M. 2007. Effects of glucose-dependent insulinotropic peptide on osteoclast function. *Am J Physiol Endocrinol Metab* 292: E543-8.

Zufferey, R., Donello, J. E., Trono, D. & Hope, T. J. 1999. Woodchuck hepatitis virus posttranscriptional regulatory element enhances expression of transgenes delivered by retroviral vectors. *J Virol* 73: 2886-92.

Zufferey, R., Dull, T., Mandel, R. J., Bukovsky, A., Quiroz, D., Naldini, L. & Trono, D. 1998. Self-inactivating lentivirus vector for safe and efficient in vivo gene delivery. *J Virol* 72: 9873-80.

13 Acknowledgments

First, a special thanks goes to Prof. Dr. Eckhard Wolf for allowing me to carry out this research work at the Chair for Molecular Animal Breeding and Biotechnology, Gene Center, Ludwig-Maximilians University Munich, his friendly and helpful support at all times as well as for reviewing this manuscript.

I also would like to thank Prof. Dr. Rüdiger Wanke for allowing me to work in his laboratories, for his support and for reviewing this manuscript.

Another acknowledgment goes to Dr. Nadja Herbach for her support in all pathological questions as well as for reviewing this manuscript.

Thanks to Dr. Dagmar von Waldthausen, who mentored the first two years of this work, for her support.

I am very grateful to Dr. Barbara Keßler for the great teamwork as well as her support concerning the entire work with the pigs.

I am grateful to Prof. Dr. Alexander Pfeifer and Dr. Andreas Hofmann (Institute of Pharmacology and Toxicology, University of Bonn, Germany) for the generation of the lentiviral vector.

I wish to express my sincere thanks to Prof. Dr. Karin Ulrichs, Dr. Irina Chodnevskaja and Bianca Schneiker (Experimental Transplantation Immunology, Surgical Clinic I, University Hospital of Wuerzburg, Germany), who carried out the islet isolations with me, for her support and the great working atmosphere.

I also would like to acknowledge Prof. Dr. Burkhard Göke and Dr. Jutta Berster for giving me so many helpful advices.

Thanks to Prof. Dr. Katrin Hartmann and the chemical laboratory team of the Medical Small Animal Clinic for carrying out the serum fructosamine measurements.

I also would like to thank Prof. Dr. Karl Heinritzi for giving me the opportunity to carry out glucose tolerance tests of adult pigs in the premises of the pig clinic as well as the entire team of the Chair for Pig Diseases for their support.

I am grateful to Prof. Dr. Holm Zerbe for giving me the opportunity to use the necropsy room of the Clinic for Ruminants as well as Dr. Ebert from the Landesamt für Gesundheit und Lebensmittelsicherheit for the good collaboration.

I am grateful to the German Mouse Clinic, especially to Dr. Corinna Moerth and Elfi Holupirek, for measuring the serum glucose levels.

Special thanks to Christian Erdle and Siegfried Elsner for their excellent animal care and to Lisa Pichl for the generation of the paraffin sections.

I am particularly thankful to my colleagues Dr. Anne Wünsch, Dr. Marc Boelhauve Dr. Susanne Thieme, Dr. Elisabeth Kemter, Dr. Daniela Diehl, Dr. Sigrid Mueller, Dr. Harald Lahm, Dr. Marlon Schneider, Hannelore Breitsameter, Eleonore Schilling, Maik Dahlhoff, Sabine Kautz, Andreas Blutke, Heidi Alt and to all the other past and present members of the group in the Gene Center as well as in the Moorversuchsgut for their support and for creating a very pleasant working atmosphere.

I wish to thank all past and present members of the graduate program 1029 for their support.

The financial support from the Deutsche Forschungsgemeinschaft (GRK 1029) is deeply acknowledged.